Field Trip the Andean Heart of Colombia: Tectonics, Volcanoes, and Geological Hazards

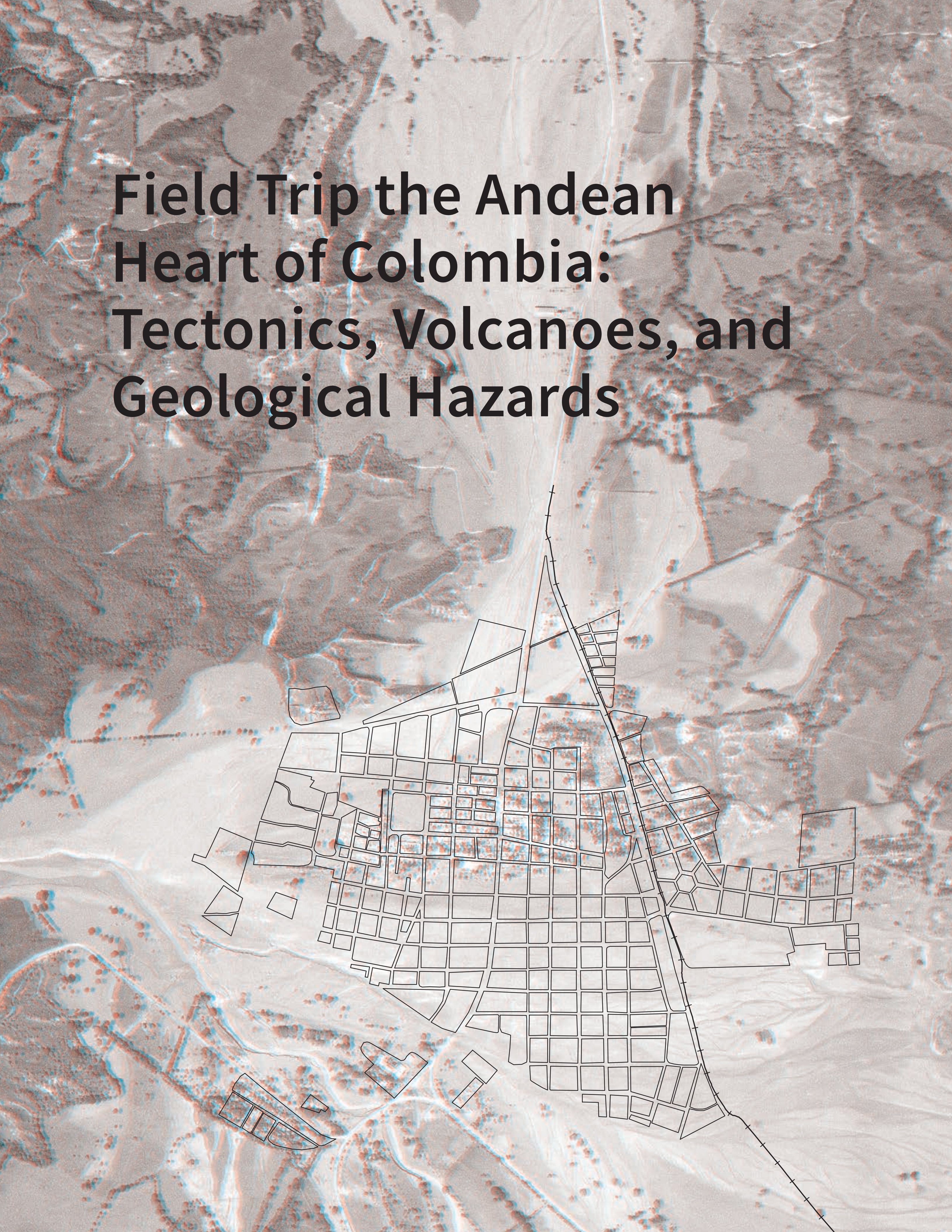

Cover

Anaglyph of Armero generated from orthophotos acquired on November 20, 1985 (Flight C–2229), showing that the November 13, 1985 Armero lahar devastated approximately 85% of the town. Anaglyph glasses provided with this field guide are required for proper viewing.

Suggested citation

Gómez, J., Avendaño, J.A., Romero, E.S. & Arboleda, M.C. 2025. Field Trip the Andean Heart of Colombia: Tectonics, Volcanoes, and Geological Hazards. Servicio Geológico Colombiano and International Union of Geological Sciences, 48 p. Bogotá, Colombia.

Geography, Landscapes, and Cultural Traditions Along the Field Trip Itinerary

January 28, 2026
Outbound journey: Bogotá–Ibagué, Tolima

Traveling from Bogotá to Armero follows one of the most representative routes of central Colombia and the Northern Andes, where Andean geography, national history, and cultural identity intertwine in a profound—and at times moving—way. This route crosses first the **Eastern Cordillera** and then the **Central Cordillera**, allowing participants, within a few hours, to appreciate the remarkable diversity of landscapes, climates, and traditions that characterize the country and the tropical Andes as a whole.

The journey begins in **Bogotá**, leaving the Sabana behind and entering the municipality of **Soacha**, one of the oldest urban areas of the plateau. From the road, the contrast between metropolitan expansion and the surrounding hills marking the exit from the city becomes evident. Nearby lies the **Tequendama Falls** area, a natural and historical symbol of the region, visible from open sections of the corridor.

After passing the **Chusacá toll**, the road descends toward warmer climates, and the towns of **Silvania** and **Fusagasugá** appear, surrounded by crops and plant nurseries. Fusagasugá stands out as the "Garden City" due to its agricultural tradition and active university environment. Farther along, the route crosses the **Chinauta plain**, an open stretch where the highway follows the **Sumapaz River**, the natural boundary between Cundinamarca and Tolima deparments, offering a marked transition toward a broader, greener, and warmer valley. The **Chinauta toll** is located in this sector and serves as a common reference point for travelers.

The journey continues toward one of the most emblematic points along the route, **La Nariz del Diablo** ("The Devil's Nose"), named for the pronounced curve and rocky relief bordering the road, which from certain angles resembles a nose profile. From this point, panoramic views of the **Magdalena River valley** can be enjoyed, making it one of the most memorable natural viewpoints of the trip. Shortly thereafter, the route reaches Melgar, a major tourist destination known for its extensive hotel infrastructure.

Farther on lies **Flandes**, where crossing the Magdalena River marks the definitive transition into Tolima and opens into a region with strong agricultural and historical traditions. The route continues through **Chicoral**, known for its political history and rural setting, and **Gualanday**, a road junction where commercial activity revolves around highway traffic. Along this stretch, the landscape follows the **Coello River**, whose waters irrigate extensive croplands, while the road is animated by roadside restaurants, tropical fruit vendors, and clearly marked access points toward **Espinal** and **Ibagué**, reinforcing the dynamic agricultural character of the region.

January 29, 2026
Return journey: Ibagué–Armero–Bogotá

The stretch from **Ibagué to Armero** traverses the heart of northern Tolima, a region where rural landscapes, historical memory, and cultural identity are constantly expressed along the road. The journey departs from **Ibagué**, the departmental capital and widely known as the "Musical City of Colombia", a title reflecting Tolima's deep artistic tradition. Andean music and folkloric festivals are closely linked to rural life and the Magdalena River valley. From the first kilometers, on clear days, it is possible to observe the **Nevado del Tolima**, an emblematic volcano that dominates the horizon and symbolizes the enduring relationship between the territory and the natural processes that have shaped regional history.

Leaving Ibagué heading north, the road cuts through warm plains and extensive croplands until reaching **Alvarado** and **Venadillo**, municipalities where rice fields and cattle ranching define both the landscape and the rhythm of rural life, always accompanied by rivers and streams that sustain agricultural activity. Farther along lies the **La Sierra** sector, a gently undulating stretch offering broad valley views and, on clear days, a privileged perspective of the Nevado del Tolima—one of the most photogenic landscapes along the route. The journey continues toward **Lérida**, a former agricultural center of northern Tolima, where vestiges of its prosperous past and a calm atmosphere are still perceptible from the road, closely tied to the region's recent history.

The route then reaches **Armero**, a site of fundamental importance to Colombia's collective memory. Prior to 1985, Armero was a prosperous agricultural town, renowned for cotton and rice production. Today, it is a place of reflection and remembrance, marked by the tragedy caused by the eruption of **Nevado del Ruiz**, which forever transformed both the geography and human history of the area. Visiting Armero is not merely a tourist stop but a cultural and educational experience that underscores the power of nature and the critical importance of risk management in volcanic regions.

The return to Bogotá follows the **western corridor**, a route that blends history, landscape, and territorial transformation. The journey begins in **Cambao**, a former river port on the Magdalena River, recalling a time when fluvial transport was central to commerce and regional integration. From there, the road ascends the western flank of the **Eastern Cordillera**, passing through **Vianí**, a coffee–growing municipality surrounded by green mountains and a mild climate, and **Albán**, known for its agricultural vocation and strategic role as a natural gateway to the Bogotá Sabana.

Farther along, the route reaches **Facatativá**, one of the most important historical and cultural centers of western Cundinamarca, famous for the **Piedras del Tunjo Archaeological Park**, where rock art and landscape reveal the deep ancestral relationship between Indigenous communities and their territory. The journey continues through **Madrid** and **Mosquera**, municipalities that today reflect the industrial and urban dynamism of the Sabana, developed over the alluvial deposits of the **Bogotá River**, before finally returning to the capital city.

Overall, the **Bogotá–Armero round trip** offers a comprehensive view of Colombia: from urban life in the high Andes and its gastronomy, through intermediate cities rich in music, tradition, and ancestral flavors, to landscapes laden with history, meaning, and geodiversity. It is a route that combines natural beauty, cultural diversity, and profound historical lessons—an ideal journey for experiencing a significant portion of the country from the heart of the Northern Andes.


Mariquita
Honda
Fresno
Palocabildo
Falan
Casabianca
Villahermosa
Guayabal
Lérida
Santa Isabel
Venadillo
Anzoátegui
Alvarado
Piedras
IBAGUÉ
Coello
Valle de San Juan
San Luis
Espinal
Guamo
Suárez
Ortega
Saldaña
Purificación
RÍO MAGDALENA
RÍO CUCUANA
RÍO SALDAÑA
Útica
La Peña
El Peñón
Villa Gómez
Quebradanegra
Nimaima
Vergara
Nocaima
Pacho
Supatá
Guaduas
Villeta
La Vega
San Francisco
Subachoque
Sasaima
Chaguaní
Tabio
Tenjo
El Rosal
Albán
Bituima
San Juan de Río Seco
Cota
Facatativá
Beltrán
Ambalema
Anolaima
Zipacón
Madrid
Bojacá
Funza
Mosquera
BOGOTÁ D.C.
Quipile
Cachipay
Pulí
La Mesa
San Antonio de Tequendama
Soacha
Anapoima
El Colegio
Jerusalén
Apulo (Rafael Reyes)
Guataquí
Granada (El Soche)
Sibaté
Tocaima
Viotá
Agua de Dios
Nariño
Silvania
Tibacuy
Fusagasugá
Girardot
Flandes
Ricaurte
Nilo
Pasca
Arbeláez
Melgar
Pandi
San Bernardo
Icononzo
Carmen de Apicalá
Cunday
Cabrera
Villarrica

Field Trip

The Andean Heart of Colombia: Tectonics, Volcanoes, and Geological Hazards

Jorge GÓMEZ TAPIAS[1]*, Maria Luisa MONSALVE[2], Juliana Andrea AVENDAÑO ASCENCIO[3], Efrén Santiago ROMERO CORTÉS[4], and María Camila ARBOLEDA GONZÁLEZ[5]

1 mapageo@sgc.gov.co
Servicio Geológico Colombiano
Dirección de Geociencias Básicas
Grupo de cartografía geológica
Diagonal 53 n.° 34–53
Bogotá, Colombia
ORCID: https://orcid.org/0000-0002-7906-7819

2 mmonsalve@sgc.gov.co
Servicio Geológico Colombiano
Dirección de Geociencias Básicas
Observatorio Vulcanológico y Sismológico de Manizales
Avenida 12 de octubre n.°.15-47
Manizales, Colombia
ORCID: https://orcid.org/0000-0001-5056-3475

3 javendano@sgc.gov.co
Servicio Geológico Colombiano
Dirección de Geociencias Básicas
Grupo de cartografía geológica
Diagonal 53 n.° 34–53
Bogotá, Colombia

4 efromeroc@unal.edu.co
Servicio Geológico Colombiano
Dirección de Geociencias Básicas
Grupo de cartografía geológica
Diagonal 53 n.° 34–53
Bogotá, Colombia

5 marboleda@sgc.gov.co
Servicio Geológico Colombiano
Dirección Técnica de Laboratorios
Grupo de geomecánica y procesos físicos
Avenida Calle 50 n.°26-20
Bogotá, Colombia

* Autor de correspondencia

Supplementary Information

S1: https://www2.sgc.gov.co/MGC/Documents/Ft_IUGS/iugsfts2.pdf

S2: https://www2.sgc.gov.co/MGC/Documents/Ft_IUGS/iugsfts1.kmz

Abstract

The field guide The Andean Heart of Colombia: Tectonics, Volcanoes, and Geological Hazards presents an integrated geological synthesis of the central Colombian Andes, combining stratigraphic, structural, volcanic, and geomorphological observations along a transect across the Eastern Cordillera, Central Cordillera, and the Upper Magdalena Valley. Prepared for the 82nd Executive Committee Meeting of the International Union of Geological Sciences, the guide highlights the links between Andean tectonic evolution and geological hazards affecting densely populated regions.

The excursion begins in the Eastern Cordillera, where Upper Cretaceous successions of the Guadalupe Group and the overlying Guaduas Formation are exposed within an overturned anticline. This structure is interpreted as a fault–propagation fold associated with west–verging thrust systems, documenting tectonic inversion of Mesozoic extensional basins during Late Cretaceous–Paleocene Andean shortening. The stratigraphic transition from shallow–marine to coal–bearing continental deposits reflects major paleogeographic and tectonic reorganization along the eastern margin of the Upper Magdalena Valley.

In the Upper Magdalena Valley, the guide emphasizes Quaternary volcanism and its geomorphic and societal impacts. Extensive Holocene lahar deposits generated by Cerro Machín Volcano are examined, including the Guamo and Espinal hyperconcentrated–flow deposits and the Chicoral debris-flow deposit. These lahars traveled more than 100 km along the Coello and Magdalena river systems, constructing large alluvial fans that today host important agricultural areas and urban settlements.

A key historical and hazard–related component of the excursion is the visit to Armero, the site of the catastrophic 13 November 1985 eruption of Nevado del Ruiz. Lahars triggered by this eruption devastated the town, causing one of the deadliest volcanic disasters in modern history. Armero serves as a powerful example of the consequences of volcanic hazards in populated valleys and underscores the importance of hazard assessment, land–use planning, and risk communication.

The guide also documents synorogenic molasse sedimentation of the Chicoral Formation (Eocene) and analyzes the Ibagué Fault, an active dextral strike–slip structure with well–preserved morphotectonic features and evidence for repeated late Quaternary surface–rupturing earthquakes. Overall, the field guide demonstrates the value of integrated field observations for understanding Andean tectonics and mitigating geological risk.

1. Introduction

The Field Trip the Andean Heart of Colombia: Tectonics, Volcanoes, and Geological Hazards is organized as one of the official activities of the 82nd Executive Committee Meeting of the International Union of Geological Sciences (IUGS). Participation in the field trip is limited to members of the IUGS Executive Committee. This two–day geological excursion follows the route Bogotá–Ibagué, returning via Ibagué–Armero–Bogotá (Cambao route). The itinerary offers an overview of Colombia's geological and geomorphological diversity through key outcrops and landscapes, including the overturned anticline of the Guadalupe Formation, lahar deposits of Cerro Machín Volcano, the Chicoral Formation, the Calicanto pressure ridge associated with the Ibagué Fault, Tabor Volcano, Guacharacos Volcano, and the Armero lahar deposits. See the itinerary of the field trip and the Supplementary Information S1.

This field trip guide was prepared by geologist Jorge GÓMEZ TAPIAS and geologist María Luisa MONSALVE BUSTAMANTE. Jorge GÓMEZ TAPIAS is the author of four editions of the Geological Map of Colombia (Gómez et al., 2007; Gómez et al., 2015; Gómez & Montes, 2020 and Gómez et al., 2023) and editor of the first comprehensive multivolume book, The Geology of Colombia (Gómez & Pinilla–Pachon, 2020a, b; Gómez & Mateus–Zabala, 2020a, b), and has worked as a researcher at the Servicio Geológico Colombiano for the past 24 years.

María Luisa MONSALVE BUSTAMANTE obtained a DEA from Université Pierre et Marie Curie (Paris VI) and pursued PhD studies at the University of Geneva, Switzerland (1988–1990). She is one of Colombia's most distinguished volcanologists and has conducted fieldwork at all active and potentially active volcanoes in the country. Her research focuses on physical volcanology, petrology, and volcanic hazard assessment.

Geologist Juliana Andrea AVENDAÑO ASCENCIO, Efrén Santiago ROMERO CORTÉS and María Camila ARBOLEDA GONZÁLEZ collaborated in the logistical preparation of the field trip, prepared the figures included in the guide, and was responsible for the layout and design of the field trip guide.

To update and refine the content of this guide, two and a half weeks of fieldwork were carried out. During this period, outcrop conditions were verified, descriptions were revised and improved, drone–based aerial imagery was acquired, and field stations were selected and optimized. In addition, new posters were prepared for use at the different field stops.

The excursion takes place within the Magdalena Valley, a region characterized by distinctive geomorphology and average temperatures close to 27 °C. Participants will overnight in th city of Ibagué.

Ibagué, the capital of the department of Tolima, founded in 1550, is located at an elevation of 1,225 m above sea level and has a mean annual temperature of approximately 26 °C.

The Armero region, located between 300 and 400 m above sea level in northern Tolima, exhibits a warm, humid tropical climate, with average annual temperatures ranging from 26 to 28 °C. During the dry season, maximum temperatures may exceed 35 °C, with a heat index (feels-like temperature) of up to 40 °C due to high relative humidity.

This guide represents an updated version of the field excursion Geological History of the Colombian Andes in the Surroundings of Ibagué (Gómez et al., 2016).

2. Geologic Evolution of Colombia: From Cratonic Foundations to an Accretionary Andean Margin

This brief overview of the geological evolution of Colombia is adapted and modified from Zuluaga et al. (2026). Colombia occupies the northwestern corner of South America, where the Caribbean, Nazca, and South American plates interact, producing frequent seismicity and volcanism (Figure 1). The Northern Andes record long–lived continental growth since the Neoproterozoic, developed west of the Guiana Shield—the exposed northwestern margin of the Amazonian Craton (Cordani et al., 2000) (Figure 2). This history includes episodic arc magmatism, medium– to high–grade metamorphism during multiple orogenies, and accretion of oceanic plateau fragments and high–pressure mélanges. While some first–order geodynamic links (e.g., Pangaea breakup vs. extension along western Gondwana) remain debated, the present crustal architecture reflects repeated convergence, accretion, and crustal reworking.

Geological mapping conducted by the Servicio Geológico Colombiano indicates that western Colombia is characterized by major faults that separate distinct lithodemic units. The San Jerónimo Fault separates the Quebradagrande Complex from the Triassic–Jurassic rocks of the Cajamarca Complex. The Silvia–Pijao Fault separates the Quebradagrande Complex from the Arquía Complex, whereas the Cauca–Almaguer Fault marks the boundary between the Arquía Complex and rocks of the Colombian–Caribbean Large Igneous Province exposed in the Western Cordillera of Colombia. The tectonic boundary separating continental–affinity crust to the east (–220 mGal; Case et al., 1973) from accreted oceanic lithosphere to the west (+75 to +135 mGal; Case et al., 1973) is the Cauca–Almaguer Fault (Figures 1, 2). The western domain comprises Pacific-derived oceanic plateau fragments, commonly interpreted as plume–type ophiolites (Nivia, 1987; Kerr et al., 1997; Dilek & Furnes, 2014).

2.1 Andean Architecture And Major Physiographic Domains

The Colombian Andes consist of three longitudinal cordilleras separated by the Magdale-na and Cauca inter–Andean foreland basins (Figure 3). Toward the north, the orogenic belt narrows and transitions into lower–relief structural domains; nevertheless, the coastal ranges of La Guajira (Jarara, Macuira, and Carpintero) persist as discrete uplifted blocks along the Caribbean margin. The Sierra Nevada de Santa Marta (Figure 3) stands out due to its elevation, margin position, and the apparent

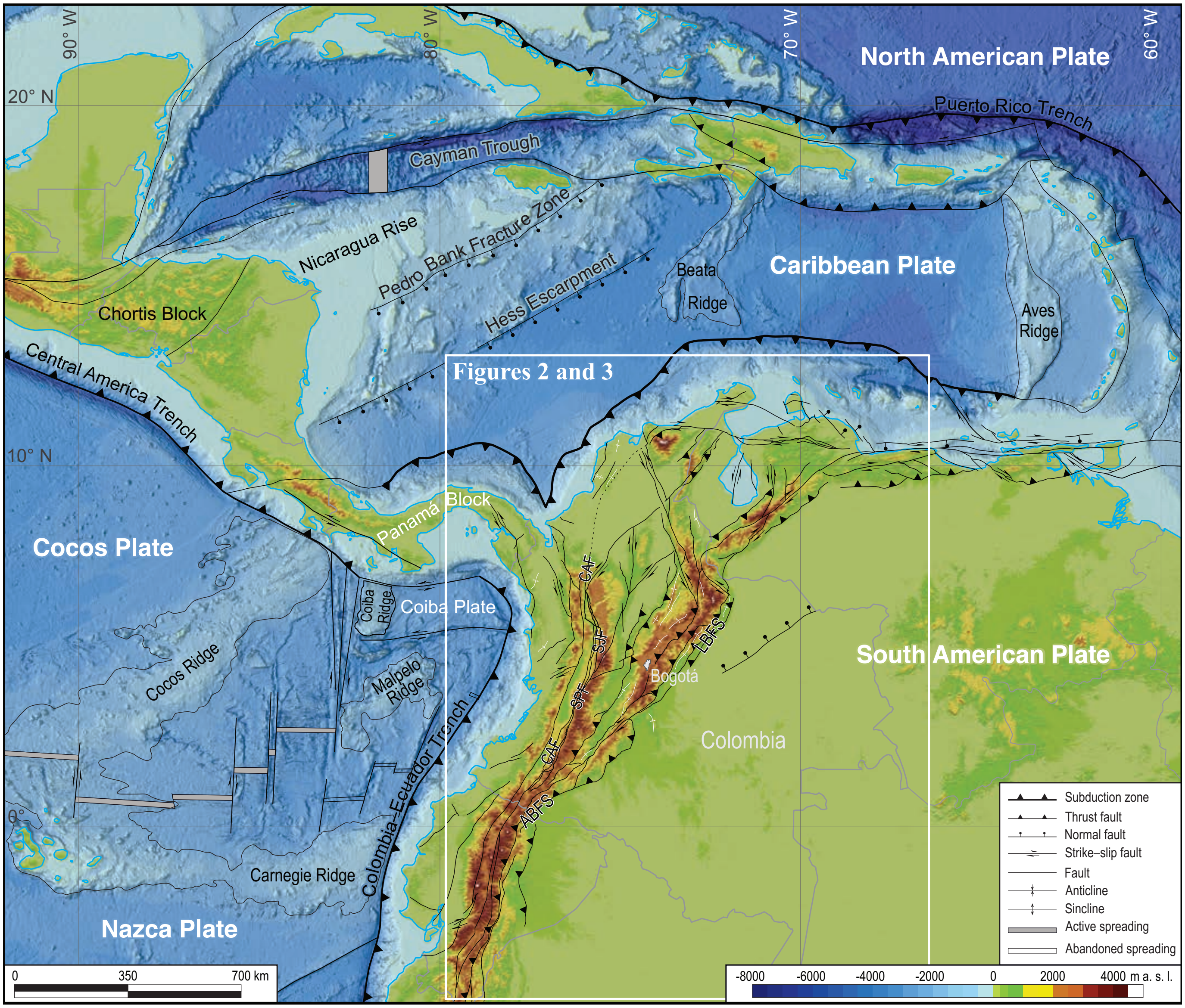

Figure 1. Tectonic framework of the northwestern corner of South America and the Caribbean (Gómez et al., 2015). CAF: Cauca–Almaguer Fault; SPF: Silvia–Pijao Fault; SJF: San Jerónimo Fault; ABFS: Amazonian Border Fault System; LBFS: Llanero Border Fault System. The area covered by Figures 1 and 2 is indicated on the map.

absence of a conventional crustal root (Case & MacDonald, 1973; Cerón, 2008; Quiroga et al., 2024). These coastal belts reflect deformation tied to Caribbean–South American in-teraction (Kellogg & Bonini, 1982). To the west, the orogen transitions toward the trench via the Serranía de Baudó and the Pacific coastal plain (Figure 3).

2.2 Guiana Shield and Proterozoic basement framework

In Colombia, direct knowledge of the Guiana Shield is limited by rainforest access. The region corresponds to the Río Negro–Juruena Province of the Amazonian Craton (Tassinari & Macambira, 1999; Santos et al., 2000), recording arc magmatism, rifting, and ano-rogenic magmatism. These rocks are grouped as the Mitú Migmatitic Complex (Galvis et al., 1979; Rodríguez et al., 2011; Kroonenberg, 2019) and have been linked to the Cauaburi and Querarí orogenies (1.86–1.72 Ga; Almeida et al.,2013, 2022; Kroonenberg, 2019) or alternatively to the Atabapo and Vaupés cycles (Cordani et al., 2016). Proterozoic basement is unconformably overlain by Mesoproterozo-ic low–grade metamorphic rocks (Serranía del Naquén; Gómez et al., 2023; Kroonenberg, 2019) and by thick Mesoproterozoic–Mesozoic marine successions exposed in plateaus such as Chiribiquete or known from subsurface datasets (Dueñas–Jiménez & Montalvo–Jónsson, 2020; Dueñas–Jiménez et al., 2020). Westward, Cenozoic Andean basin fills blanket much of the region. The Amazonian and Llanero Border Fault Systems separate cratonic and Andean domains (Figures 1, 2).

La Guajira Peninsula
Caribbean Sea
Pacific Ocean
Barranquilla
Caracas
Panamá
Medellín
Bogotá
Cali
Quito
Venezuela
Colombia
Brazil
Peru
Guiana Shield
Western Cordillera
Central Cordillera
Eastern Cordillera
Pacific coastal plain
Cesar River
Atrato River
Cauca River
Magdalena River
Meta River
Orinoco River
Guaviare River
Caquetá River
Putumayo River
Amazonas River
68° W
70° W
72° W
74° W
76° W
78° W
12° N
10° N
8° N
6° N
4° N
2° N
0°
2° S
4° S
1
2
3
4
5
6
7
8
9
10
11
12
13
14
15
16
17
River
City
0
200 km
-8000
-6000
-4000
-2000
0
2000
4000 m a. s. l.

Figure 2. Physiographic map of the northwestern corner of South America. The geographic features mentioned in the paper are indicated and numbered as follows: (1) Serranía de Jarara, (2) Serranía de Macuira, (3) Serranía de Carpintero, (4) Serranía de Cocinas, (5) Sierra Nevada de Santa Marta, (6) Serranía del Baudó, (7) Serranía del Naquén, (8) Serranía del Chiribiquete, (9) Macarena Massif, (10) Santander Massif, (11) San Lucas Massif, (12) Las Minas Massif, (13) Floresta Massif, (14) Quetame Massif, (15) Serranía del Perijá, (16) Plato Basin, and (17) San Jorge Basin. The features are numbered according to the order in which they are mentioned in the paper (modified from Gómez et al. 2020).

Proterozoic crystalline inliers (migmatites and granulites of Mesoproterozoic–Neoproterozoic age) occur as fault–bounded blocks in the Macarena Massif, Guajira, Sier-ra Nevada de Santa Marta, Santander Massif, and Central Cordillera (San Lucas and Las Minas) (Ibañez–Mejía, 2020; Kroonenberg, 2019) (Figure 3). They record Grenvillian–Rodinia assembly metamorphism (1300–900 Ma; Li et al., 2008) and later overprints in places; for example, the Santander Massif preserves protolith ages <1.71 Ga, Grenvillian metamorphism (~1.1 Ga), and superposed Ordovician metamorphism (Cordani et al., 2005; Ordóñez–Carmona et al., 2006; van der Lelij et al., 2016; Zuluaga et al., 2017).

2.3 Famatinian Orogeny (sensu Ramos 2018)

Opening of the Iapetus Ocean (~570–535 Ma) established Gondwana's western margin, which became an active convergent boundary by ~500–480 Ma and has remained so in broad terms (Cawood et al., 2001; Pankhurst et al., 2000; van der Lelij, 2013). This early Paleozoic event is generally interpreted as accretionary orogenesis rather than continent–continent collision (van Staal & Hatcher, 2010). In Colombia, Ordovician metamorphism and local migmatization are preserved in the Santander, Floresta, and Quetame massifs (Forero, 1990; Restrepo-Pace, 1995; van der Lelij et al., 2016; Zuluaga et al., 2017) (Figure 3). Ordovician marine strata in adjacent basins were later overlain by Devonian–Carboniferous sequences following mid–Paleozoic collapse (Moreno–Sánchez et al., 2020).

2.4 The assembly and subsequent breakup of Pangaea

U–Pb data (ca. 333 and 300 Ma) support a Carboniferous arc along the eastern Central Cordillera and the Lower Magdalena Valley, likely tied to terminal Rheic closure during Gondwana–Laurasia collision (Leal–Mejía, 2011; Silva–Arias et al., 2016; Rodríguez et al., 2022; Zapata–Cardona et al., 2023). After Pangaea assembly (Blakey, 2003), widespread magmatism and metamorphism affected the NW South American margin between ~290 and 240 Ma. Remnants of a Permian arc occur in blocks within the Sierra Nevada de San-ta Marta, near the Ibagué Fault Zone, and across northern Colombia–Venezuela (Dasch, 1982; Viscarret et al., 2009; van der Lelij, 2013) (Figure 3). This arc has been modeled above an east–dipping subduction zone and may connect to the Permian belt of southern Mexico (Cochrane et al., 2014a, 2014b; Spikings et al., 2015).

Triassic metamorphic and igneous rocks—cf. especially the Cajamarca Complex in An-tioquia—record an anatexis event around 255–250 Ma that marks the waning of the Per-mian arc (Maya & González, 1995; Cardona et al., 2010) (Figure 3), with correlative sig-nals in Mexico and Peru (Weber et al., 2007; Mišković et al., 2009). Subsequently, Triassic peraluminous (S–type) plutonism indicates extension and rifting, with enhanced melting of pelitic sources, plausibly driven by mafic underplating (Spikings et al., 2015; Cochrane et al., 2014a). This phase is linked to early western Pangaea breakup and rapid transition from rifting to drifting within ~20–25 My, consistent with associated ophiolite develop-ment (Vinasco et al., 2006; Martínez, 2007; Cochrane et al., 2014a; Spikings et al., 2015; Spikings & Paul, 2019). Regional comparisons suggest contrasting stress regimes along the margin (compression in Mexico vs. limited compression in Peru), implying more pro-nounced terrane accretion in ancestral Central America than along much of western Gondwana (Weber et al., 2007; Mišković et al., 2009; Ramos & Aleman, 2000; Ramos, 2008; Cochrane et al., 2014a).

2.5 Mesozoic arc migration and basin development (Late Triassic–Early Cretaceous)

Following Triassic extension, two major continental arc phases are recognized: a Late Triassic–Jurassic high–K calc–alkaline arc (210–180 Ma) and an Early Cretaceous tholeiitic to primitive arc (130–115 Ma; Quebradagrande). Both unfolded during Pangaea breakup, including Central Atlantic opening (~200–180 Ma) and rift–drift transition between North America and Africa (~200 Ma), as well as Tethyan rifting in NW South America (Withjack et al., 1998; Fourcade et al., 1990; Bortolotti & Principi, 2005; Peace et al., 2020). The Ear-ly Cretaceous episode overlaps the South Atlantic opening (~140–104 Ma; Heine et al., 2013). Jurassic granitoids are widespread in the eastern Central Cordillera, Santander Massif, Sierra Nevada de Santa Marta, and Guajira, consistent with a long-lived arc system (Bustamante et al., 2016; Cochrane et al., 2014b; López–Isaza & Zuluaga, 2020; Bayona et al., 2020; Rodríguez-García et al., 2020) (Figure 3). Jurassic volcaniclastic successions in-clude syn–extensional deposits in the Eastern Cordillera that were later overlain by the well–known Cretaceous marine succession (Mojica & Dorado, 1987; Sarmiento–Rojas, 2019). Isotopic trends (more juvenile Nd–Hf westward in younger intrusions) and basin–axis volcaniclastic records support an extensional setting and a low–relief orogen with the arc in an intra–arc basin (Spikings et al., 2015; Zuluaga et al., 2015). A broad Jurassic thermal imprint also produced low–grade metamorphism in Early Devonian strata and locally overprinted Ordovician basement under low–pressure conditions (Zuluaga et al., 2017; Zuluaga & López, 2019).

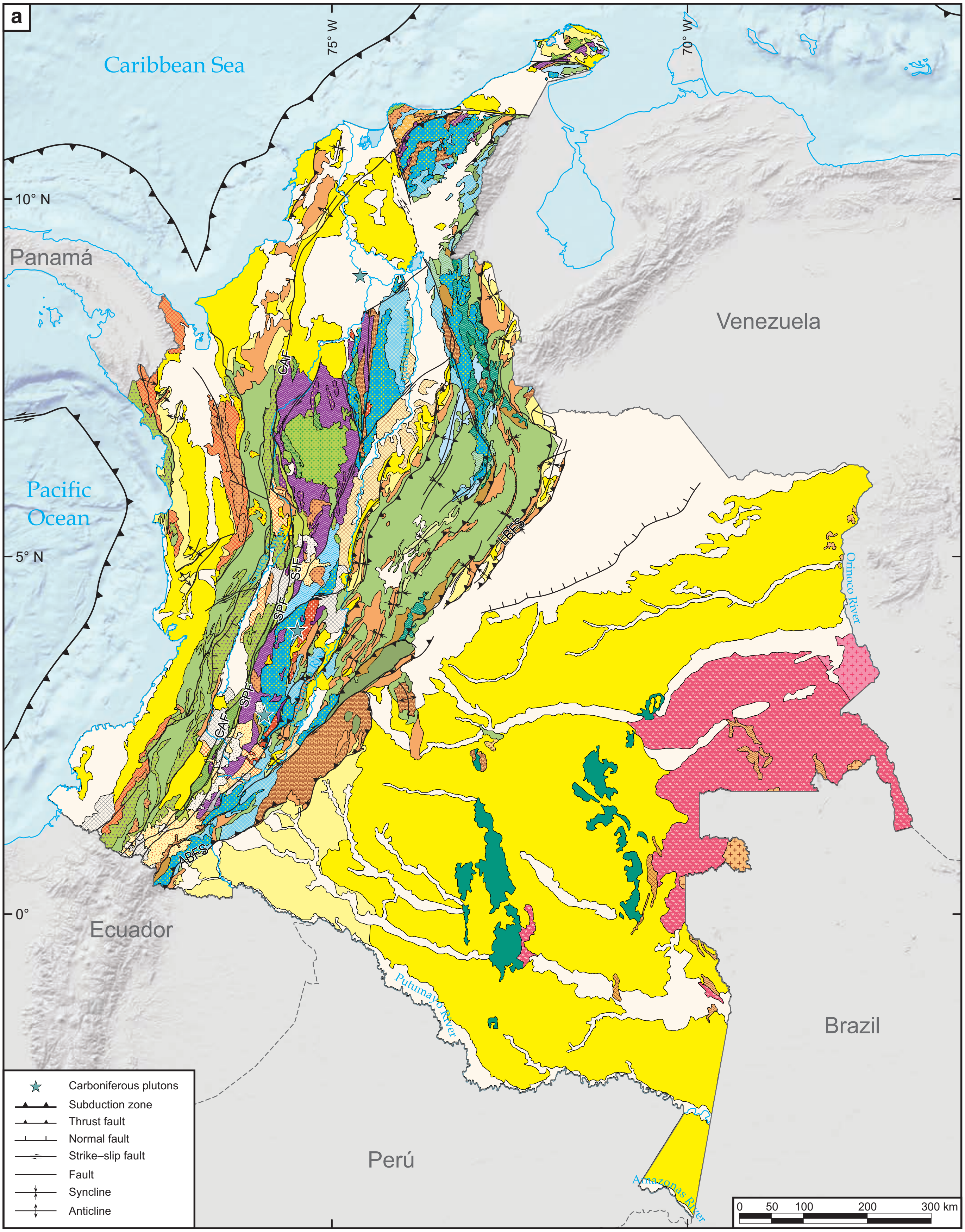
a
Caribbean Sea
75° W
70° W
10° N
5° N
0°
Panamá
Pacific Ocean
Venezuela
Ecuador
Brazil
Perú
CAF
SJF
SPF
LBFS
APFS
Orinoco River
Putumayo River
Amazonas River
Carboniferous plutons
Subduction zone
Thrust fault
Normal fault
Strike–slip fault
Fault
Syncline
Anticline
0 50 100 200 300 km

Figure 3. (a) Geological map of Colombia, simplified from Gómez et al. (2023). **(b)** Legend of the map. CAF: Cauca–Almaguer Fault; SPF: Silvia–Pijao Fault; SJF: San Jerónimo Fault.

The Quebradagrande Complex comprises a 145–112 Ma volcano–sedimentary package with low–grade metamorphic overprint (Maya & González, 1995; Nivia et al., 2006; Vi-llagómez et al., 2011; Cochrane, 2013). Competing interpretations exist (oceanic vs. conti-nental arc vs. marginal basin), but combined datasets favor arc migration oceanward above the same east–dipping subduction system after the Jurassic (Spikings et al., 2015). Continued extension generated back–arc basins later incorporated into the Eastern Cordil-lera and filled with thick Cretaceous marine deposits reaching into Guajira (Toussaint & Restrepo, 1994; Cooper et al., 1995; Sarmiento–Rojas et al., 2006; Pindell & Kennan, 2009; Vásquez et al., 2010). New U–Pb constraints from the Cajamarca Complex east of the Palestina Fault suggest Jurassic or Early Cretaceous metamorphism? (167–137 Ma) in some sectors, differing from Triassic ages farther north (Bustamante, 2016; Naranjo et al., 2018; Pindell et al., 2020) (Figure 3).

2.6 Plateau collisions and terrane accretion

The Quebradagrande Complex is bounded eastward by Cajamarca and westward by Sil-via–Pijao Fault from the Arquía Complex, which interpreted as a former subduction chan-nel later modified by thrusting (Bustamante & Bustamante, 2019), Figure 3. The Arquía Complex includes blocks of low– to medium–grade rocks, localized high–pressure assem-blages, serpentinites, and granitoids and correlated with Ecuador's Raspas Complex. High–pressure metamorphism is commonly dated at ~130–120 Ma (Arculus et al., 1999; John et al., 2010; Bustamante et al., 2012; García–Ramírez et al., 2017). Cooling ages span ~110–125 to 70–60 Ma in Arquía and ~129–123 to 85–60 Ma in Raspas (Restrepo & Toussaint, 1976; Toussaint & Restrepo, 1978; Brook, 1984; Bustamante et al., 2011; Bosch et al., 2002; Spikings et al., 2005).

West of the Cauca–Almaguer Fault, the Western Cordillera and the Chocó–Panamá block contain ophiolitic fragments with metasediments, thick metabasalts, and ultramafic roots (Barrero, 1979; Bourgois et al., 1982; Kerr et al., 1997; Ariza–Acero et al., 2022). These sequences are widely interpreted as hotspot–formed oceanic plateau crust (99–86 Ma) accreted to the margin and linked to the Colombian–Caribbean Large Igneous Province (CLIP) (Kerr et al., 1997; Vallejo et al., 2006; Villagómez et al., 2011; Ariza-Acero et al., 2022). An intraoceanic arc (98–89 Ma; e.g., Buga and Santa Fe batholiths, Altamira Gab-bro) developed within the plateau prior to accretion (Villagómez et al., 2011; Weber et al., 2015; Zapata–Villada et al., 2017), Figure 3. Two key accretionary stages are com-monly recognized: Late Cretaceous (~75 Ma) accretion along the Cauca–Almaguer Fault with westward trench migration to near the modern position, and Oligocene–Early Mio-cene (<28 Ma) collision of the Chocó–Panamá block, followed by rapid Middle Miocene uplift supported by detrital zircon, thermochronology, and foraminiferal biostratigraphy (Duque–Caro, 1990; Farris et al., 2011; Montes et al., 2012, 2015; Spikings et al., 2015; Ariza–Acero et al., 2022).

2.7 Late Cretaceous–Eocene arcs, metamorphism, and Andean pulses

Late Cretaceous arc magmatism (100–75 Ma) in the Central Cordillera is represented by large plutonic bodies such as the Antioquia and Córdoba batholiths (Ibañez–Mejía et al., 2007; Ordóñez–Carmona et al., 2008; Leal–Mejía, 2011; Villagómez et al., 2011). A younger Paleocene–Eocene calc–alkaline arc is documented by U–Pb zircon ages and may have been segmented and spatially diffuse, potentially reflecting shallow subduction fol-lowing CLIP collision and subduction of thickened oceanic plateau crust (Bayona et al., 2012; Cardona et al., 2014; Bustamante et al., 2017; Leal–Mejia, 2011), see Figure 3.

Oblique Caribbean–South American convergence from the Late Cretaceous to early Eo-cene promoted continental growth along the NW margin, especially in the Sierra Nevada de Santa Marta and Guajira (James, 2000). This Caribbean orogenic phase produced low– to medium–grade metamorphism in Mesozoic sedimentary sequences now exposed in the Caribbean Mountain System, and the Santa Marta metamorphic belt has been linked to low–angle underthrusting of the Caribbean plate beneath South America (Tschanz et al., 1974; Restrepo–Pace et al., 1997; Zuluaga and Stowell, 2012).

The Andean Orogeny in Colombia is commonly placed as initiating in the Late Cretaceous and evolving through diachronous Paleogene–Neogene pulses of deformation, uplift, and exhumation (Horton et al., 2020; Mora et al., 2020; Cardona et al. 2020). The Western Cordillera largely reflects Late Cretaceous CLIP accretion, crustal thickening, uplift, and establishment of a new margin farther west (Spikings et al., 2005, 2015; Villagómez & Spikings, 2013). The Central Cordillera preserves Jurassic arc roots overprinted by Late Cretaceous–Paleogene magmatism, including Antioquia Batholith emplacement north of ~5°N, whereas active volcanism dominates south of this latitude (Leal–Mejía, 2011; Vil-lagómez & Spikings, 2013; Marín–Cerón et al., 2019), see Figure 3. In the Eastern Cordille-ra, deformation began in the Eocene with inversion of Mesozoic extensional basins, but major shortening and exhumation occurred in Middle–Late Miocene through Pliocene–Pleistocene time (Mora et al., 2020; Bayona et al., 2021; Gómez et al., 2005; Mora et al., 2008; Parra et al., 2009a, b). The Santander Massif experienced earlier rapid exhumation in late Oligocene–Early Miocene time, emphasizing along–strike diachroneity (Amaya et al., 2017, 2020; Velandia et al., 2021; Villamizar–Escalante et al., 2024).

These tectonic phases strongly controlled adjacent basin fills: eastern Colombia records a transition from Cretaceous shallow–marine mudstone–sandstone–carbonate systems to Paleogene–Neogene coarse continental fluvial, lacustrine, and deltaic deposits, consistent with increasing relief and erosional unroofing of crystalline rocks (Horton et al., 2020; Mora et al., 2020; Gómez et al., 2023).

2.8 Modern configuration and active volcanism

The present–day configuration of northwestern South America reflects ongoing subduction of the Nazca Plate beneath South America, interaction with the Caribbean Plate, and collision of the Panama–Chocó Block at a complex triple-junction scale (Figure 1). South of the Caldas Tear, the Nazca Plate subducts at angles greater than ~25°, feeding the active Colombian volcanic arc (Vargas & Mann, 2013; González et al., 2023). Geodetic data indicate an ENE–-directed Nazca Plate motion of ~53–55 mm/yr, NE–directed motion of the Northern Andes of ~9 mm/yr, and eastward collision of the Panama Arc at ~15–18 mm/yr (Mora–Páez et al., 2019). The modern volcanic arc is dominated by large polygenetic volcanoes with geochemical and isotopic signatures consistent with subduction–related magmatism and generally limited crustal assimilation (James & Murcia, 1984; Faure, 2013).

In the Colombian Andes, volcanoes currently considered active are large polygenetic edifices distributed in three main segments: the northern and central segments, separated by a 265 km volcanic gap and located along the crest of the Central Cordillera, and the southern segment, which is situated within the Cauca–Patía Depression and the Western Cordillera (Figure 4). Compositionally, volcanic products range from basaltic andesites to andesites and dacites. Magma generation has been attributed to a combination of processes, including mantle melting, slab–fluid—induced metasomatism of the mantle wedge, crustal contamination, magma mixing, and fractional crystallization.

Systematic study of active volcanoes in Colombia began in 1985 with continuous monitoring by the Servicio Geológico Colombiano, complemented by stratigraphic and eruptive–history reconstructions. Several volcanoes have documented historical activity, including Nevado del Ruiz, Puracé, Doña Juana, and Galeras. In recent decades, eruptive activity has occurred at Nevado del Ruiz, Galeras, and the northwestern sector of the Coconucos Volcanic Chain (including Puracé), while other volcanoes have shown signs of reactivation, such as Cerro Machín, Chiles–Cerro Negro, and Sotará.

The area visited during this excursion (Tolima Department) lies within the distal influence zone of Cerro Machín and Nevado del Ruiz volcanoes, both located in the northern volcanic segment. Cerro Machín Volcano, situated in the Central Cordillera south of the northern volcanic segment (Figure 4), is considered one of the most dangerous volcanoes in Colombia due to its highly explosive behavior, large–magnitude eruptions—mainly Plinian–type dacitic eruptions—and proximity to major population centers. Nevado del Ruiz Volcano is infamous for the catastrophic eruption of 13 November 1985, which devastated the town of Armero, located approximately 45 km east of the volcano. Monogenetic volcanoes identified in recent years near the city of Ibagué will also be observed during the excursion.

Holocene eruptions of Cerro Machín Volcano have generated pyroclastic flows and surges, fallout deposits, and dome emplacement and destruction (Cepeda et al., 1995; Rueda, 2000; Méndez, 2001; Murcia et al., 2010; Laeger et al., 2013). These deposits constitute the geological record and eruptive history of the volcano and are correlated with lahar deposits that have traveled distances exceeding 100 km along the Coello and Magdalena rivers. Such lahars have devastated and inundated large areas, leading to the formation of extensive terraces and coalescing alluvial fans (Cortés, 2001a, b; Murcia et al., 2008). Numerous population centers in the departments of Tolima and Cundinamarca are built on lahar deposits, where intensive agricultural activity, industrial development, and extraction of construction materials occur, making this region of significant economic importance to Colombia (Navarro et al., 2011). Lahars represent one of the greatest volcanic hazards associated with Cerro Machín Volcano (Cortés, 2001a; Méndez et al., 2002). Along the Chicoral variant, sequences of lahar deposits—including debris flows and hyperconcentrated flow deposits of different ages—are well exposed and can be examined in the field.

3. Itinerary

3.1 Day one, Stop 1

Upper Cretaceous and Overturned Anticline
74° 33’ 59.6” W; 4° 15’ 60.0” N
650 m.a.s.l.

After descending past the Chinauta toll station, a ridge composed of rocks of the Guadalupe Formation (Campanian–Maastrichtian) can be observed when looking toward the northwest. These strata strike approximately NE and dip more than 50° to the SE (Figure 5). The abrupt change in slope and topography marks the contact between the Guadalupe Group and the Guaduas Formation. It is important to note that the transition from marine to continental environments occurs through tidal deposits at the base of the Guaduas Formation (Maastrichtian).

The Guadalupe Group (Hubach, 1931, 1957; redefined by Renzoni, 1962) is composed of three formations. The basal unit is the Arenisca Dura Formation, represented by thick-bedded quartz sandstones with occasional interbeds of mudstone in medium to thick layers. A characteristic porcelanite horizon occurs in the lower to middle part of the sequence and constitutes the host unit for phosphorites. The Plaeners Formation consists of mudstones rich in benthic foraminifera, alternating with packages of chert, whereas the Arenisca Tierna Formation is composed of friable quartz sandstones arranged in very thick beds. Reported ages indicate that the Arenisca Dura Formation is early Campanian, the Plaeners Formation is late Campanian, and the Arenisca Tierna Formation is Maastrichtian. These units were deposited in littoral to sublittoral environments, associated with intertidal plains.

The Guaduas Formation (Hettner, 1892, in De Porta, 1974) is an argillaceous–sandy sequence containing coal seams throughout the succession; economically exploitable seams are located in the lower part, below the marker horizon known as the Arenisca La Guía. Sarmiento (1994) reported a thickness of approximately 1100 m for this unit. The assigned age ranges from late Maastrichtian to early Paleocene. The Guaduas Formation was deposited in a coastal plain that evolved into swamps and lakes connected to the sea, ultimately grading into low coastal plains dominated by meandering rivers.

Looking toward the west, a narrow V–shaped valley carved by the Sumapaz River can be observed. From this point to the next stop, the road follows this narrow valley, allowing observation of a stratigraphic section of the Guadalupe Group repeated by two west-verging thrust faults.

Along the valley, repeated sections of the Guadalupe Group can be recognized, displaying its characteristic lithologies: Arenisca Tierna, Arenisca de Labor, Plaeners, and Arenisca Dura (or Raizal). Beneath the latter sandstone, centimeter–thick layers of siliceous mudstone are observed. This is the last locality where the typical stratigraphy of the Guadalupe Group, as recognized in the Bogotá Savanna, can be observed.

At this site of the stop, a well developed overtuned anticlinal

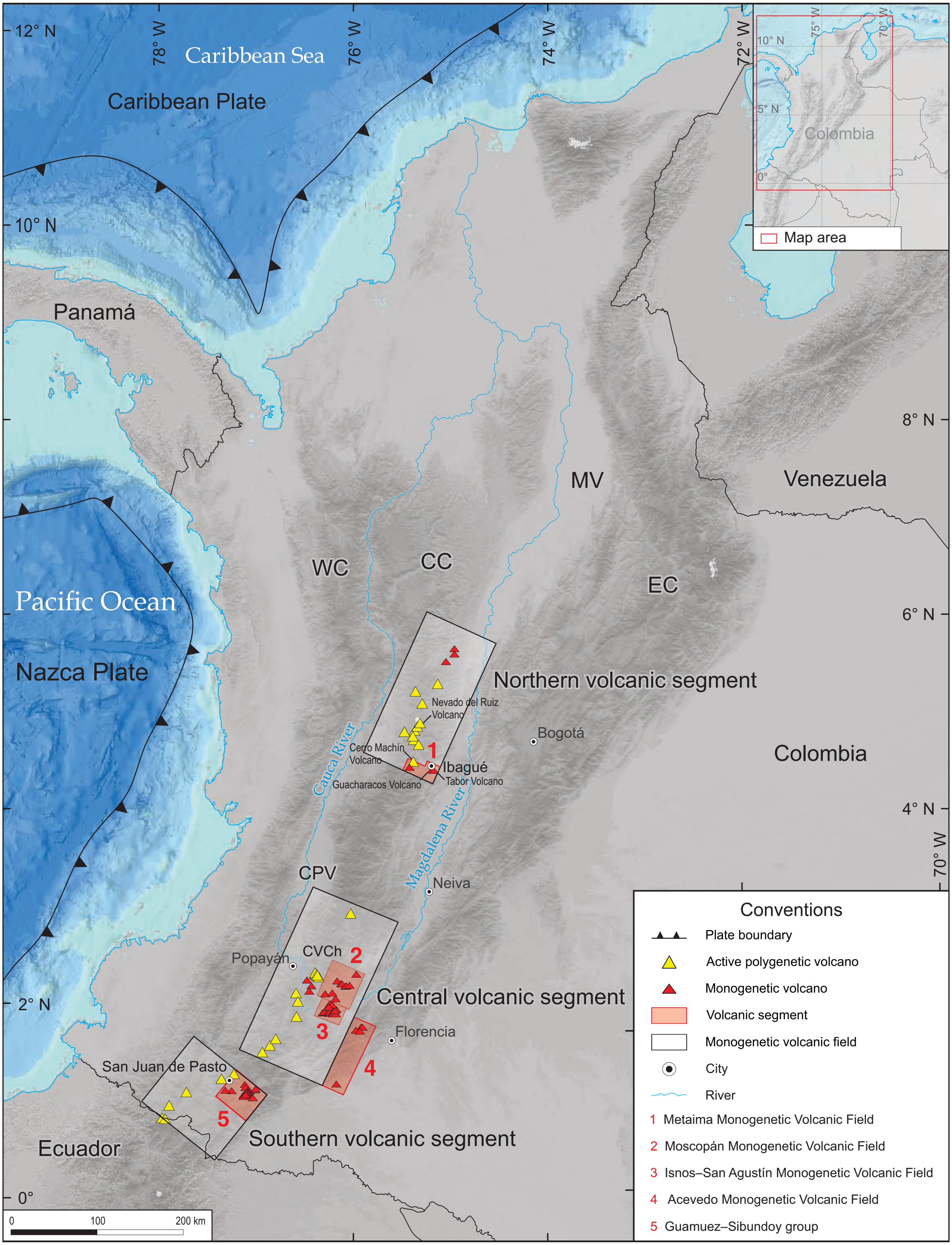

Caribbean Sea
Caribbean Plate
Panamá
Pacific Ocean
Nazca Plate
Ecuador
Venezuela
Colombia
WC
CC
EC
MV
CPV
CVCh
Northern volcanic segment
Central volcanic segment
Southern volcanic segment
Nevado del Ruiz Volcano
Cerro Machín Volcano
Guacharacos Volcano
Tabor Volcano
Ibagué
Bogotá
Neiva
Popayán
Florencia
San Juan de Pasto
Cauca River
Magdalena River
12° N
10° N
8° N
6° N
4° N
2° N
0°
78° W
76° W
74° W
72° W
70° W
75° W
10° N
5° N
0°
Colombia
Map area
0
100
200 km
Conventions
Plate boundary
Active polygenetic volcano
Monogenetic volcano
Volcanic segment
Monogenetic volcanic field
City
River
1 Metaima Monogenetic Volcanic Field
2 Moscopán Monogenetic Volcanic Field
3 Isnos–San Agustín Monogenetic Volcanic Field
4 Acevedo Monogenetic Volcanic Field
5 Guamuez–Sibundoy group

Figure 4. Map of Colombia showing the Quaternary active polygenetic volcanoes and monogenetic volcanic fields. WC: Western Cordillera; CC: Central Cordillera; EC: Eastern Cordillera; MV: Magdalena Valley; CPV = Cauca–Patía Valley (adapted from Gómez et al. 2023).

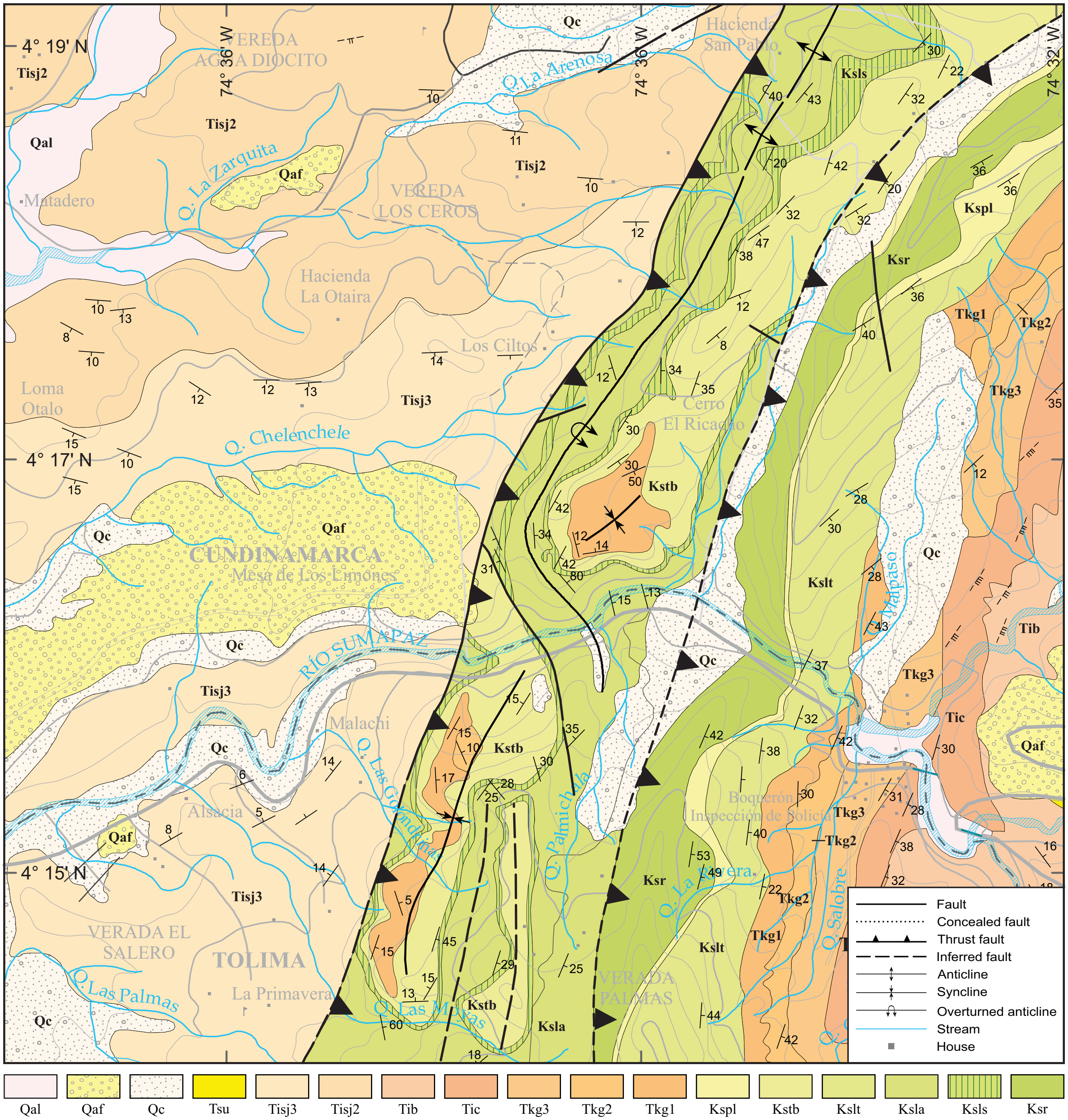

Figure 5. Geological map of the Boqueron area (after Etayo–Serna, 2001). Lithological units are listed and labeled according to their stratigraphic position, from youngest to oldest, as follows: Tsu: Usme Formation; Tisj3: San Juan de Rioseco Formation, conglomerates; Tisj2: San Juan de Rioseco Formation, claystones and sandstones; Tisj1: San Juan de Rioseco Formation, lidite-fragment breccia; Tib: Bogotá Formation, claystone with interbeds of sandstone; Tic: Cacho Formation, sandstones; TKg: Guaduas Formation; TKg1: Guaduas Formation, claystones; TKg2: Guaduas Formation, sandstones, claystones, and coal beds; TKg3: Guaduas Formation, claystone with interbeds of sandstone; Kstb: La Tabla and Buscavida formations; Kspl: Plaeners Formation, mudstone, siltstone, and chert; Kslt: Tierna–Labor Formation, sandstones; Ksla: beds composed of mudstone and sandstone; Ksls: Lidita Superior Formation; Ksr: Raizal Formation, sandstones.

Figure 6. Structural view of an overturned anticline in Upper Cretaceous sandstones, Boquerón area, Eastern Cordillera (eastern flank).

structure involving sandstones of the Guadalupe Group is exposed (Figure 6). This structure was likely formed by fault–propagation folding. It is noteworthy that a few kilometers south of this locality, within similar structures, lies the Guando oil field.

Continuing westward toward the next stop, a fault breccia zone is encountered, produced by the westernmost thrust fault in this sector.

Upon exiting this narrow valley, lithic sandstones and red beds of Paleogene age crop out. These sediments were deposited in small piggyback basins developed between two major thrust faults. The deposits are interpreted as synkinematic and represent an excellent example of growth strata.

3.2 Stop 2

Holocene Volcán Machín´s Lahars.
Espinal-Ibagué Highway
74° 54’ 43.895” W; 4° 13’ 58.951” N
343 m.a.s.l.

The so–called Chicoral Debris Flow forms terraces 3–20 m thick along the Coello and Magdalena rivers and extends up to 109 km from its source area. The deposit covers a minimum area of 62 km^2, with an estimated minimum volume of 0.57 km^3, and comprises two dacite–rich units. Radiocarbon dating suggests that this lahar is related to the eruption known as El Guaico, dated at 2550 ± 70 yr BP (Méndez, 2001), which produced a block–and–ash flow that filled the Toche River valley approximately 5 km from the volcano. Subsequent remobilization of this material by water generated debris flows that traveled 91 km along the Toche and Coello rivers (Figure 7), crossed the Espinal Fan, entered the Magdalena River, and continued a further 18 km upstream (Murcia et al., 2008).

Figure 7. Panoramic view of the morphology produced by the Chicoral Debris Flow deposit, showing a flat, non–dissected surface and the characteristic vertical walls of the deposit, on the right bank of the Coello River (Gualanday sector).

3.2.1 Description of Stop 2

At this stop, located along the access road to the Pavimentos Colombia company, the stratigraphic relationship between three lahar–deposit units can be observed: the Guamo and Espinal Hyperconcentrated–Flow deposits, and the Chicoral Debris–Flow deposits (Cortés, 2001a, b). This exposure also allows observation of the processes and dynamics that occurred between these lahar–generating events (Figure 8). The outcrop summarizes much of the lahar stratigraphy that is widely distributed across the area and that gave rise to the Guamo and Espinal alluvial fans, where some of the most important rice-producing regions in Colombia are located.

Navarro et al. (2011) describe the sequence exposed at this stop as follows:

> The basal unit corresponds to the Guamo Hyperconcentrated Flow

Figure 8. Stratigraphic sequence of lahar deposits from Cerro Machín Volcano exposed on the right bank of the Coello River, at a road cut along the access road to the Pavimentos Colombia facilities. The sequence includes the Guamo and El Espinal Hyperconcentrated–Flow deposits, a paleosol dated at ~2,500 yr BP, and an overlying Chicoral Debris–Flow deposit (photo from Navarro et al., 2011).

> deposit, dated at 4360 ± 105 yr BP. This unit is characterized by its wide areal distribution and an average thickness of approximately 20 m. The deposit comprises several hyperconcentrated-flow units of gray coloration, with a massive to pseudo-stratified appearance. It is heterolithic, vesicular, and matrix-supported by fine- to medium-grained sand, and contains abundant subrounded white pumice clasts up to 30 cm in diameter. Subangular lithic clasts of dacitic lavas and schists occur in lesser proportions, ranging in size from fine gravel to several tens of centimeters. Dacitic lava clasts vary in color from gray to reddish, whereas schist clasts are typically black to green. The presence of pumice lenses is also characteristic of this unit. The matrix is composed of crystal fragments and pumice, together with lithic fragments of dacitic lava and schist. The crystals are euhedral and consist predominantly of biotite, hornblende, plagioclase, and quartz.

The Guamo Hyperconcentrated Flow is regarded as the largest–magnitude lahar deposit generated by Cerro Machín Volcano (CMV), covering an approximate area of 1,009 km^2 and having a minimum estimated volume of 20.18 km^3 (Cortés, 2001a, b). At the outcrop, the Guamo sequence is partially eroded and overlain by a greenish–gray silty unit interpreted as lacustrine in origin, indicating the development of a low–energy depositional environment within the Guamo deposit. Thin interbedded sandy layers record temporary changes in depositional conditions.

Overlying the lacustrine unit, across an erosional contact and following a channelized topography, the Espinal Hyperconcentrated–Flow deposit (3136–3618 yr BP) is exposed. This unit is characterized by its relatively small thickness (averaging ~2 m throughout the area), wide spatial distribution, and geomorphic expression as the Espinal Fan. The fan covers an approximate area of 294 km^2 and has a minimum estimated volume of 1.35 km^3. The deposit is beige in color, massive, and matrix–supported by fine sand, containing predominantly subrounded, low–density pumice clasts; dark gray vitreous lithic clasts occur sporadically. The matrix is composed mainly of crystals of biotite, hornblende, plagioclase, and quartz (Cortés, 2001b).

This unit is overlain by a ~40–cm–thick brown, crystalline, indurated paleosol, which represents a significant period of volcanic quiescence. Subsequently, the Chicoral Debris Flow was emplaced, including a basal sole layer approximately 30 cm thick that marks the onset of a new lahar–generating episode associated with CMV. The Chicoral Debris Flow originated from the remobilization of a block–and–ash pyroclastic–flow deposit related to the collapse and destruction of dacitic domes that obstructed the volcanic crater.

The Chicoral deposit is characterized by the formation of terraces with flat, undissected surfaces and steep vertical scarps (Figure 7). These terraces are discontinuously distributed along the margins of the Coello and Magdalena rivers, extending as far as the town of Nariño (Cundinamarca), located approximately 113 km from the CMV edifice. The deposit is massive, gray in color, heterolithic, vesicular, indurated, and matrix–supported by sand. It is composed mainly of subangular to subrounded clasts of porphyritic dacitic lava with gray to reddish coloration, together with accidental clasts incorporated from the river and stream channels. The matrix consists of lithic fragments of similar composition to the clasts, along with crystals of biotite, amphibole, plagioclase, and quartz.

Radiocarbon dating of paleosols underlying and overlying the Chicoral deposit constrains its relative age to between 2505 ± 65 and 1640 ± 45 yr BP (Cortés, 2001a, b; Hurtado & Murcia, 2003; Murcia et al., 2008).

3.3 Stop 3

Chicoral Group (Eocene molase).
Espinal–Ibagué Highway
74° 58’ 31.879” W; 4° 13’ 24.949” N
434 m.a.s.l.

3.3.1 Description of Stop 3

At this stop, rocks of the Chicoral Formation (sensu Laverde, 1989), belonging to the Gualanday Group, are exposed. The formation is composed of tabular to lenticular beds of clast-supported conglomerates, moderately sorted, with clast sizes ranging from pebbles to small cobbles (predominantly 5–6 cm in diameter). Clasts are subrounded to well–rounded, and chert is the dominant lithology (approximately 70%), accompanied by siliceous mudstone clasts. The matrix consists of medium-grained quartz sand with subordinate chert lithic fragments (Figure 9).

Within the chert and siliceous mudstone clasts, molds of foraminifera derived from the Oliní Group can be observed.

The conglomerate bedding strikes N58°E and dips 60°W. This outcrop is located on the eastern flank of the Gualanday

Figure 9. Conglomerate of the Chicoral Formation. The clasts are predominantly composed of chert and siliceous siltstones derived from the erosion of Upper Cretaceous geological units of the Upper Magdalena Valley.

Syncline (Figure 10). Within the exposure, small fault planes associated with hydrocarbon seepage are observed; these structures strike N64°W, dip 55°W, and display slickenside lineations with a pitch of 33° toward the southwest.

Figure 10. Tectonosedimentary model illustrating the accumulation of sediments of the Chicoral and Potrerillo formations (after Caicedo & Roncancio, 1994).

The accumulation of the sediments of the Gualanday Group has been related to the uplift of the Central Cordillera (van Houten & Travis, 1968; Anderson, 1972). These deposits correspond to alluvial environments, including alluvial fans, braided river systems, and floodplains, and are associated with the development of a thrust system with southeastward vergence and tectonic transport affecting the western sector of the Upper Magdalena Valley. Two main thrusting pulses are recorded within the deposits of the three formations of the Gualanday Group (Caicedo & Roncancio, 1994).

The first tectonic pulse occurred nearly contemporaneously with the accumulation of the Chicoral Formation. During this episode, a mountain front developed as a result of folding of the hanging-wall units, exposing Upper Cretaceous rocks to erosion and leading to the dismantling of the stratigraphic section at least down to the Lower Lidite Formation of the Oliní Group by the late Eocene (Figure 11). Adjacent to the mountain front, alluvial fans were formed; in proximal sectors these deposits rest unconformably on Cretaceous units, whereas toward more distal areas the contact becomes progressively conformable (Caicedo & Roncancio, 1994).

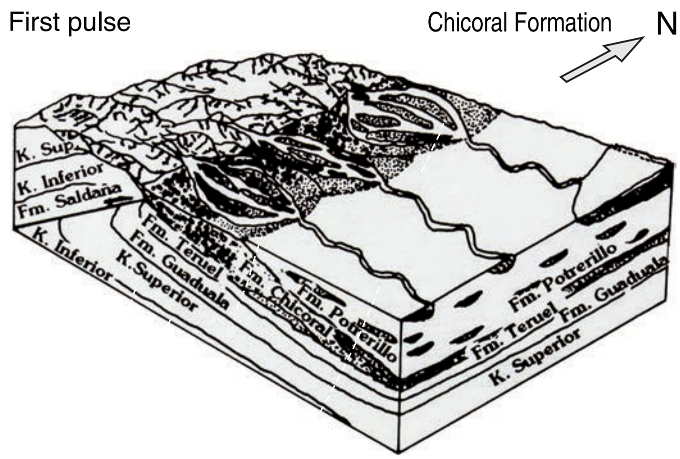

Figure 11. Tectonosedimentary model showing the depositional evolution of the Chicoral and Potrerillo formations during their accumulation (after Caicedo & Roncancio, 1994).

The second tectonic pulse represents a rejuvenation or reactivation of the first event and resulted in the accumulation of the upper units of the Gualanday Group (Potrerillos and Doima formations). These sediments were deposited in alluvial fan environments and braided river systems (Caicedo & Roncancio, 1994).

3.3.2 Panoramic view of the Ibagué, Guamo, and Espinal alluvial fans

At this stop, the group will ascend to the second bench of the slope, from where the spatial relationships among the Ibagué, Guamo, and Espinal alluvial fans can be clearly observed (Figure 11). The Ibagué Fan, of Pleistocene age, is composed of lahar deposits derived from Nevado del Tolima Volcano that were ponded against the barrier formed by the Gualanday Group (figures 12 and 13). At that time, the ancestral Coello River drained southward through a valley developed along the Potrerillo Formation—an argillaceous unit of the Gualanday Group (Figure 12).

With the onset of activity at Cerro Machín Volcano, lahars reached the Payandé corregimiento in the municipality of San Luis and were subsequently channelized along the Coello River valley, flowing southward. At the latitude of San Luis, these flows were diverted eastward toward the Magdalena Valley, leading to the formation of the Guamo Fan (Figure 12).

Later, as sedimentation progressively filled the ancestral

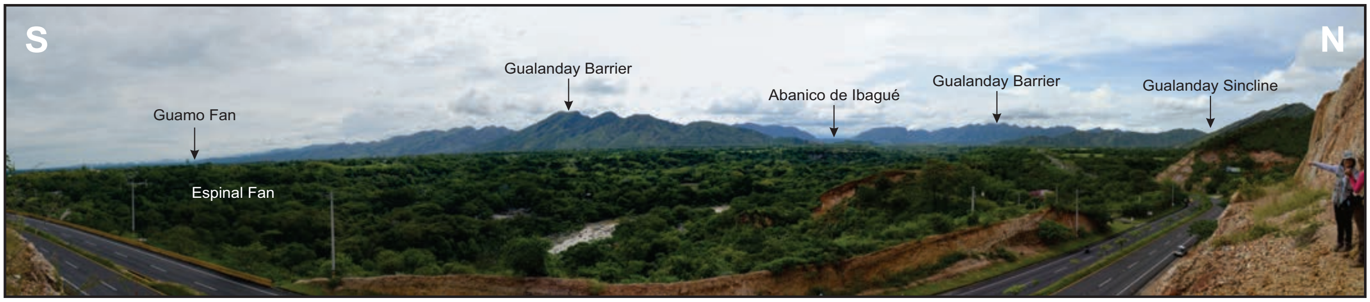

Figure 12. Panoramic view showing the Espinal Fan in the foreground; the Ibagué Fan visible in the background at the location where the Coello River breached the Gualanday Barrier. The apex of the Guamo Fan is visible on the left.

Coello River drained southward through a valley developed along the Potrerillo Formation—an argillaceous unit of the Gualanday Group (Figure 12).

With the onset of activity at Cerro Machín Volcano, lahars reached the Payandé corregimiento in the municipality of San Luis and were subsequently channelized along the Coello River valley, flowing southward. At the latitude of San Luis, these flows were diverted eastward toward the Magdalena Valley, leading to the formation of the Guamo Fan (Figure 13).

Later, as sedimentation progressively filled the ancestral Coello River valley, the river breached and incised the Gualanday barrier, carving a valley that today reaches approximately 3,000 m in width and up to 130 m in depth (Figure 14). From that point onward, new lahars generated by Cerro Machín Volcano were routed through this incised valley and, downstream of the Gualanday barrier, contributed to the development of the Espinal Fan.

3.4 Stop 4

Ibagué Fault (neotectonic activity).
Hacienda Calicanto
74° 59’ 46.388” W, 4° 28’ 47.968” N
662 m.a.s.l.

The Ibagué Fault is a dextral strike–slip structure with an E–NE strike, located in the central sector of the Central Cordillera of the Colombian Andes. It forms part of a major transcurrent shear zone that affects the mountain range (Figure 3). The fault cuts across much of the urban area of Ibagué, from which it takes its name, and along its trace it offsets metamorphic rocks of the Cajamarca Complex (Jurassic?), Jurassic igneous rocks, Paleogene and Neogene sedimentary units, and Quaternary deposits forming the Ibagué Fan. The city of Ibagué is situated at the apex of this fan, which corresponds to a broad alluvial plain composed mainly of Pleistocene volcaniclastic sediments generated during multiple eruptive events of the Nevado del Tolima Volcano.

The fault offsets a crustal block of the Central Cordillera by approximately 29 km (Figure 3). At a regional scale, the Ibagué Fault appears as a single, continuous trace; however, where it crosses the Quaternary deposits of the Ibagué Fan, it develops a wide array of morphotectonic features characteristic of active transcurrent deformation. These include pressure ridges, linear ridges, pull–apart basins with associated lakes, fault scarps, fault trenches, domes, and laterally displaced drainage networks (Montes et al., 2005), see Supplementary Information 2. These landforms conform to a simple–shear kinematic model, in which the deformation ellipsoid exhibits alternating zones of compression and extension, accompanied by the development of synthetic and antithetic Riedel–type shear fractures and folds oriented parallel to the longitudinal axis of the ellipsoid (Wilcox et al., 1973; Harding, 1974) (Figure 15). The concentration and diversity of diagnostic geomorphic indicators of active dextral strike–slip faulting along a single fault segment is exceptional (Diederix et al., 2006).

The Ibagué Fault comprises three segments characterized by distinct deformation features, with deformation intensity increasing eastward. At this station, we are standing directly on the trace of the Ibagué Fault at the Calicanto Pressure Ridge. From this location, a 1,020 m traverse will be conducted to observe Quaternary deformation of the Ibagué Fan, with panoramic views to both the west and east of the ridge.

To the west, the first two deformation segments can be observed. The first segment crosses the city of Ibagué and is expressed as a linear fault trace marked by fault scarps and aligned, laterally displaced drainages. The second segment consists of a succession of synthetic structures that generate a linear array of en echelon pressure ridges, locally interrupted by small pull-apart basins (Figure 16).

The most common and prominent morphological features along the fault trace are pressure ridges, which are elongate landforms that represent the surface expression of transpressive conditions within the main deformation zone (Diederix et al., 2006). These structures result from the interaction between variations in fault–plane curvature and strike–slip motion along the fault (Sylvester, 1988) (Figure 17). Along the Ibagué Fault, a total of 30 pressure ridges have been identified, with lengths ranging from 60 to 1,480 m, whereas only five pull–apart basins are present. The predominance of pressure ridges over basins is attributed to the kinematics of a dextral en echelon Riedel shear system characterized by numerous left–stepping offsets, which promote transpressive deformation and ridge formation.

In contrast, right-stepping relay zones—which generate transtensive conditions and favor basin development—are comparatively rare, explaining the limited number of pull–apart

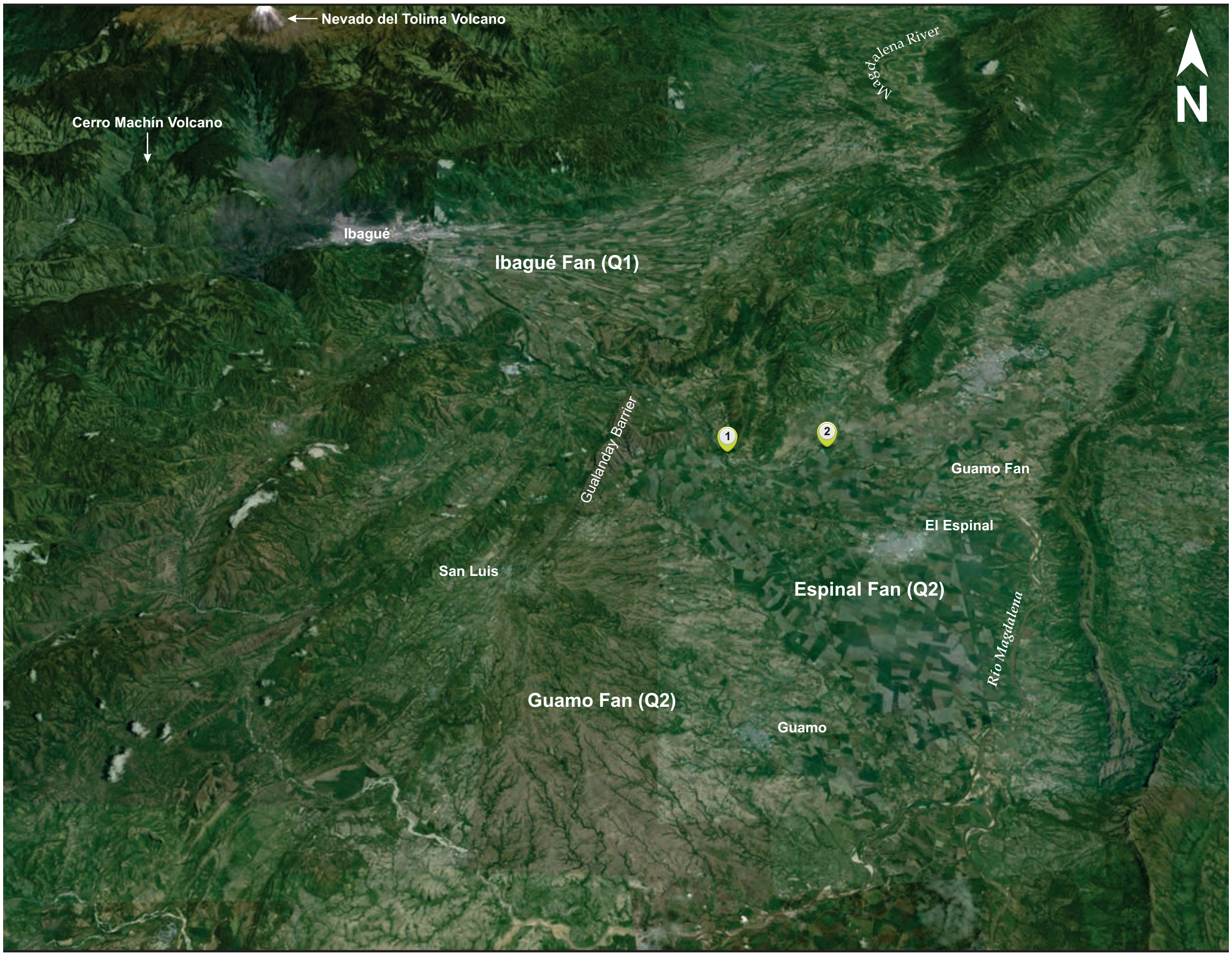

Figure 13. Google Earth image showing the temporal relationships between the Pleistocene Ibagué Fan (Nevado del Tolima Volcano) and the Guamo and Espinal fans formed by Holocene lahars from the Cerro Machín Volcano. The Gualanday Group acted as a geological barrier to the advance of the Ibagué Fan. K1: Lower Cretaceous; Q1: Pleistocene; Q2: Holocene.

basins observed along the fault.

East of the Calicanto Pressure Ridge, the third deformation segment of the Ibagué Fault is characterized by multiple en echelon fault traces, prominent pressure ridges (including the El Púlpito Pressure Ridge), and localized bulging and folding of Quaternary deposits. West of the town of Piedras, this deformation includes the exhumation of a block of the Ibagué Batholith (Figure 18) and the uplift and warping of the Ibagué fan. This structural configuration is interpreted as the result of transpression generated by a slight northward curvature of the fault zone. The spatial arrangement of structures across the Ibagué fan suggests that the Ibagué Fault terminates eastward in a transpressive front, with deformation propagating from west to east along a lateral ramp. This mechanism has facilitated the northward displacement of the Central Cordillera relative to the fault (Osorio et al., 2008).

The Calicanto Pressure Ridge is one of the largest features observed along the fault trace, measuring approximately 1,485 m along its major axis and reaching a height of about 40 m (Figure 19). This ridge formed as a result of a gentle leftward curvature of the main fault trace, which generated transpressive conditions. In cross section, the ridge is asymmetric, with a gentler southern flank and a steeper northern flank.

At the northeastern end of the ridge, and separated from it by a deep trench (Figure 18), another elongated ridge of lesser height is present. This ridge is interpreted as the displaced northern flank of the Calicanto Pressure Ridge, offset by approximately 565 m in a dextral sense. The course of the Chipalo River, which flows east of the ridge, has been displaced by a similar amount. This landform is interpreted as the result of straightening of the main fault trace, which effectively cuts across and truncates the earlier curvature of the fault (Figure 19). Although the exact age of this readjustment cannot be determined, it likely occurred during a late stage of ridge development, after the ridge had already attained its present dimensions (Diederix et al., 2006).

Figure 14. Google Earth image showing the temporal relationships between the Pleistocene Ibagué Fan (Nevado del Tolima Volcano) and the Guamo and Espinal fans formed by Holocene lahars from the Cerro Machín Volcano. The Gualanday Group acted as a geological barrier to the advance of the Ibagué Fan. K1: Lower Cretaceous; Q1: Pleistocene; Q2: Holocene.

Several major population centers, including Ibagué, Bogotá, Armenia, Pereira, and Manizales, lie within the zone potentially affected by activity along the Ibagué Fault. For this reason, and to evaluate the associated seismic hazard, the Colombian Geological Survey (CGS) conducted a paleoseismological study in a pull–apart basin containing a fault–related lake. This study identified ten surface–rupture events over the past approximately 15,000 years, with an average estimated magnitude of Mw ~7.2 and a slip rate of about 2.8 mm/yr. Historical earthquakes associated with the fault include the 1825 Ibagué earthquake and the 1942 event, which reached a surface–wave magnitude (Ms) of 5.8 and an epicentral intensity of VII in the city of Ibagué (Gómez & Salcedo, 2000).

Following detailed morphotectonic and paleoseismological investigations aimed at understanding the long-term behavior of

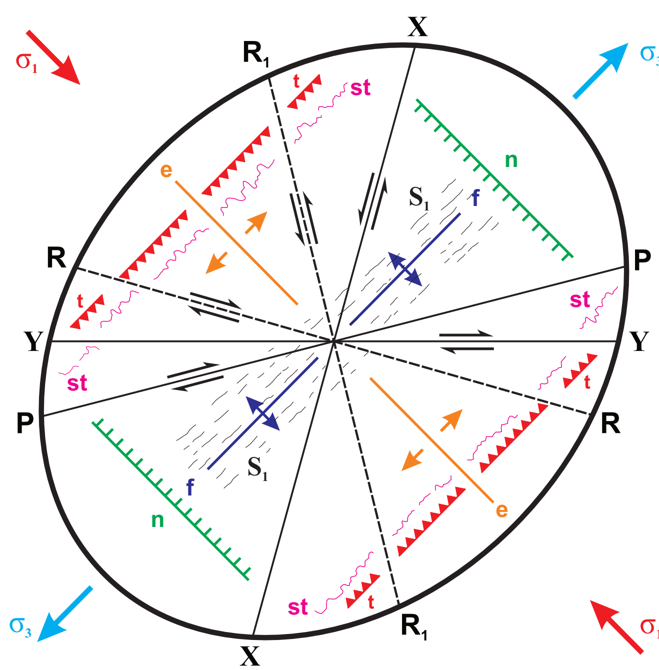

→ **Figure 15.** Orientation of major and minor structures associated with dextral strike–slip faulting under ideal simple–shear conditions (after Rossello, 2001). Shown are the main fault (Y); synthetic Riedel shears (R, P); antithetic Riedel shears (X, R1); folds (f); normal faults (n); thrust faults (t); extensional fractures (e); stylolites (st); and cleavage or foliation (S1).

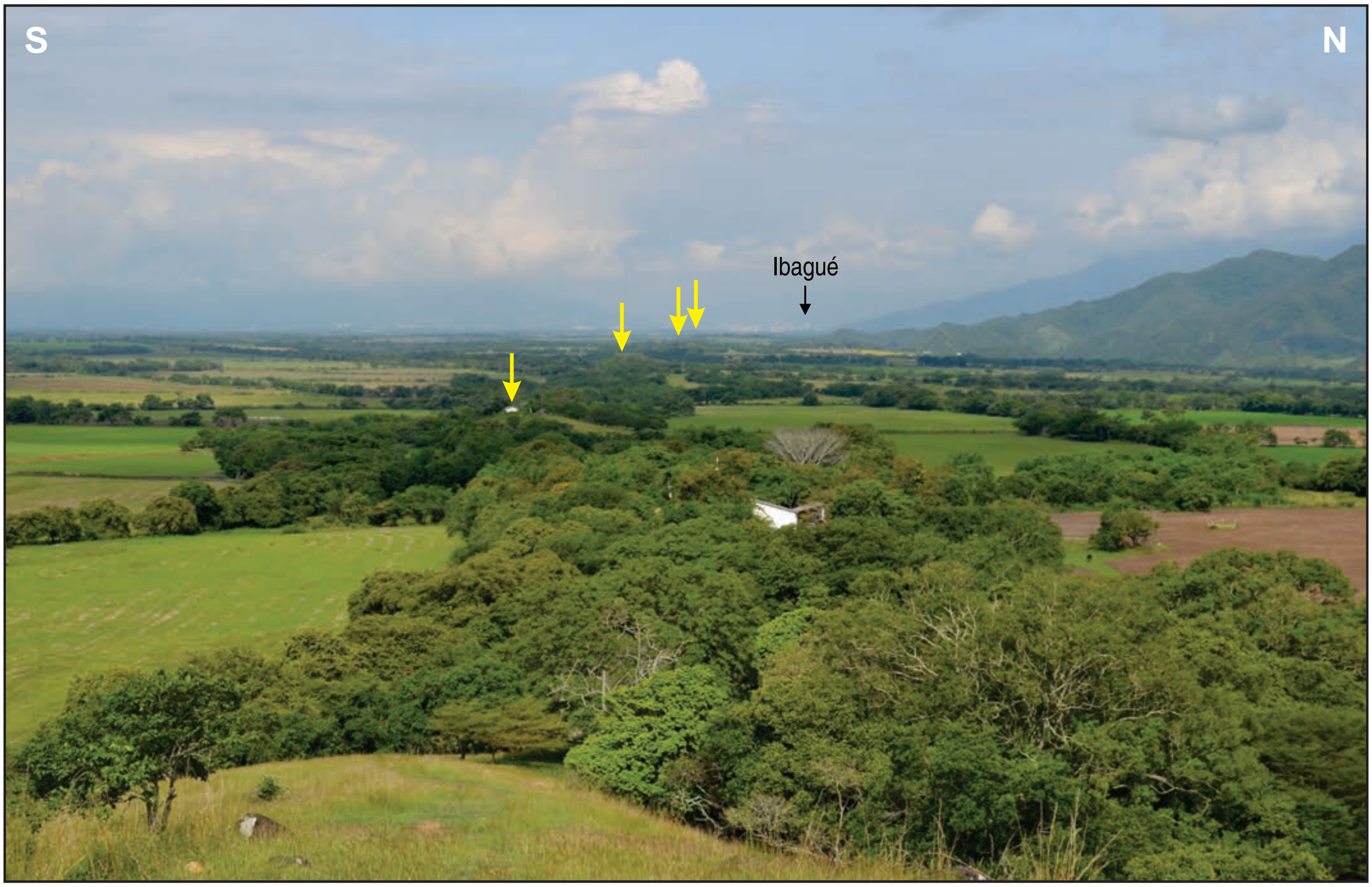

Figure 16. Westward view of the Ibagué Fault from the Calicanto Pressure Ridge. The fault trace is primarily expressed by the alignment of pressure ridges (yellow arrows), with the city of Ibagué visible in the background.

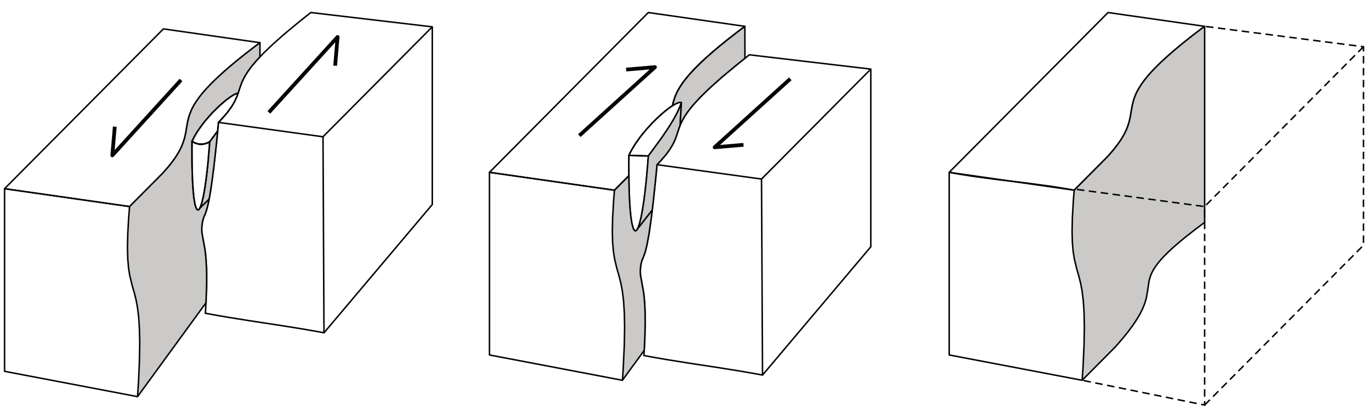

Figure 17. Block diagrams illustrating models for the formation of fault–related pressure ridges and pull–apart basins, resulting from the interaction between fault–plane geometry and the direction of transcurrent movement (after Diederix et al., 2006).

the Ibagué Fault, the GEORED Project of the Servicio Geológico Colombinao installed 15 seismic monitoring stations around the fault. These stations form part of a passive seismic network that operates for approximately 120 hours per year. Two of these stations are located on the Calicanto Pressure Ridge and on the displaced ridge to the northeast.

3.5 Day 2, Stop 5

Tabor Volcano and view of Guacharacos Volcano (Quaternary)
Ibagué–Armenia Highway
75° 10’ 38.676” W, 4° 23’ 58.106” N
1050 m.a.s.l.

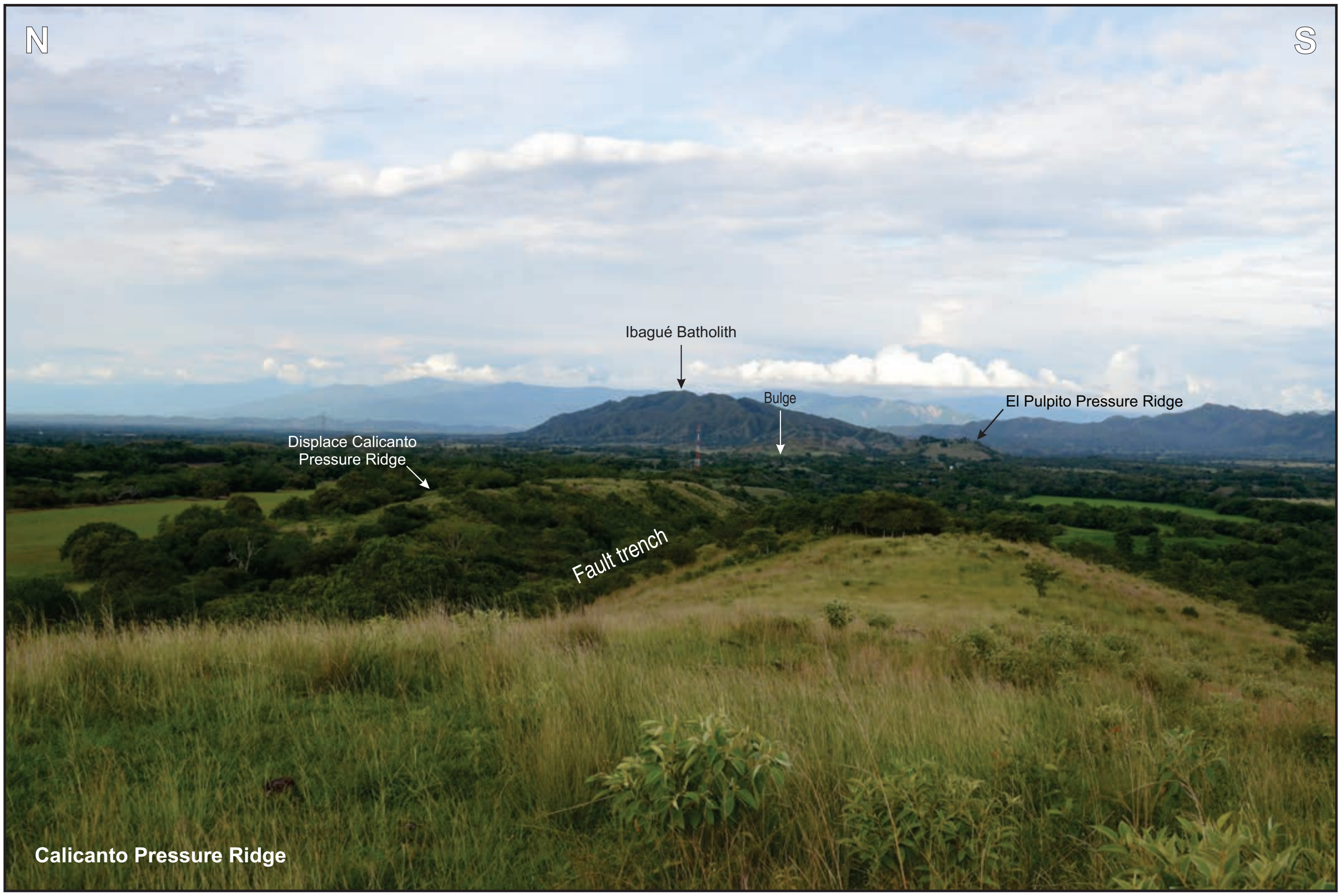

Figure 18. Fault trench produced by displacement of the northern part of the Calicanto Pressure Ridge. In the background, the El Púlpito Pressure Ridge and the Piedras Bulge are visible.

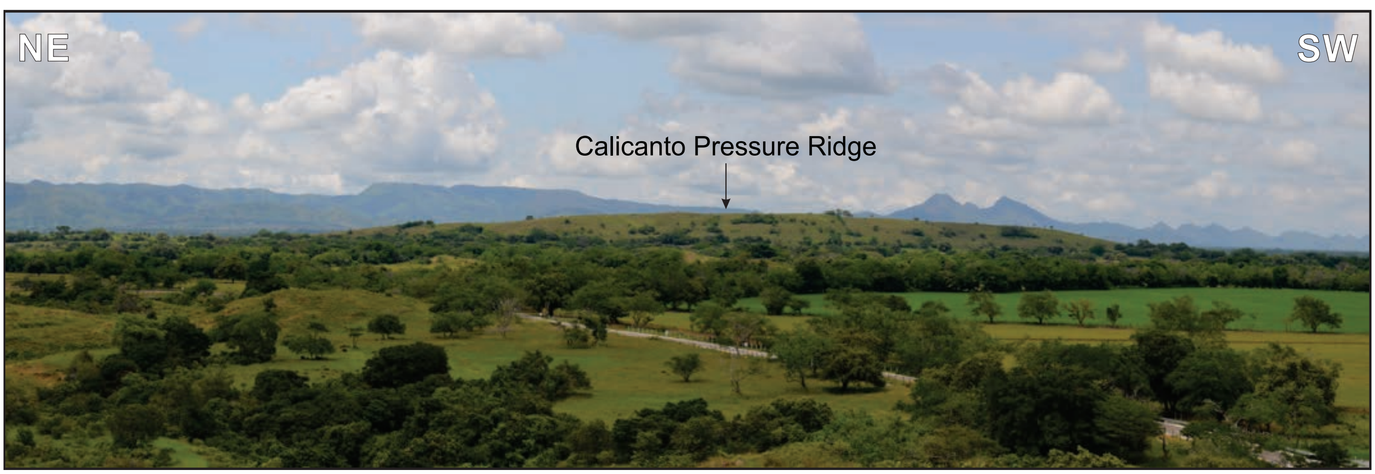

Figure 19. Longitudinal view of the Calicanto Pressure Ridge, looking from the northeast.

In the Tolima Department, several eruptive centers with characteristics of monogenetic volcanism have been identified, some of which are located very close to the city of Ibagué, such as the Guacharacos and Tabor volcanoes (Figure 21). These volcanoes correspond to lava cones and pyroclastic cones whose main products are olivine- and pyroxene-bearing andesitic basalts. Geochemically, these rocks correspond to calc-alkaline basalts with high magnesium contents, interpreted as near-primary magmas (Núñez et al., 2001; Galindo, 2012; Monsalve & Gómez, 2015).

The volcanic products of these structures lie on the volcanic–sedimentary deposits of the Ibagué fan from the Pleistocene, suggesting that the volcanic event is considered one of the most recent geological events to have occurred in this region,

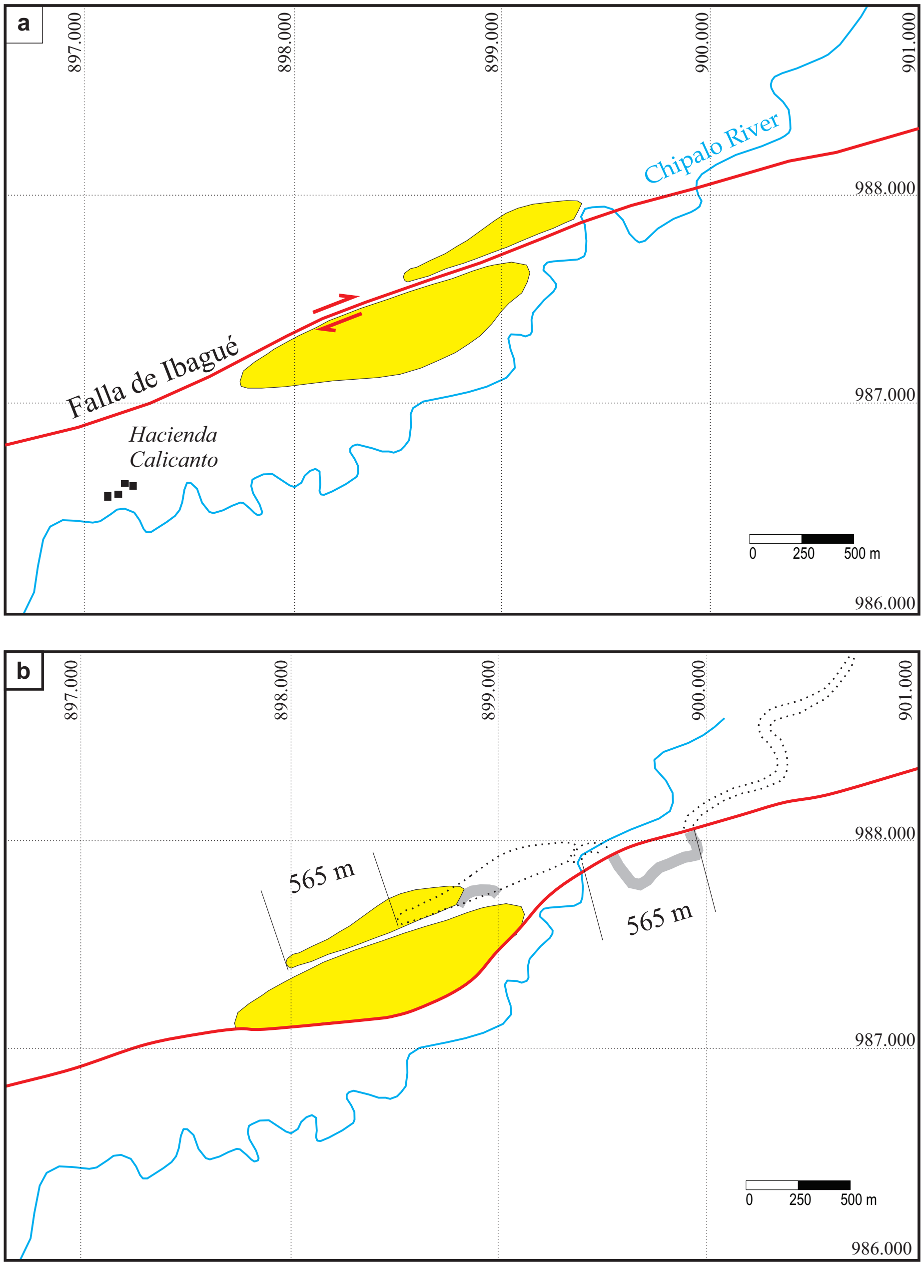

Figure 20. Conceptual model illustrating the formation of the Calicanto Pressure Ridge. (a) Present–day configuration of the Calicanto Pressure Ridge, which has been cut and displaced in a dextral sense by the Ibagué Fault as the fault trace straightened. (b) Reconstructed earlier stage of the pressure ridge prior to renewed activity along the Ibagué Fault, when neither the ridge nor the course of the Chipalo River had yet been displaced. Gray shading indicates the present–day meanders of the Chipalo River. Restoration of the inferred dextral displacement shows the coincidence of the river channel north and south of the fault. The present locations of the ridge and river are shown with dashed lines. An approximate horizontal displacement of ~565 m is inferred.

possibly during the Holocene (Núñez et al., 2001). In the area where the city of Ibagué is built, several geological faults converge, some of them showing clear evidence of neotectonic activity. It is likely that the Tabor Volcano was emplaced along Riedel faults related to the Ibagué Fault system, such as the Martinica and Buenos Aires faults (Figure 22).

The Tabor Volcano is a crescent-shaped pyroclastic cone with a crater approximately 350 m in diameter. It displays a gentle slope toward its western sector and is partially destroyed toward its E–SE sector (Figure 23). The volcanic products identified to date mainly consist of basaltic blocks, ranging from massive to vesicular, exposed along the inner crater walls and locally on the surface of the cone. These blocks likely represent material detached from the pyroclastic layers forming the cone. Volcanic bombs are scarce, and a thin layer of lithic to vesicular lapilli has been recognized on the western flank. A single lava flow associated with this volcano has been identified west of the cone. Petrographically, these materials correspond to olivine

Figure 21. Aerial view of the Guacharacos and Tabor volcanoes. Arrows indicate the directions of lava flows. Guacharacos Volcano comprises two scoria cones and two lava flows, one to the north and one to the south. Tabor Volcano has an open crater toward the NNE and a lava flow directed to the west. Note the close proximity of both volcanoes to the Ibagué and Buenos Aires faults. Photograph courtesy of Forest Engineer César Augusto Gutiérrez (after Monsalve et al. 2020).

basalts (Monsalve et al., 2020).

From the summit of the Tabor Volcano, the Guacharacos Volcano can be observed approximately 1.7 km to the southwest (Figure 24). This volcanic cone has a relief of less than 100 m and an elongated east–west geometry with a major axis of approximately 250 m (Núñez et al., 2001). The products of the Guacharacos Volcano consist mainly of lava flows and pyroclastic fall deposits, including bombs and lapilli. The surrounding pyroclastic materials are highly weathered and have been transformed into dark red clay-rich soils.

Two lava flows originated from the Guacharacos cone (Figure 21). One flowed northward along the Guacharacos stream valley, reaching the Combeima River and locally modifying its course. This flow is approximately 1300 m long and has an average thickness of 20 m. The second flow descended southward along the Zanja Honda stream valley; although it has a similar length (~1300 m), its volume is smaller than that of the northern flow (Núñez et al., 2001). Both flows are covered by abundant pyroclastic fall deposits, and brecciated zones formed by volcanic bombs incorporated into the lava while still molten are observed on their surfaces.

3.6 Stop 6

Lava flow from the Guacharacos Volcano (Quaternary). Ibagué–Armenia Highway.
75° 11’ 12.8907” W, 4° 24’ 41.648” N
1086 m.a.s.l.

During construction of the Ibagué bypass, lava flows and pyroclastic deposits associated with the Guacharacos Volcano were exposed (Núñez et al., 2001). At this stop, a cross-sectional exposure of the northern lava flow is observed, with an average exposed thickness of approximately 8 m (Figure 25).

The basaltic lava exhibits a massive interior core and a scoriaceous, brecciated upper surface with irregular thickness. Remnants of altered pyroclastic material are also present. The rock is light gray, locally pale red due to oxidation, and displays a porphyritic texture with an aphanitic matrix. Phenocrysts consist mainly of olivine crystals smaller than 2 mm.

Petrographically, the lava corresponds to olivine–pigeonite andesitic basalt, with phenocrysts comprising approximately 23–29% of the rock. These are set within a trachytic matrix characterized by aligned plagioclase (labradorite) microlites

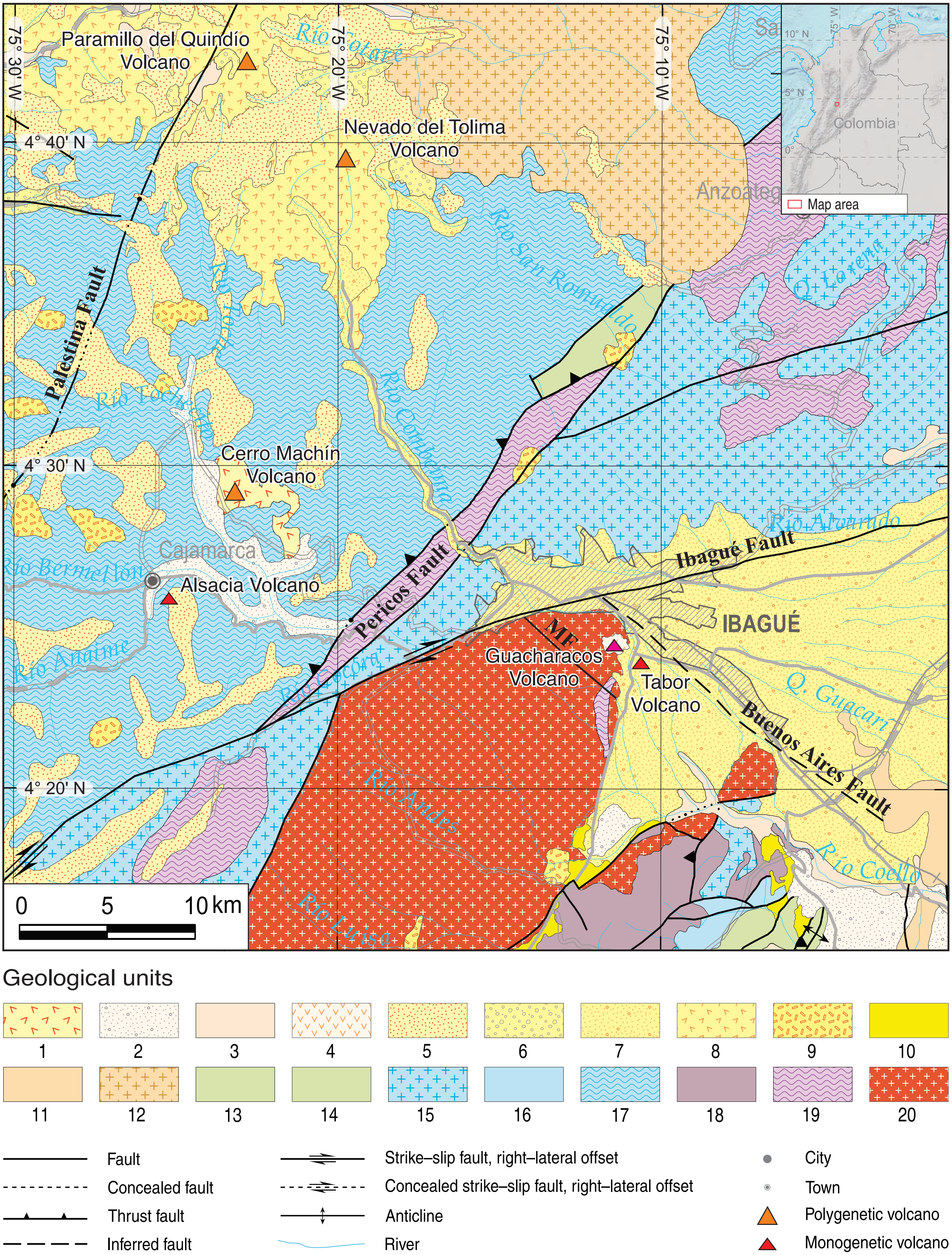
Paramillo del Quindío Volcano
Nevado del Tolima Volcano
Cerro Machín Volcano
Alsacia Volcano
Guacharacos Volcano
Tabor Volcano
Cajamarca
IBAGUÉ
Anzoátegui
Colombia
Map area
10° N
5° N
0°
75° W
70° W
75° 30' W
75° 20' W
75° 10' W
4° 40' N
4° 30' N
4° 20' N
Palestina Fault
Pericos Fault
Ibagué Fault
Buenos Aires Fault
MF
Río Gualí
Río Totaré
Río San Romualdo
Río Combeima
Río Toche
Río Bermellón
Río Anaime
Río Cocora
Río Andes
Río Luisa
Río Alvarado
Río Coello
Q. Lorena
Q. Guacarí
0
5
10 km
Geological units
1
2
3
4
5
6
7
8
9
10
11
12
13
14
15
16
17
18
19
20
Fault
Concealed fault
Thrust fault
Inferred fault
Strike–slip fault, right–lateral offset
Concealed strike–slip fault, right–lateral offset
Anticline
River
City
Town
Polygenetic volcano
Monogenetic volcano

Figure 23. Drone view of the Tabor Volcano, illustrating its crater and moon–shaped.

(Núñez et al., 2001).

Although only a limited number of monogenetic volcanoes have been identified in this area, previous studies (Núñez et al., 2001; Galindo, 2012; Monsalve & Gómez, 2015; Monsalve et al., 2020) suggest that monogenetic volcanic activity may persist for up to one million years. Therefore, the presence of additional, as–yet–unrecognized monogenetic volcanic centers in the region cannot be ruled out.

3.7 Armero before the tragedy: A necessary portrait to understand the magnitude of the catastrophe that shocked the entire world

Through the following chronicle, the aim is to portray the historical and economic importance enjoyed by Armero during much of the twentieth century, prior to the calamity that forever marked the history of an entire country. Imagining what life was like before the tragedy allows us to understand, with greater closeness, the profound grief experienced by thousands of Colombians as a result of the long–foretold catastrophe that occurred on the fateful night of November 13, 1985.

3.7.1 Overview of agricultural production and Armero's main economic activity

It was in the year 1895 when Antioquian settlers Demetrio González, Cirilo García, and José María Alzate arrived in what is now known as the territory of Armero, seeking to take advantage of the region's highly productive lands to establish their livelihoods. This took place in the context of the episode known

←

Figure 22. Regional geological map of the Metaima Monogenetic Volcanic Field. (1) Holocene volcanic rocks from Cerro Machín Volcano, (2) Holocene volcaniclastic deposits from Cerro Machín Volcano, (3) Quaternary aluvial deposits, (4) Quaternary volcanic rocks and pyroclastic deposits from Guacharacos Volcano, (5) Quaternary pyroclastic deposits, (6) Quaternary morraines, (7) Quaternary volcanoclastic deposits, (8) Pliocene – Quaternary volcanic rocks, (9) Neogene porphyries, (10) Neogene sedimentites, (11) Paleogene sedimentites, (12) Eocene intrusives, (13) Cretaceous? metasedimentites, (14) Cretaceous sedimentites, (15) Jurassic Ibagué Batholith, (16) Jurassic volcanosedimentites, (17) Jurassic metamorphic rocks, (18) Triassic sedimentites, (19) Triassic metamorphic rocks, and (20) Permian plutons and orthogneisses. (MF) Martica Fault. Simplified from Gómez et al. (2023).

Figure 24. Panoramic view of the Guacharacos Volcano from Tabor Volcano.

Figure 25. Lava flow from the Guacharacos Volcano exposed along the Ibagé–Armenia Highway.

in Colombia as the Antioquian colonization, which extended from the late eighteenth century to the early twentieth century and consisted of the large–scale migration of impoverished rural families from Antioquia in search of fertile land where they could establish farms and found villages or towns. As a result of this migration, an agrarian revolution took place along the Central and Western Cordilleras, as well as in their foothills and surrounding regions (Valencia, 2017).

During its golden years, Armero was nationally recognized as "The White City of Colombia," a nickname earned due to its extensive cotton production. By 1959, cotton occupied approximately 50% of all cultivated land in Armero, representing 23% of the total cotton production of the Tolima Department for that year, according to data from the National Administrative Department of Statistics (DANE, 1960, cited in Barajos et al., 2023). Cotton cultivation began in 1935, promoted by the Ministry of Agriculture, with the objective of taking advantage of the area's geomorphological characteristics and highly productive soils.

However, cotton was not the only crop grown in Armero. The following figures illustrate the municipality's agricultural production in 1959: sesame accounted for 12.45% of Armero's total production and 5% of Tolima's; maize represented 13.65% in Armero and 5% in Tolima; rice accounted for 8.30% in Armero and 4% in Tolima; and coffee, which reached 6.17% of the municipality's total agricultural output that year.

This major agricultural and economic boom was accompanied, as expected, by a population increase in subsequent years that surpassed that of nearby towns such as Fresno, Honda, and Purificación, which in 1938 had larger populations than Armero.

In approximately 50 years, Armero doubled its population, growing from about 14 000 inhabitants in 1938 to a maximum of slightly over 29 000 inhabitants in 1985, according to official DANE figures (Barajos et al., 2023). Such was Armero's economic and demographic growth that, by the year of the tragedy, it had consolidated itself as the second–largest urban center and the fastest-growing economy in the Tolima Department (Figure 26a).

As shown throughout this historical portrait, the Armero region has been characterized by the remarkable fertility of its soils throughout its history. Paradoxically, this fertility is a direct consequence of ancient laharic flows associated with the activity of Nevado del Ruiz Volcano. Evidence of these eruptive episodes is not only documented in historical records and ancient written accounts, but is also preserved in situ through lahar deposits associated with past eruptions, such as the event of March 12, 1595 (Martínez et al., 2014).

3.7.2 Emerging economic activities

Armero also hosted other emerging and innovative economic activities for the time, including a soft drink company (La Bogotana), clothing store branches that would later gain significant regional influence, branches of major banks such as Banco Agrario and Bancolombia, terrestrial transportation companies, and even aviation services, among others. In total, Armero came to host approximately 31 manufacturing facilities, second only to the departmental capital, Ibagué. Recreational centers, health services, and scientific institutions for the people of Armero.

3.7.3 We now present a brief overview of some cultural, scientific, and lifestyle aspects of the municipality's inhabitants

For survivors of the tragedy and those who had personal ties to Armero, the town represented childhood and adolescence, a place called home, as well as broad opportunities for employment, development, and education. By the second half of the twentieth century, it was common to hear that Armero had some of the highest–quality schools in the region. According to the map produced by the Colombian Geographic Institute (IGAC) as part of the municipality's historical reconstruction project (Barajos et al., 2023), seven educational institutions—schools and high schools—were identified, along with a campus of the University of Tolima, which still exists today.

Scientific institutions also flourished in Armero, including the Carlos Roberto Darwin Anthropological Museum and the most important institute in Colombia dedicated to the study and exhibition of snakes, known as the Armero Serpentarium, which ranked second in Latin America in this field (Mora, 2022).

Healthcare facilities were also notable, including a psychiatric hospital and a third–level hospital (Figure 26d). Even today, it is uncommon in Colombia to find municipalities with tertiary–level hospitals that do not also have high population densities and significant regional economic importance.

Finally, among Armero's recreational spaces were nightclubs, country clubs, cafés, parks, and even a movie theater (Figure 26b)—a luxury at the time reserved for only the most prosperous cities in the country—as well as sports facilities such as football stadiums. Not to be forgotten are the railway lines that crossed the urban center, along which thousands of travelers passed while journeying from southern to northern Colombia (Figure 26c).

(Figure 26c).

3.7.4 Conclusions and final reflections

Through this account, we travel across the memories of a municipality with a brilliant past and one of the greatest promises of prosperity seen in Colombia during the twentieth century. This memory, though seemingly distant and overshadowed by an event that undoubtedly marked—and will continue to mark—multiple generations, not only of Colombians but also of scientists and professionals worldwide who dedicate their lives to volcanic hazard risk reduction, deserves to be told.

As stated in Barajos et al. (2023), Armero is not merely a tragic memory portrayed through sensationalist press images; it also represents the history of one of the most prosperous towns with the greatest economic potential that Colombia has ever known. These images of a resilient and opportunity-filled Armero should also form part of the global collective memory, serving as a powerful reminder that motivates us to work tirelessly so that a disaster of such magnitude never occurs again anywhere in the world

3.8 Stop 7

Armero´s Lahars. Holocene
Intersection of the Lérida–Armero and Cambao–Armero roads.
74° 54' 27,907" W, 4° 57' 28,411" N
352 m.a.s.l.

3.8.1 Introduction

Nevado del Ruiz Volcano (NRV) is an active composite volcano (Figure 27) with an elevation of 5321 m, located approximately 140 km northwest of Bogotá, at the northern end of the Northern Volcanic Segment of the Central Cordillera. The volcano lies within Los Nevados National Natural Park and spans the departments of Caldas and Tolima. Holocene eruptions have been predominantly explosive, characterized by episodes of dome extrusion and destruction, debris avalanches, pyroclastic fall and flow deposits, and pyroclastic surges that interacted with the summit ice cap, generating lahars (Thouret et al., 1990).

On November 13, 1985, Nevado del Ruiz erupted, producing a complex sequence of pyroclastic flows and surges that interacted with snow and ice from the summit glacier, triggeringthe deadliest lahar sequence in recent human history. Lahars flowed westward, northward, and eastward from the volcano,

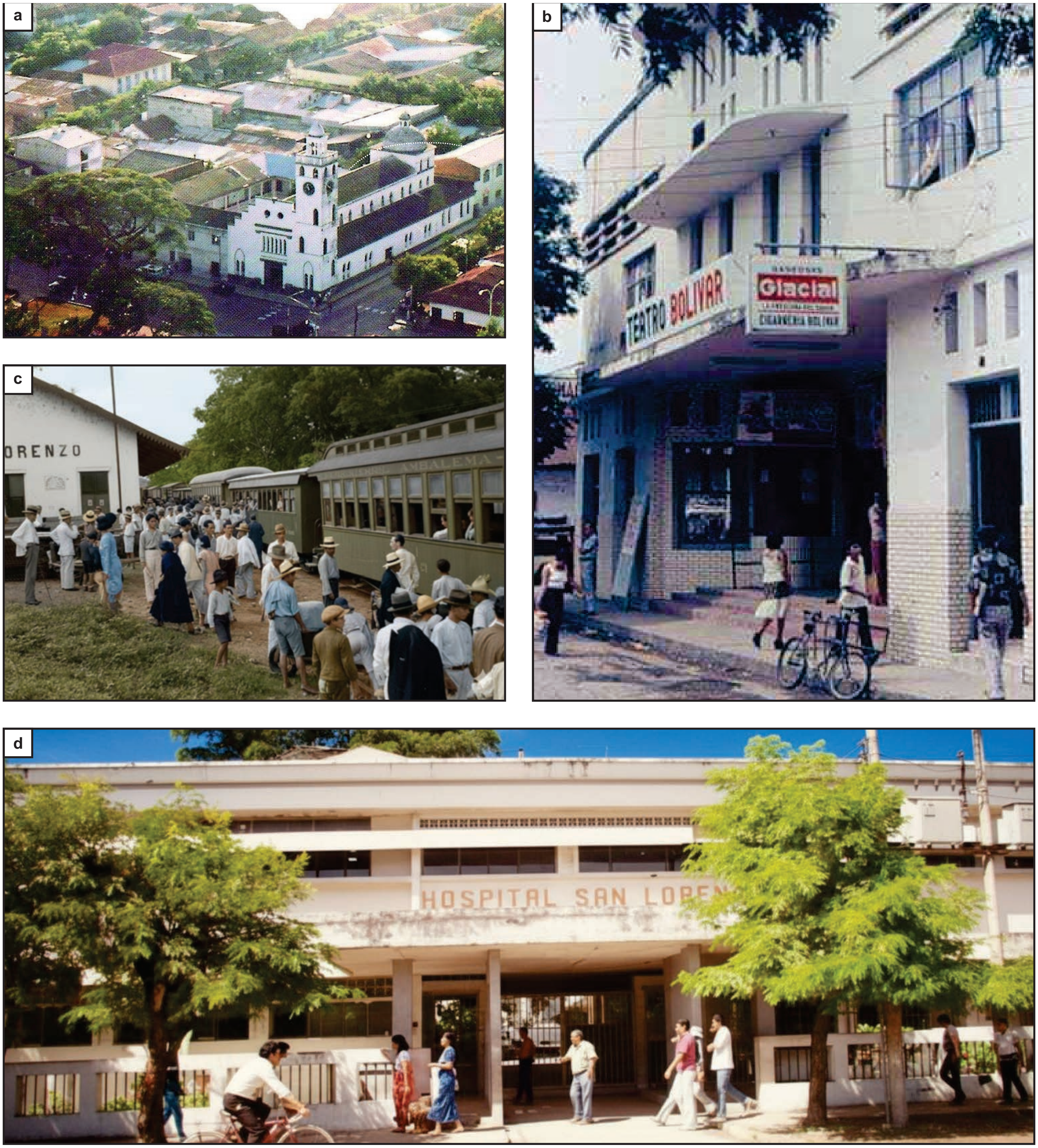

Figure 26. Historical images of Armero before the tragedy, some of them enhanced using AI. (a) Aerial view of the central park and the widely known Church of the Municipality. (b) Bolivar Theater.of Armero. (c) The Railway of Armero. On the figure, part of the name San Lorenzo is displayed, which was a former name for the municipality of Armero. Enhanced and colored image using AI. (d) San Lorenzo Hospital in Armero. Photographs taken from: https://www.facebook.com/SiempreArmero.

following three of the four main drainage systems originating at the edifice: the Chinchiná River (Caldas Department) and the Gualí and Lagunilla rivers (Tolima Department). Within approximately four hours of the onset of the eruption, the lahars descended about 5100 m in elevation and traveled distances of up to 104 km, leaving a trail of catastrophic destruction (Piers-

Figure 27. Panoramic view of Nevado del Ruiz Volcano (northern sector). Headwaters of the Azufrado River (a tributary of the Lagunilla River), one of the valleys through which the lahars generated during the November 13, 1985 eruption were channeled.

on et al., 1990).

The lahars caused the near–total destruction of the town of Armero (figures 28 and 29), located in northern Tolima at the mouth of the Lagunilla River canyon and 42 km east of the volcano's summit. The event resulted in the deaths of more than 20 000 inhabitants of Armero, as well as residents of other affected areas in the department of Caldas (Navarro et al., 2011).

The tragic consequences of the November 13, 1985 eruption marked the beginning of systematic volcanological studies in Colombia and became a global lesson, demonstrating the need for detailed volcanic studies to prevent and mitigate the effects of future eruptions through monitoring and the production of volcanic hazard maps. Accordingly, under Decree 3815 of December 26, 1985, the Servicio Geológico Colombiano (SGC) *was officially designated as the government institution responsible for the study and monitoring of active volcanoes in the country.*

Historical accounts of Nevado del Ruiz eruptions indicate that the area now occupied by Armero had already been devastated twice by lahars triggered by volcanic activity, in 1595 and 1845 (Ramírez, 1975; Espinosa, 2012). Several studies address the 1985 NRV lahars, including Mojica et al. (1985), Naranjo et al. (1986), Pierson et al. (1990), and Cortés et al. (2006). These works integrate geological data with eyewitness accounts collected immediately after the disaster and up to 20 years later.

Notably, Pierson et al. (1990) provided detailed stratigraphic descriptions, indirect measurements of flow velocity and discharge, reconstruction of lahar hydrographs (discharge versus time), and volume calculations. The lahar that devastated Armero resulted from the merging of two nearly simultaneous flows that developed along the Lagunilla and Azufrado river channels and converged approximately 23 km west of Armero. Upon exiting the Lagunilla canyon and encountering relatively flat topography—corresponding to a fan built by previous lahars and floods—the flow geometry changed dramatically, resulting in rapid deceleration, lateral spreading over a wide area, and rapid deposition (Pierson et al., 1990).

3.8.2 Description of Stop 2

At the intersection of the Ibagué–Mariquita and Cambao–Bogotá roads, an outcrop exposes two lahar deposits: one corresponding to the 1985 event and another very likely related to the 1845 eruption, separated by a brown paleosol. The paleosol is overlain by a pinkish layer of irregular thickness, composed of a silty matrix with sporadic rounded clasts. This layer is, in turn, capped by a concrete slab or sidewalk (Figure 30).

At this outcrop, the upper deposit, corresponding to the 1985 lahar, is approximately 1.30 m thick and consists of a massive, vesicular, poorly sorted debris-flow deposit of Havana-brown color. It is matrix-supported by very coarse sand and locally displays zones of yellow oxidation. The deposit is heterolithic and contains subangular, subrounded, and rounded gravel-sized clasts, with diameters of up to 30 cm. Clast lithologies include andesitic lavas of various shades, green, gray, and black schists, green phyllites, amphibolites, and granodiorites. These materials derive from pyroclastic deposits of the 1985 eruption and earlier eruptions, preexisting channel sediments, and bedrock eroded by the lahar. The deposit also contains wood fragments, tree trunks, glass, plastics, and debris from destroyed buildings.

The lower lahar deposit exhibits macroscopic compositional characteristics similar to those of the upper unit and, in some sections of the outcrop, appears as a single massive deposit. The pinkish layer developed above the paleosol is interpreted as the product of a flood event reported to have occurred approximately 50 years prior to the destruction of Armero (Navarro et al., 2011). In proximal and mid-fan areas affected by the 1985 lahar, surface accumulations of block–sized, subrounded, and rounded clasts derived from the debris flow are still commonly observed.

3.9 Stop 8

Panoramic view of the former town of Armero, with the Lagunilla River canyon in the background
La Aurora Farm, 2 km east of the central park of Armero
74° 53' 28,835" W; 4° 57' 33,804" N
345 m.a.s.l.

From one of the nearby low hills, a panoramic view of the former town of Armero can be observed. Despite their modest elevation, these hills served as refuges during the lahar event, saving the lives of many people who were able to escape the force of the mudflow (Navarro et al., 2011). The Lagunilla River canyon is clearly visible, opening onto the flat terrain where Armero was established. At this point, the lahar split into three main branches.

The largest branch flowed eastward along the course of the Viejo River for approximately 18 km, reaching the hamlet of Santuario. A second branch flowed northward along the Santo Domingo creek valley toward the Sabandija River, while a third branch followed Lagunilla River channel for about 10 km.

Figure 28. Orthophoto of Armero before November 13, 1985 tragedy. Photo taken on May 5, 1985. Scale of the photo 1:14000.

The lahar inundated an area of approximately 34 km² and advanced in successive pulses, producing the greatest destruction in the central sector of Armero's urban area (figures 31 and 32), which was completely razed to its foundations (Mojica et al., 1985).

Historical records indicate that the Armero valley had been affected by even larger mud-flows prior to the November 1985 event, notably in March 1595 and February 1845 (Ramí-rez, 1975; Mojica et al., 1985; Espinosa, 2012).

3.10 Stop 9

Ruins of the town of Armero, San Antonio Church, and Los Fundadores Park (Parque a la Vida).
Former Armero.
74° 54' 10,397" W; 4° 57' 42,934" N
357 m.a.s.l.

"Gather now your memories,
keep them in your heart,
let silence accompany you,
and enter the temple of God,
bow your head before Him
and tell Him that even today,

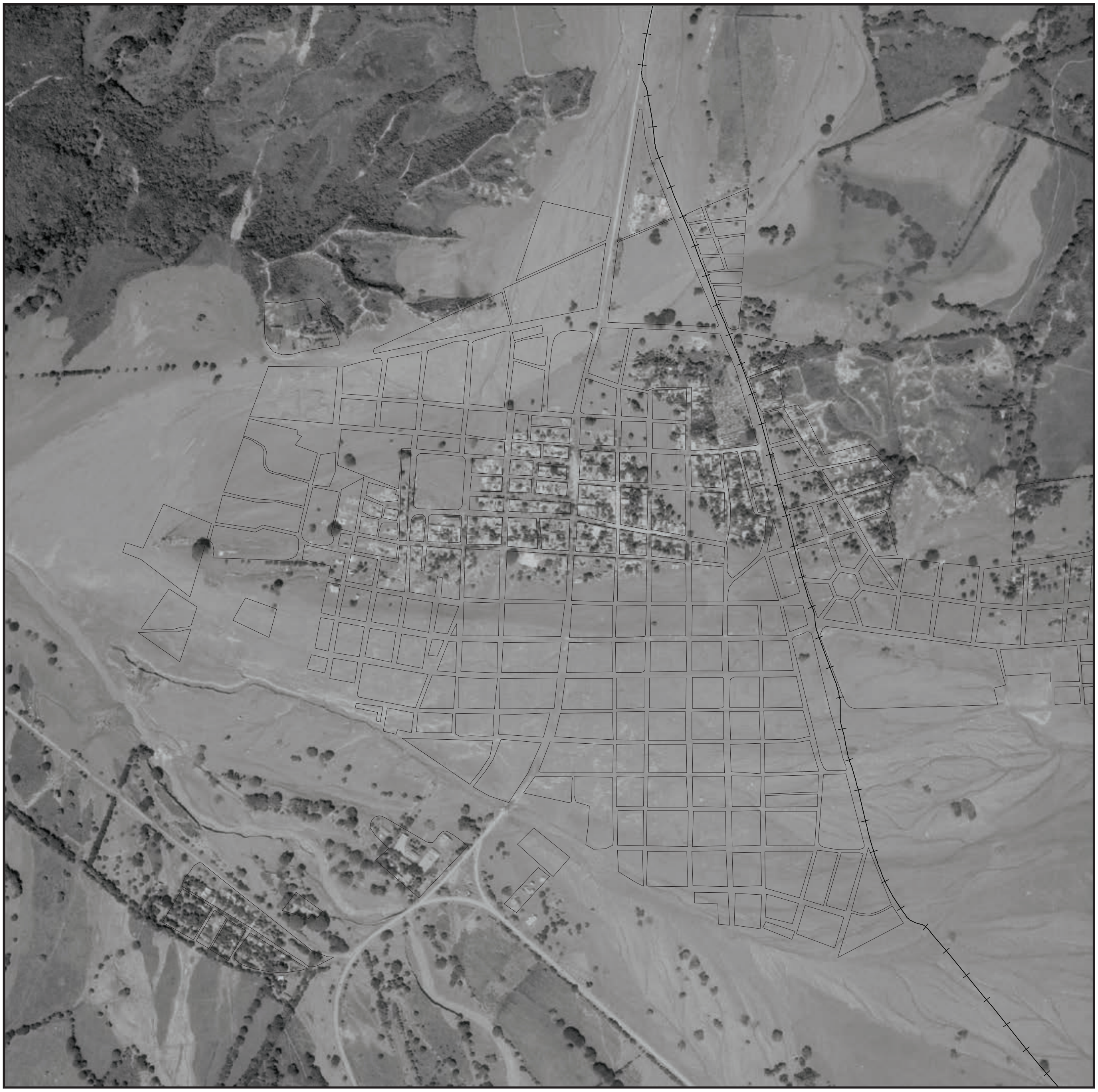

Figure 29. Orthophoto of Armero after November 13, 1985 tragedy. Photo taken on November 20, 1985, Flight C–2229, photo No. 62. Over the photo is overlap the contour on the blocks and the railway. Scale of the photo 1:14000.

though years have passed…
you still do not understand what happened."
— Luz García

The visit allows observation of several significant ruins, including remnants of the San Antonio Church dome; the original pavement of the main square and of San Lorenzo Church; the vault of the Banco de la República building; and various symbolic monuments commemorating the disaster and the many lives lost on the night of November 13, 1985.

These monuments were constructed at different times following Colombia's largest natural disaster and include Parque a la Vida and the Pope's Cross.

3.11 Chronicle by geologist Sofía del Rosario NAVARRO ALARCÓN, geologist and survivor of the Nevado del Ruiz Eruption

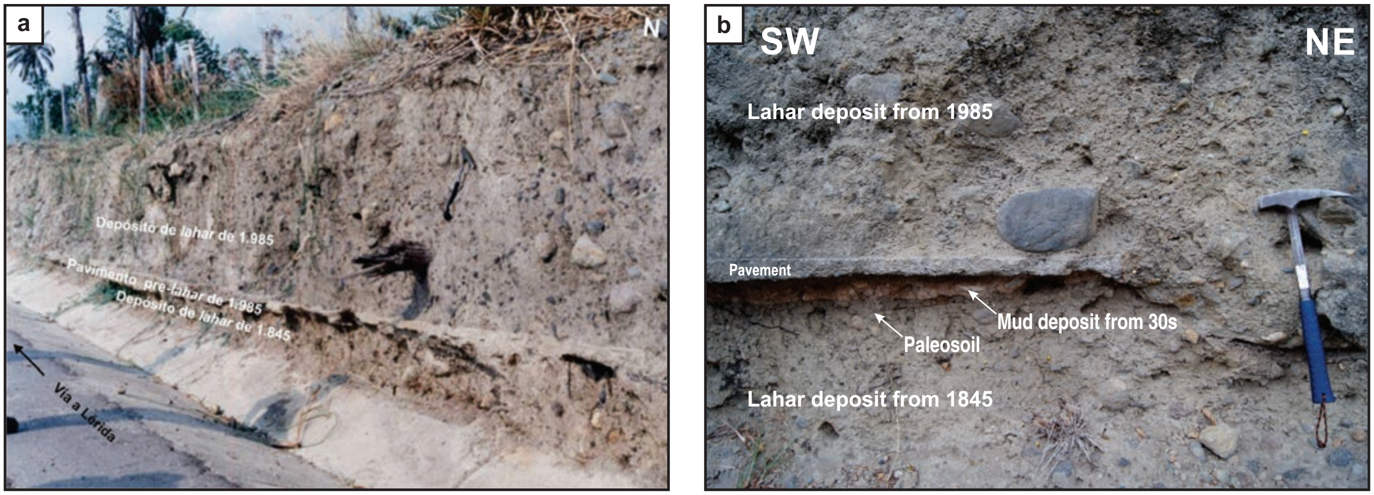

Figure 30. Armero lahars at the intersection of the Ibagué–Mariquita and Cambao–Bogotá roads. **(a)** Contact zone between the 1985 and 1845 (?) debris-flow deposits. The paleosol, the layer associated with a flood that occurred around the 1930s, and the concrete slab separating the two deposits are visible. **(b)** Detail of the contact zone. Note the paleosol developed atop the 1845 lahar deposit.

On the occasion of the field trip organized within the framework of the 82nd Executive Meeting of the IUGS, Colombian geologist Sofía del Rosario NAVARRO ALARCÓN—survivor of the 1985 Armero tragedy—revisits one of the most devastating volcanic events of the twentieth century. Her testimony offers an intimate and deeply human perspective on the eruption of Nevado del Ruiz Volcano, an event that forever transformed the relationship between geology, volcanic risk, and society.

In this chronicle, NAVARRO recounts how she managed to survive along with some of her classmates while participating in a field excursion in the vicinity of the volcano, at a time when she was still an undergraduate geology student at the University of Caldas. Her experience—marked by uncertainty, limited scientific knowledge, and the overwhelming power of nature—bridges personal experience with geological lessons that continue to resonate within the international scientific community today.

"We arrived in Armero at around 7:00 p.m. on the fateful night of November 13, 1985, accompanied by an intense, unrelenting rainfall. We ended up there despite having expressed my disagreement to the professor in charge of our field excursion regarding his decision to spend the night in Armero due to the heavy rain. For me, the idea of staying there overnight was unthinkable—not because I anticipated an imminent eruption, but because at the time the news frequently warned about the instability of a dam which, if it were to fail, could cause a catastrophic flood in the town and surrounding areas. I knew there was a latent flood hazard and I expressed this concern to my professor.

At that time, we were unaware of the newly produced—and first—volcanic hazard map in Colombia for Nevado del Ruiz, as we belonged to a lower academic semester than those students who had been able to participate in the mapping project. The supervising professor, Jorge DORADO, and the teaching assistant, Jorge Mario ESTRADA, who were responsible for leading our field trip, were aware of the map, as they had participated directly in its preparation together with other geologists from the Colombian Geological Survey. Personally, I believe they cannot be blamed. To give just one example, even today, when one looks at the hazard map of Machín Volcano, one does not necessarily rule out staying in towns located near the volcano.

That night, the rain was so heavy that some of my friends and I decided to stay in the same room and not go out for dinner. Around 11:00 p.m., after a football match broadcast, those who had gone out to eat finally learned that Nevado del Ruiz Volcano had erupted. They ran back to the hotel to wake us and inform us of the eruption, showing us that ash was falling with clasts reaching up to 2 cm in size, known as lapilli. Earlier that same day, while we were in Falán, a nearby town, an ash emission had also occurred in the afternoon, but with much finer grain sizes—similar to what we were accustomed to in Manizales, a city very close to Ruiz. This detail surprised some of my colleagues years later when I recounted my experience, as official reports only mentioned fine–grained ash emissions on that day.

After being alerted to the eruption, everything unfolded as described in other survivors' accounts from that night in Armero. The town's priest went out to speak and ask the residents to remain calm; however, shortly afterward, the power went out and panic spread. All the inhabitants began running toward the same area, and we left the hotel in fear, asking where we should run to escape the danger. Everyone pointed in the same direction. As soon as we started running that way, one of our classmates warned us that it would be better to climb to the hotel in fear, asking where we should run to escape the danger. Everyone pointed in the same direction. As soon as we started running that way, one of our classmates warned us that it would be better to climb to the hotel terrace for shelter. Some of us followed his advice and turned back.

The Residencias Popular in Armero had two floors, with a terrace on the top level. That is where we took refuge, together with some classmates and nearby residents. From there, we first saw a flood arrive, carrying food stalls and large objects.

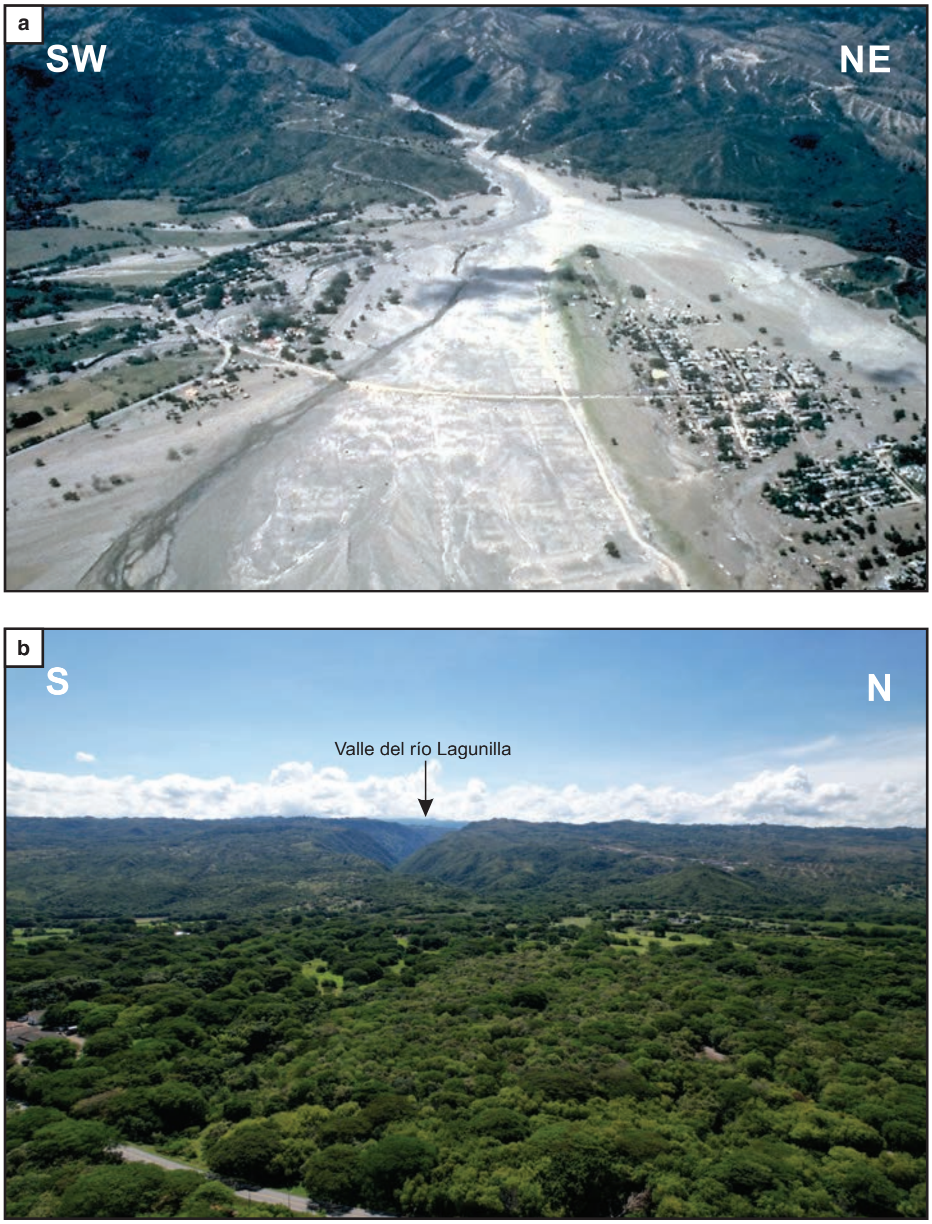

Figure 31. Panoramic view of the former town of Armero, with the Lagunilla River valley in the back-ground, along which the lahar descended, inundating and destroying the town. (a) Aerial view showing the Lagunilla River canyon, the leveled terrain on which Armero was estab-lished, and the distribution of the main lahar deposit that destroyed the town on November 13, 1985, as it reoccupied the course of the so-called Viejo River (from Navarro et al., 2011). (b) View of the Lagunilla River valley and Armero 30 years after the tragedy (photograph taken on April 30, 2016).

This flood consisted of relatively clean water displaced from the Lagunillas River by the enormous volume of volcanic material mobilized after the eruption. At that moment, the tragedy had only just begun. Shortly afterward, we heard a tremendous roar caused by the lahars, which rose before us as a wave that appeared taller than the five–story hotel we were standing on, carrying cars, debris from houses, and other structures in its path.

As we watched this immense wave approach at high speed, a lower but still powerful flow destroyed all the lower floors of the hotel, leaving us standing on tiles that had once formed part of the terrace. Moments later, one of my friends and I went down a staircase to the floor below. At that instant, the roof above us collapsed, and a large water tank fell down with us. We became trapped by debris from the wall and ceiling when suddenly a second wave arrived, mobilizing all the surrounding material. Thanks to this, my friend and I were freed from the rubble—I pulled him toward me to help him escape. Immediately, we climbed onto the fallen water tank, and the flow carried us over the debris beneath our feet. This was possible due to a process that occurs in lahars known as bulking, whereby the volume of the flow increases and larger, heavier clasts are transported at the top of the flow, effectively floating above the finer material being carried along.

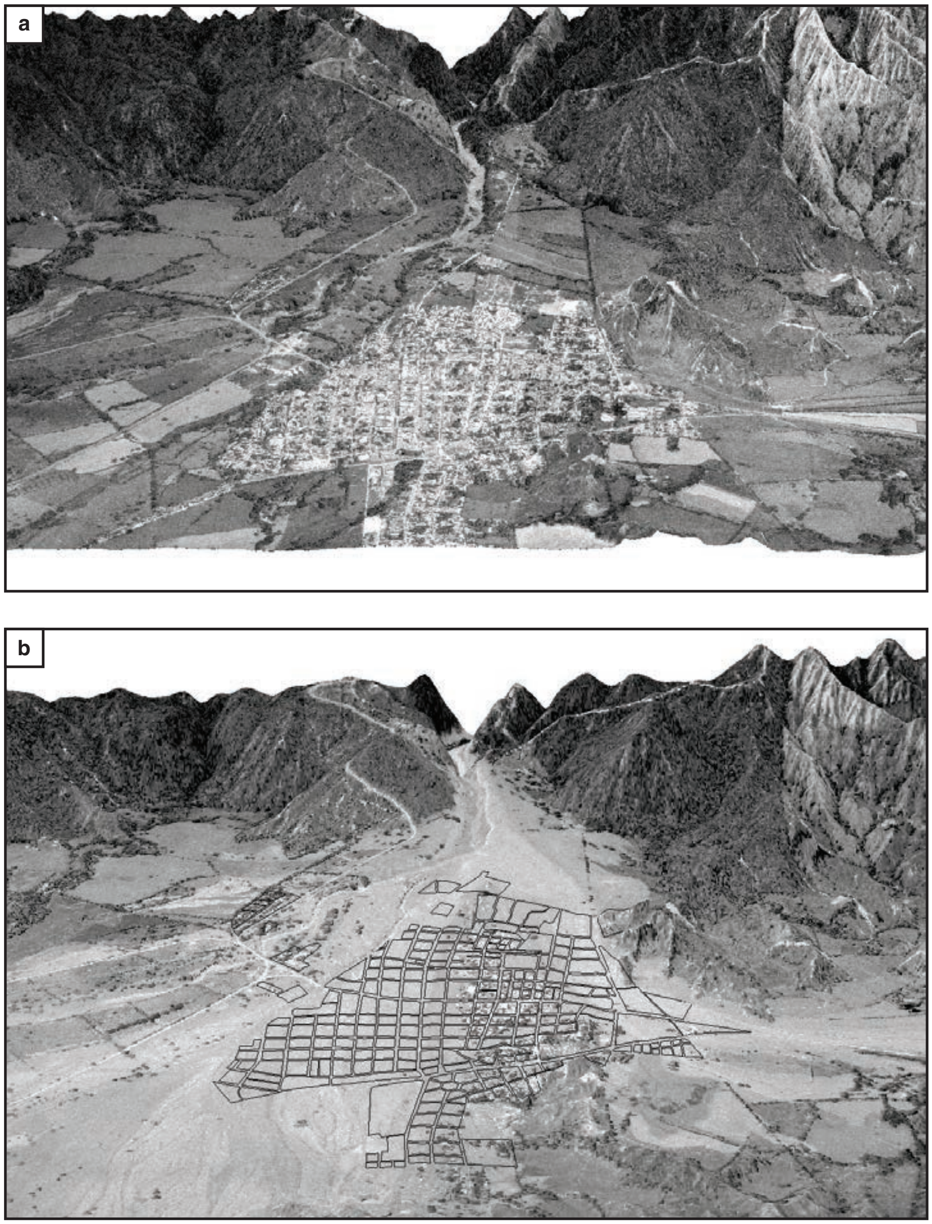

Figure 32. 3D models of Armero generated in ArcScene with a 3× vertical exaggeration. (a) Image based on data from November 20, 1985. (b) Image based on data from May 5, 1985.

Fortunately, the hotel was not located along one of the main lahar pathways; had it been, the outcome of this story would have been entirely different. Instead, we were transported by the lahar for several meters to an area known as El Mercadito, in the central part of the town, where the level of destruction was comparatively lower. For us, the transport by the flow ended there

As the hours passed, more survivors began to appear, whom we assisted as best we could amid the chaos. In addition to my friend, another classmate emerged who had managed to remain on top of the water tank and, almost inexplicably, had not a single trace of mud on his clothing. Another was freed from between mattresses and debris where he had been trapped. After several hours, the first helicopters and humanitarian aid arrived, but the intense rain mixed with volcanic ash soon prevented further landings and forced us to spend the night there. One helicopter managed to evacuate my friend, who had sustained severe injuries to his leg, along with another injured classmate. The following day, we were reunited with two more classmates who, fortunately, had not suffered serious injuries. By then, exhaustion and the urgency to leave the area were overwhelming. I approached a group of police officers and rescue workers who, together with other survivors near El Mercadito, were improvising an escape route: bed planks and fragments of furniture laid over the mud to prevent us from sinking and to allow us to finally leave the area devastated by the lahar. Of the 30 classmates in our group, 11 died that night. Not all of us were staying in the same hotel, and not all were as fortunate as we were."

3.12 Stop 10

Ruins of San Lorenzo Hospital in Armero and the sector of the town not destroyed by the lahar
Ibagué–Mariquita Road
74° 54’ 20.621” W; 4° 57’ 50.278” N
369 m.a.s.l.

At this stop, the ruins of San Lorenzo Hospital in Armero can be observed. The lower floor of the building was buried by the 1985 lahar deposit, leaving only the second floor partially destroyed and exposed. In addition, the ruins of several houses that remained standing in the hospital sector are visible.

This area corresponds to the zone where the lahar split into two branches, isolating this sector and preventing it from being completely destroyed like the rest of the town.

4. Final considerations

As demonstrated throughout these stops, lahars represent one of the greatest potential hazards associated with volcanic eruptions. Areas that have been affected by lahars on multiple occasions may be impacted again by future events of similar nature. Although the lahar deposits observed differ in formation mechanisms, composition, and magnitude, the destructive power of the events that generated them—and the resulting severe human and economic losses—is evident.

Figure 33 compares the areal distribution of lahars from Cerro Machín Volcano (CMV) and Nevado del Ruiz Volcano (NRV). If technical information derived from volcanic hazard assessments is not incorporated into risk management strategies, development plans, land-use planning, educational programs, contingency measures, and emergency protocols, the potential consequences for life and property in future lahar events may be devastating. Continuous monitoring and research of active volcanoes are essential to provide timely information to communities within their areas of influence and to strengthen communication and coordination among the various actors involved in volcanic risk management (Navarro et al., 2011).

Acknowledgments

We would like to express our gratitude to Geologist Juan Manuel HERRERA GONZÁLEZ, Technical Director of the Basic Geoscience Directorate, who approved two field campaigns aimed at verifying the condition of the outcrops and conducting drone–based photographic documentation. We also thank the Geomatics Group of the Colombian Geological Survey, particularly Yuri Lorena BECERRA MARTÍNEZ, for the preparation of the orthophotos, anaglyphs, and digital elevation models of the Armero area.

Likewise, we extend our appreciation to the Director General of the Servicio Geológico Colombiano, Julio FIERRO, for authorizing the funding of the field excursion for the members of the IUGS Executive Committee.

Finally, we sincerely thank Sofía del Rosario NAVARRO ALARCÓN of the Servicio Geológico Colombiano, who shared her personal experiences as a survivor of the Armero tragedy and granted permission for their inclusion in this guide.

References

Almeida, M., Macambira, M.J., Santos, J.O., Nascimento, R.S.C., & Paquette, J. 2013. Evolução crustal do noroeste do Cráton Amazônico (Amazonas, Brasil) baseada em dados de campo, geoquímicos e geocronológicos. In: SBG/Núcleo Norte, Simposio de Geologia Da Amazônia, 13°, Belém. Anais, 1–4.

Almeida, M. E., Nascimento, R. S. C., Mendes, T. A., Santos, J. O. S., Macambira, M. J. B., Vasconcelos, P., & Pinheiro, S. S. 2022. An outline of Paleoproterozoic-Mesoproterozoic crustal evolution of the NW Amazon craton and implications for the Columbia Supercontinent. International Geology Review, 64(22), 3195–3229. https://doi.org/10.1080/00206814.2021.2025158

Amaya, S., Zuluaga, C., & Bernet, M. 2017. New fission-track age constraints on the exhumation of the central Santander Massif: implications for the tectonic evolution of the Northern Andes, Colombia, Lithos, 282-283, 388-402. https://doi.org/10.1016/j.lithos.2017.03.019

Amaya–Ferreira, S., Zuluaga, C.A., & Bernet, M. 2020. Different levels of exhumation across the Bucaramanga Fault in the Cepitá area of the southwestern Santander Massif, Colombia: Implications for the tectonic evolution of the Northern Andes in northwestern South America. In: Gómez, J. & Mateus–Zabala, D. (editors), The Geology of Colombia, Volume 3 Paleogene – Neogene. Servicio Geológico Colombiano, Publicaciones Geológicas Especiales, 37, 689–727. Bogotá. https://doi.org/10.32685/pub.esp.37.2019.17

Anderson, T.A. 1972. Paleogene Nonmarine Gualanday Group, Neiva Basin, Colombia, and Regional Development of the Colombian Andes. Geological Society of America Bulletin, 83(8): 2423–2438. https://doi.org/10.1130/0016-7606(1972)83[2423:PNGGNB]2.0.CO;2

Arculus, R. J., Lapierre, H., & Jaillard, E. 1999. Geochemical window into subduction and accretion processes: Raspas metamorphic complex, Ecuador. Geology, 27(6), 547-550. https://doi.org/10.1130/0091-7613(1999)027<0547:GWISAA>2.3.CO;2

Ariza–Acero, M. M., Spikings, R., Beltrán-Triviño, A., Ulianov, A., & von Quadt, A. (2022). Geochronological, geochemical and isotopic characterisation of the basement of the Chocó-Panamá Block in Colombia. Lithos, 412, 106598. https://doi.org/10.1016/j.lithos.2022.106598

Barajos, B., Camacho, I., Cadena, G., Cedeño, C., Cortes, Y., Craig, J., Serrato, A., Gómez, D., González, J., Guerrero, A., Lache, M., Oliveros, M., Pérez, S., Prieto, Y., Ramírez, G., & Ramírez, D. 2023. Armero: imaginarios territoriales – Diálogos Geográficos XIX. IGAC. 34 p. Bogotá, Colombia. ISBN: 978-958-5494-95-4. ISBN en línea: 978-958-5494-96-1

Barrero, D. 1979. The geology of the central Western Cordillera, west of Buga and Roldanillo, Colombia. Publciaciones Geológicas Especiales del Ingeominas, 4, 1-75.

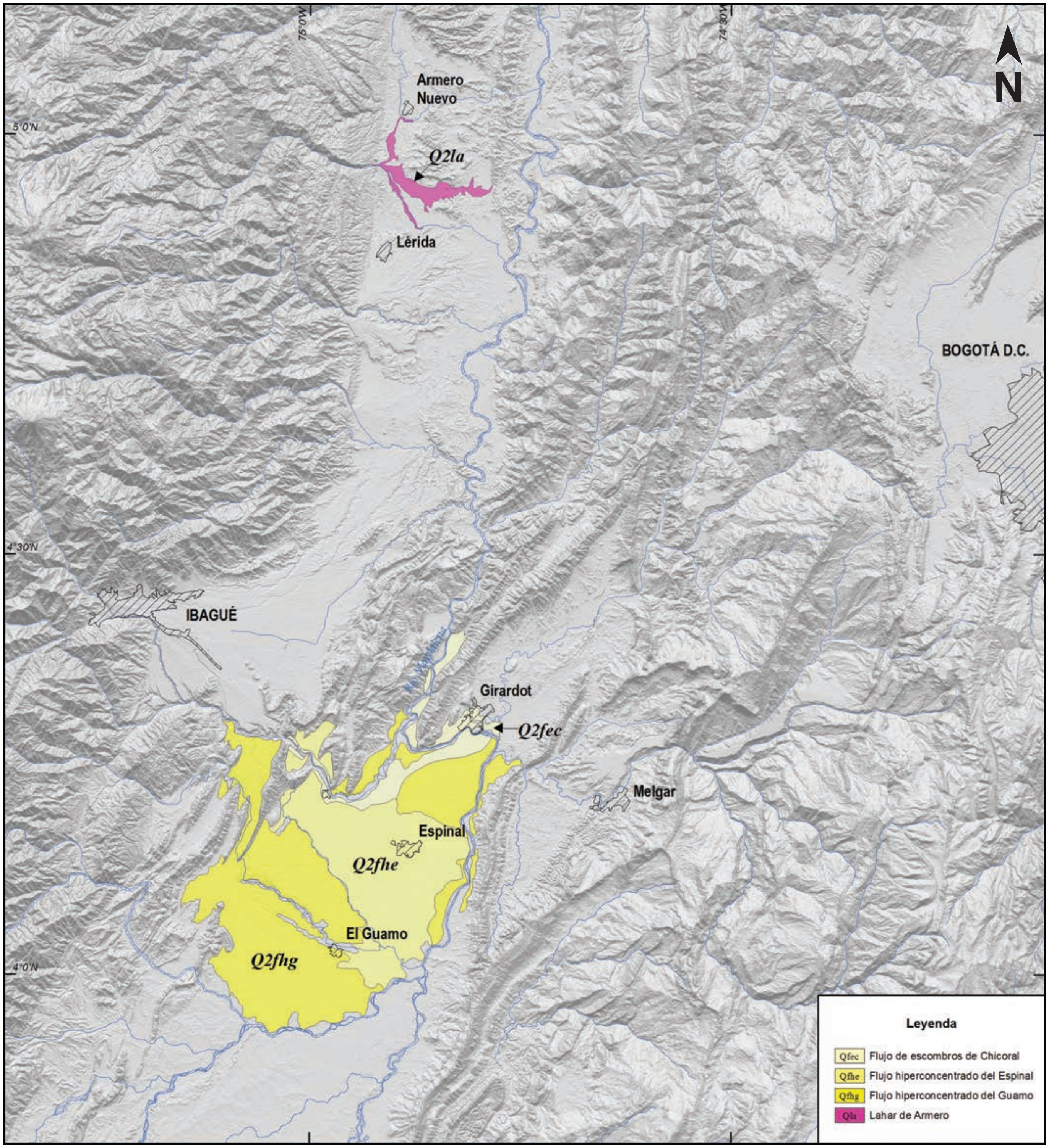

Figure 33. Comparison of the areal distribution of the 1985 Armero lahar and the lahars of Cerro Machín Volcano documented in the geological record, adapted from Cortés et al. (2006) (modified from Navarro et al., 2011).

Bayona, G., Cardona, A., Jaramillo, C., Mora, A., Montes, C., Valencia, V., Ayala, C., Montenegro, O. & Ibañez-Mejia, M. (2012). Early Paleogene magmatism in the Northern Andes: Insights on the effects of Oceanic Plateau–continent convergence. Earth and Planetary Science Letters, 331, 97–111. https://doi.org/10.1016/j.epsl.2012.03.015

Bayona, G., Bustamante, C., Nova, G. & Salazar–Franco, A.M. 2020. Jurassic evolution of the northwestern corner of Gondwana: Present knowledge and future challenges in studying Colombian Jurassic rocks. In: Gómez, J. and Pinilla–Pachon, A.O. (eds) The Geology of Colombia, Volume 2 Mesozoic. Servicio Geológico Colombiano, Bogotá, Publicaciones Geológicas Especiales, 36, 171–207, https://doi.org/10.32685/pub.esp.36.2019.05

Bayona, G., Baquero, M., Ramírez, C., Tabares, M., Salazar, A.M., Nova, G., Duarte, E., Pardo, A., Plata, A., Jaramillo, C., Rodríguez, G., Caballero, V., Cardona, A., Montes, C., Gómez-Marulanda, S., & Cárdenas-Rozo, A.L. 2021. Unravelling the widening of the earliest Andean northern orogen: Maastrichtian to early Eocene intra-basinal deformation in the northern Eastern Cordillera of Colombia. Basin Research, 33, 809–845. https://doi.org/10.1111/bre.12496

Blakey, R.C. 2003. Carboniferous–Permian paleogeography of the assembly of Pangaea. In: Wong, T. E. (ed), Proceedings of the XVth International Congress on Carboniferous and Permian Stratigraphy. Utrecht (Vol. 10, p. 16).

Bortolotti, V. & Principi, G. 2005. Tethyan ophiolites and Pangaea break–up. The Island Arc, 14, 442–470. https://doi.org/10.1111/j.1440-1738.2005.00478.x

Brook, M. 1984. New radiometric age data from SW Colombia: Cali, Colombia. INGEOMINAS-Misión Británica (BGS) Report No 10, 25 p.

Bosch, D., Gabriele, P., Lapierre, H., Malfere, J.-L. & Jaillard, E. 2002. Geodynamic significance of the Raspas Metamorphic Complex (SW Ecuador): geochemical and isotopic constraints. Tectonophysics, 345, 83–102. https://doi.org/10.1016/S0040-1951(01)00207-4

Bourgois, J., Calle, B., Toumon, J. & Toussaint, J-F. 1982. The Andean ophiolitic megastructures on the Buga-Buenaventura transverse (Western Cordillera-Valle Colombia). Tectonophysics, 82, 207-229. https://doi.org/10.1016/0040-1951(82)90046-4

Bustamante, A., Juliani, C., Hall, C.M. & Essene, E.J. 2011. 40Ar/39Ar ages from blueschists of the Jambaló region, Central Cordillera of Colombia: Implications on the styles of accretion in the northern Andes. Geologica Acta, 9(3–4): 351–362. https://doi.org/10.1344/105.000001697

Bustamante, A., Juliani, C., Essene, E.J., Hall, C.M. & Hyppolito, T. 2012. Geochemical constraints on blueschist– and amphibolite–facies rocks of the Central Cordillera of Colombia: The Andean Barragán region. International Geology Review, 54(9), 1013–1030. https://doi.org/10.1080/00206814.2011.594226

Bustamante, C. & Bustamante, A. 2019. Two Cretaceous subduction events in the Central Cordillera: Insights from the high P–low T metamorphism. In: Gómez, J. & Pinilla–Pachon, A.O. (editors), The Geology of Colombia, Volume 2 Mesozoic. Servicio Geológico Colombiano, Publicaciones Geológicas Especiales 36, p. 485–498. Bogotá. https://doi.org/10.32685/pub.esp.36.2019.14

Bustamante, C., Archanjo, C.J., Cardona, A. & Vervoort, J.D. 2016. Late Jurassic to Early Cretaceous plutonism in the Colombian Andes: A record of long–term arc maturity. Geological Society of America Bulletin, 128, 1762–1779, https://doi.org/10.1130/B31307.1

Bustamante, C., Cardona, A., Archanjo, C. J., Bayona, G., Lara, M., & Valencia, V. 2017. Geochemistry and isotopic signatures of Paleogene plutonic and detrital rocks of the Northern Andes of Colombia: A record of post-collisional arc magmatism. Lithos, 277, 199-209. https://doi.org/10.1016/j.lithos.2016.11.025

Caicedo, J.C. & Roncancio, J.H. 1994. El Grupo Gualanday como ejemplo de acumulación sintectónica, en el Valle Superior del Magdalena, durante el Paleógeno. En: Etayo Serna, F. (Editor), Estudios Geológicos del Valle Superior del Magdalena. Universidad Nacional, p. X1–X19. Bogotá.

Cardona, A., Valencia, V., Garzón, A., Montes, C., Ojeda, G., Ruiz, J. & Weber, M. 2010. Permian to Triassic I to S–type magmatic switch in the northeast Sierra Nevada de Santa Marta and adjacent regions, Colombian Caribbean: Tectonic setting and implications within Pangea paleogeography. Journal of South American Earth Sciences, 29, 772–783. https://doi.org/10.1016/j.jsames.2009.12.005

Cardona, A., Weber, M., Valencia, V., Bustamante, C., Montes, C., Cordani, U. & Muñoz, C.M. 2014. Geochronology and geochemistry of the Parashi granitoid, NE Colombia: Tectonic implication of short–lived Early Eocene plutonism along the SE Caribbean margin. Journal of South American Earth Sciences, 50, 75–92. https://doi.org/10.1016/j.jsames.2013.12.006

Cardona, A., León, S., Jaramillo, J.S., Valencia, V., Zapata, S., Pardo–673 Trujillo, A., Schmitt, A.K., Mejía, D. & Arenas, J.C. 2020. Cretaceous record from a Mariana– to an Andean–type margin in the Central Cordillera of the Colombian Andes. In: Gómez, J. and Pinilla–Pachon, A.O. (eds) The Geology of Colombia, Volume 2 Mesozoic, Servicio Geológico Colombiano, Bogotá, Publicaciones Geológicas Especiales, 36, 335–373. https://doi.org/10.32685/pub.esp.36.2019.10

Case, J.E. & MacDonald, W.D. 1973. Regional gravity anomalies and crustal structure in Northern Colombia. Geological Society of America Bulletin, 84, 2905-2916. https://doi.org/10.1130/0016-7606(1973)84<2905:RGAACS>2.0.CO;2

Case, J. E., Barnes, J., París, G., González, I. H. & Viña, A., 1973. Trans-Andean geophysical profile, southern Colombia. Geological Society of America Bulletin 84, 2895–2904. https://doi.org/10.1130/0016-7606(1973)84<2895:TGPSC>2.0.CO;2

Cawood, P. A., McCausland, P. J., & Dunning, G. R. 2001. Opening Iapetus: constraints from the Laurentian margin in Newfoundland. Geological Society of America Bulletin, 113(4), 443-453. https://doi.org/10.1130/0016-7606(2001)113<0443:OICFTL>2.0.CO;2

Cepeda, H., Murcia, L.A., Monsalve, M.L., Méndez, R.A & Núñez, A. 1995. Volcán Cerro Machín, departamento del Tolima Colombia: Pasado, presente y futuro. Ingeominas, informe interno, 48 p. Popayán.

Cerón, J.F., 2008. Crustal structure of the Colombian Caribbean basin and margins. Ph.D. thesis, University of South Carolina, 165 p.

Cochrane, R., 2013. U–Pb thermochronology, geochronology and geochemistry of NW South America: rift to drift transition, active margin dynamics and implications for the volume balance of continents (PhD thesis) Terre & Environment, 118. University of Geneva,Switzerland, 191 p.

Cochrane, R., Spikings, R., Gerdes, A., Ulianov, A., Mora, A., Villagómez, D., Putlitz, B., & Chiaradia, M. 2014a. Permo–Triassic anatexis, continental rifting and the disassembly of western Pangaea. Lithos, 190–191, 383–402, https://doi.org/10.1016/j.lithos.2013.12.020

Cochrane, R., Spikings, R., Gerdes, A., Winkler, W., Ulianov, A., Mora, A., & Chiaradia, M. 2014b. Distinguishing between in-situ and accretionary growth of continents along active margins. Lithos, 202, 382-394. https://doi.org/10.1016/j.lithos.2014.05.031

Cooper, M. A., Addison, F. T., Alvarez, R., Coral, M., Graham, R. H., Hayward, A. B., Howe, S., Martinez, J., Naar, J., Peñans, R., Pulham, A. J., & Taborda, A. 1995. Basin Development and Tectonic History of the Llanos Basin, Eastern Cordillera, and Middle Magdalena Valley, Colombia. AAPG 716 Bulletin, 79(10), 1421–1443. https://doi.org/10.1306/7834D9F4-1721-11D7-8645000102C1865D

Cordani, U.G., Sato, K, Teixeira, W, Tassinari, C.G.G. & Basei, M.A.S. 2000. Crustal evolution of the South American platform. In: Cordani, U.G., Milani, E.J., Thomaz–Filho, A. and Campos, D.A. (eds) Tectonic evolution of South America. 31st International Geological Congress, Río de Janeiro, Proceedings, 19–40.

Cordani, U.G., Cardona, A., Jimenez, D.M., Liu, D., & Nutman, A.P. 2005. Geochronology of Proterozoic basement inliers in the Colombian Andes: tectonic history of remnants of a fragmented Grenville belt. Geological Society, London, Special Publications, 246, 329–346. https://doi.org/10.1144/GSL.SP.2005.246.01.13

Cordani, U.G., Sato, K., Sproessner, W., & Fernandes, F.S. 2016. U–Pb zircon ages of rocks from the Amazonas territory of Colombia and their bearing on the tectonic history of the NW sector of the Amazonian Craton. Brazilian Journal of Geology, 46, 5–35, http://doi.org/10.1590/2317-4889201620150012

Cortés, G.P. 2001a. Estudio Geológico de los depósitos de lahar asociados a la actividad eruptiva del Volcán Cerro Machín. Ingeominas, informe interno, 96 p. Manizales.

Cortés, G.P. 2001b. Lahares Asociados a la actividad eruptiva del Volcán Cerro Machín. VIII Congreso Colombiano de Geología. Memorias, 12p. Manizales.

Cortés, G.P., Murcia, H.F., Hurtado B.O, Cepeda, H. & Nuñez, A. 2006. Comparison of the lahar deposits of the eruption of Nevado del Ruiz volcano on 13th of november 1985 and the pre-historic eruptions of Cerro Machín volcano in the central zone of Colombia. Abstracts volume. Fourth Conference Cities on Volcanoes – IAVCEI, Quito, Ecuador, January 22-27, 2006. p4.

Dasch, L., 1982. U-Pb Geochronology of the Sierra de Perijá, Venezuela (PhD thesis) Case Western Reserve University (183 pp).

De Porta, J., 1974. Lexiqui Internationale Stratigraphique. Amerique Latina, Vol. V. CNRS. Paris.

Departamento Administrativo Nacional de Estadística (DANE). 1960. Censo agropcuario de 1960 [Censo agropecuario]. Departamento del Tolima. Colombia. DANE.

Diederix, H., Audemard, F., Osorio, J.A., Montes, N., Velandia, F. & Romero, J. 2006. Modelado morfotectónico de la falla transcurrente de Ibagué. Revista Asociación Geológica de Argentina, 61(4): 492–503. Buenos Aires.

Dilek, Y., & Furnes, H. 2014. Ophiolites and their origins. Elements, 10(2), 93-100. https://doi.org/10.2113/gselements.10.2.93

Dueñas–Jiménez, H. & Montalvo–Jónsson, J. 2020. Neoproterozoic records of the Llanos Orientales Basin, Colombia. In: Gómez, J. and Mateus–Zabala, D. (eds) The Geology of Colombia, Volume 1 Proterozoic – Paleozoic. Servicio Geológico Colombiano, Bogotá, Publicaciones Geológicas Especiales, 35, 91–99. https://doi.org/10.32685/pub.esp.35.2019.05

Dueñas–Jiménez, H., Corredor–Bohórquez, V.E., & Montalvo–Jónsson, J. 2020. Paleontology of the Paleozoic rocks of the Llanos Orientales Basin, Colombia. In: Gómez, J. and Mateus–Zabala, D. (eds) The Geology of Colombia, Volume 1 Proterozoic – Paleozoic. Servicio Geológico Colombiano, Bogotá, Publicaciones Geológicas Especiales, 751 35, 133–148, https://doi.org/10.32685/pub.esp.35.2019.07

Duque-Caro, H. 1990. Neogene stratigraphy, paleoceanography and paleobiogeography in northwest South America and the evolution of the Panama Seaway. Palaeogeography, Palaeoclimatology, Palaeoecology, 77(3-4), 203-234. https://doi.org/10.1016/0031- 0182(90)90178-A

Espinosa, A. 2012. Enciclopedia de Desastres Naturales Históricos de Colombia, volúmenes 1 a 7. Academia Colombiana de Ciencias Exactas, Físicas y Naturales–Universidad del Quindío. Banco de Historia Sísmica de Colombia (Banco interactivo de sismos sentidos en Colombia entre 1550 y 2000). Edición electrónica, 1999 p. Bogotá.

Etayo–Serna, F., Cáceres, C. & Cediel, F. 2001. Mapa geológico de la plancha 246 Fusagasugá. Scale 1:100 000. Servicio Geológico Colombiano. Bogotá.

Farris, D.W., Jaramillo, C., Bayona, G., Restrepo-Moreno, S.A., Montes, C., Cardona, A., & Valencia, V. 2011. Fracturing of the Panamanian Isthmus during initial collision with South America. Geology, 39(11), 1007–1010. https://doi.org/10.1130/G32237.1

Faure, G. 2013. Origin of igneous rocks: the isotopic evidence. Springer Science & Business Media.

Forero, A. 1990. The basement of the Eastern Cordillera, Colombia: An allochthonous

terrane in northwestern South America. Journal of South America Earth Sciences, 3, 141–151. https://doi.org/10.1016/0895-9811(90)90026-W

Fourcade, E., J. Azema, J. P. Bassoullet, F. Cecca, & J. Dercourt 1990. Paleogeography and Paleoenvironment of the Tethyan Realm During the Jurassic Breakup of Pangea. In: Nairn, A.E.M., Ricou, LE., Vrielynck, B., Dercourt, J. (eds) The Tethys Ocean. Springer, Boston, MA. https://doi.org/10.1007/978-1-4899-1558-0_6

Galindo, D.A. 2012. Caracterización y modelo genético del Volcán Guacharacos (Ibagué–Tolima). Tesis de pregrado, Universidad de Caldas, 68p. Manizales.

Galvis, J., Huguett, A., & Ruge, P. 1979. Geología de la Amazonía Colombiana. Boletín Geológico, XXII (3), 1–86.

García–Ramírez, C.A., Ríos–Reyes, C.A., Castellanos–Alarcón, O.M. & Mantilla–Figueroa, L.C. 2017. Petrology, geochemistry and geochronology of the Arquía Complex's metabasites at the Pijao–Génova sector, Central Cordillera, Colombian Andes. Boletín de Geología, 39(1): 105–126. http://dx.doi.org/10.18273/revbol.v39n1-2017005

González, R., Oncken, O., Faccenna, C., Le Breton, E., Bezada, M., & Mora, A. 2023. Kinematics and convergent tectonics of the Northwestern South American plate during the Cenozoic. Geochemistry, Geophysics, Geosystems, 24, e2022GC010827. https://doi.org/10.1029/2022GC010827

Gómez, A. & Salcedo, E. 2000. Atlas de sismicidad histórica de Colombia. Ingeominas, informe interno, 136p. Bogotá.

Gómez, E., Jordan, T.E., Allmendinger, R.W., & Cardozo, N. 2005. Development of the Colombian foreland-basin system as a consequence of diachronous exhumation of the northern Andes. Geological Society of America Bulletin, 117, 1272–1292. https://doi.org/10.1130/B25456.1

Gómez, J., Nivia, Á., Montes, N.E., Tejada, M.L., Jiménez, D.M., Sepúlveda, M.J., Osorio, J.A., Gaona, T., Diederix, H., Uribe, H. & Mora, M., compilers. 2007. Geological Map of Colombia. Scale 1:1 000 000. Ingeominas. Bogotá, Colombia.

Gómez, J., Montes, N.E., Nivia, Á. & Diederix, H., compilers. 2015. Geological Map of Colombia 2015. Scale 1:1 000 000. Servicio Geológico Colombiano, 2 sheets. Bogotá, Colombia. https://doi.org/10.32685/10.143.2015.936

Gómez, J., Monsalve–Bustamante, M.E., Montes, NE. & Ortiz, L.S. 2016. Geological History of the Colombian Andes in the Surroundings of Ibagué. Simposio Servicio Geológico Colombiano: 100 años de producción científica al servicio de los colombianos, 39 p. Bogotá, Colombia.

Gómez, J., Núñez–Tello. A., Mateus–Zabala, D., Alcárcel–Gutiérrez, F.A., Lasso–Muñoz, R.M., Marín–Rincón, E. & Marroquín–Gómez, M.P. 2020. Physiographic and geological setting of the Colombian territory. In: Gómez, J. & Mateus–Zabala, D. (editors), The Geology of Colombia, Volume 1 Proterozoic – Paleozoic. Servicio Geológico Colombiano, Publicaciones Geológicas Especiales 35, p. 1–16. Bogotá, Colombia. https://doi.org/10.32685/pub.esp.35.2019.01

Gómez, J. & Montes, N.E., compilers. 2020. Geological Map of Colombia 2020. Scale 1:1 000 000. Servicio Geológico Colombiano, 2 sheets. Bogotá, Colombia.

Gómez, J. & Mateus–Zabala, D., editors. 2020a. The Geology of Colombia, Volume 1 Proterozoic – Paleozoic. Servicio Geológico Colombiano, Publicaciones Geológicas Especiales 35, 239 p. Bogotá, Colombia. ISBN: 978-958-52959-7-1. https://doi.org/10.32685/pub.esp.35.2019

Gómez, J. & Mateus–Zabala, D., editors. 2020b. The Geology of Colombia, Volume 3 Paleogene – Neogene. Servicio Geológico Colombiano, Publicaciones Geológicas Especiales 37, 507 p. Bogotá, Colombia. ISBN: 978-958-53131-0-1. https://doi.org/10.32685/pub.esp.37.2019

Gómez, J. & Pinilla–Pachon, A.O., editors. 2020a. The Geology of Colombia, Volume 2 Mesozoic. Servicio Geológico Colombiano, Publicaciones Geológicas Especiales 36, 498 p. Bogotá, Colombia. ISBN: 978-958-52959-8-8. https://doi.org/10.32685/pub.esp.36.2019

Gómez, J. & Pinilla–Pachon, A.O., editors. 2020b. The Geology of Colombia, Volume 4 Quaternary. Servicio Geológico Colombiano, Publicaciones Geológicas Especiales 38, 569 p. Bogotá, Colombia. ISBN: 978-958-52959-9-5. https://doi.org/10.32685/pub.esp.38.2019

Gómez, J., Montes, N.E. & Marín, E., compilers 2023. Mapa Geológico de Colombia 2023. Scale 1:1 500 000. Servicio Geológico Colombiano. Bogotá.

Harding, T.P. 1974. Petroleum traps associated with wrench faults. American Association of Petroleum Geologists Bulletin 58(7): 1290–1304.

Heine, C., Zoethout, J., & Müller, R.D. 2013. Kinematics of the South Atlantic rift: Solid Earth, 4, 215–253. https://doi.org/10.5194/se-4-215-2013

Hettner, A. (1892). Die Kordillere von Bogotá, Petermanns Mitt., Bd. 22, Erganzungsheft 104, 131 p., figs., Gotha.

Horton, B.K., Parra, M. & Mora, A. 2020. Construction of the Eastern Cordillera of Colombia: Insights from the sedimentary record. In: Gómez, J. and Mateus–Zabala, D. (eds) The Geology of Colombia, Volume 3 Paleogene – Neogene. Servicio Geológico Colombiano, Bogotá, Publicaciones Geológicas Especiales, 37, 67–88, https://doi.org/10.32685/pub.esp.37.2019.03

Hubach, E. 1931. Geología Petrolífera del Departamento de Norte de Santander. Informe del S.GN. No. 176, inédito.

Hubach, E. 1957. Estratigrafía de la Sabana de Bogotá y alrededores, Bol. Geol., Vol. V., 93-112 p. Bogotá, Colombia.

Hurtado, B.O. & Murcia, H.F. 2003. Caracterización del depósito de flujo de escombros de Chicoral, Volcán Cerro Machín, Colombia. Tesis de pregrado, Universidad de Caldas, 148p. Manizales.

Ibañez–Mejia M., Tassinari C.C.G., & Jaramillo-Mejia J. 2007. U-Pb ages of the “Antioquian Batholith” – Geochronological constraints of late Cretaceous magmatism in the central Andes of Colombia. Abstract presented at the XI Congreso Colombiano de Geología, Bucaramanga, 14–17.

Ibañez–Mejia, M. 2020. The Putumayo Orogen of Amazonia: A synthesis. In: Gómez, J. & Mateus–Zabala, D. (editors), The Geology of Colombia, Volume 1 Proterozoic – Paleozoic. Servicio Geológico Colombiano, Publicaciones Geológicas Especiales 35, p. 101–131. Bogotá. https://doi.org/10.32685/pub.esp.35.2019.06

James, D. E., & Murcia, L. A. 1984. Crustal contamination in northern Andean volcanics. Journal of the Geological Society, 141(5), 823-830. https://doi.org/10.1144/gsjgs.141.5.0823

James, K.H. 2000. The Venezuelan Hydrocarbon Habitat, Part 1, Tectonics, structure, palaeogeography and source rocks. Journal of Petroleum Geology, 23(1): 5–53. https://doi.org/10.1111/j.1747-5457.2000.tb00483.x

John, T., Scherer, E. E., Schenk, V., Herms, P., Halama, R., & Garbe-Schönberg, D. 2010. Subducted seamounts in an eclogite-facies ophiolite sequence: the Andean Raspas Complex, SW Ecuador. Contributions to Mineralogy and Petrology, 159, 265-284. https://doi.org/10.1007/s00410-009-0427-0

Kellogg, J. N., & Bonini, W. E. 1982. Subduction of the Caribbean plate and basement uplifts in the overriding South American plate. Tectonics, 1(3), 251-276. https://doi.org/10.1029/TC001i003p00251

Kerr, A. C., Tarney, J., Marriner, G. F., Nivia, A. & Saunders, A. D. 1997. The Caribbean- Colombian Cretaceous Igneous Province: The Internal Anatomy of an Oceanic Plateau. Large Igneous Provinces: Continental, Oceanic, and Planetary Flood Volcanism. American Geophysical Union Geophysical Monograph 100, 123-144. https://doi.org/10.1029/GM100p0123

Kroonenberg, S. 2019. The Proterozoic Basement of the 844 Western Guiana Shield and the Northern Andes. In: Cediel, F. and Shaw, R.P. (eds) Geology and Tectonics of Northwestern South America: The Pacific–Caribbean–Andean Junction. Frontiers in Earth Sciences, Springer, Cham, 115–192. https://doi.org/10.1007/978-3-319-76132-9_3

Laeger, K., Halama, R., Hansteen, T., Savov, I.P., Murcia, H.F., Cortés, G.P. & Garbe Schönberg, D. 2013. Crystallization conditions and petrogenesis of the lava dome from the ~900 years BP eruption of Cerro Machín Volcano, Colombia. Journal of South American Earth Sciences, 48: 193–208. https://doi.org/10.1016/j.jsames.2013.09.009

Laverde, F.E. 1989. Stratigraphy of the Tertiary sequence southwest of Bogotá, Colombia: Northeastern Upper Magdalena Valley, western border of the cordillera Oriental. Tesis de maestría, University of South Carolina, 66 p. Columbia, USA.

Leal-Mejía, H. 2011. Phanerozoic gold metallogeny in the Colombian Andes: A tectono–magmatic approach. Ph.D. thesis, Universidad de Barcelona, 989 p. Barcelona. https://doi.org/10.1007/978-3-319-76132-9_6

Li, Z. X., Bogdanova, S., Collins, A.S., Davidson, A., De Waele, B., Ernst, R.E., Fitzsimons, I.C.W., Fuck, R.A., Gladkochub, D.P., Jacobs, J., Karlstrom, K.E., Lu, S., Natapov, L.M., Pease, V., Pisarevsky, S.A., Thane, K. & Vernikovsky, V. 2008. Assembly, configuration, and break-up history of Rodinia: a synthesis. Precambrian research, 160(1-2), 179-210. https://doi.org/10.1016/j.precamres.2007.04.021

López–Isaza, J.A. & Zuluaga, C.A. 2020. Late Triassic to Jurassic magmatism in Colombia: Implications for the evolution of the northern margin of South America. In: Gómez, J. & Pinilla–Pachon, A.O. (editors), The Geology of Colombia, Volume 2 Mesozoic. Servicio Geológico Colombiano, Publicaciones Geológicas Especiales, 36, p. 77–116. Bogotá. https://doi.org/10.32685/pub.esp.36.2019.03

Marín-Cerón, M.I., Leal-Mejía, H., Bernet, M., & Mesa-Garcia, J. 2019. Late Cenozoic to Modern-Day Volcanism in the Northern Andes: A Geochronological, Petrographical, and Geochemical Review. In Cediel, F., and Shaw, R.B. (eds.), Geology and Tectonics of Northwestern South America, The Pacific-Caribbean-Andean Junction. Springer, Chapter 8, 603-648. https://doi.org/10.1007/978-3-319-76132-9_8

Martínez, A.M.C., 2007. Petrogenesis and evolution of Aburra Ophiolite, Colombian Andes, Central Range (Ph.D. thesis). University of Brasilia, p. 178.

Martínez, L., Valencia, L., Ceballos, J., Narváez, B., Pulgarín, B., Correa, A., Navarro, S., Murcia, H., Zuluaga, I., Rueda, J., & Pardo, N. 2014. Geología y estratigrafía del Complejo Volcánico Nevado del Ruiz. Servicio Geológico Colombiano. 853 p. Bogotá – Manizales – Popayán, Colombia.

Maya, M. & González, H. 1995. Unidades litodémicas en la cordillera Central de Colombia. Boletín Geológico, 35, 43–57. https://doi.org/10.32685/0120-1425/bolgeol35.2-3.1995.316

Méndez, R.A. 2001. Informe sobre la geología y estratigrafía de flujos piroclásticos asociados al Volcán Cerro Machín. Ingeominas, informe interno, 36p. Manizales.

Méndez, R.A., Cortés, G.P. & Cepeda, H. 2002. Evaluación de la Amenaza Volcánica del Volcán Cerro Machín. Ingeominas, informe interno, 64p. Manizales.

Mišković, A., Spikings, R.A., Chew, D.M., Košler, J., Ulianov, A., Schaltegger, U., 2009. Tectonomagmatic evolution of Western Amazonia: Geochemical characterization and zircon U-Pb geochronologic constraints from the Peruvian Eastern Cordilleran granitoids. Geol. Soc. Am. Bull. 121, 1298–1324. https://doi.org/10.1130/B26488.1

Mojica, J., Colmenares, F., Villarroel, C., Macía, C. & Moreno, M. 1985. Características del flujo de lodo ocurrido el 13 de Noviembre de 1985 en el valle de Armero (Tolima, Colombia): Historia y comentarios de los flujos de 1595 y 1845. Geología Colombiana, 14, 107–140.

Mojica, J., & Dorado, J. 1987. El Jurásico anterior a los movimientos intermálmicos en los Andes Colombianos, Parte A: Estratigrafía. Bioestratigrafía de los sistemas regionales del Jurásico y Cretácico de América del Sur, In: Volkheimer (Ed.), Bioestratigrafía de los Sistemas Regionales del Jurásico y Cretácico de América del Sur, Comité Sudamericano del Jurásico y Cretácico, 1, 49-110.

Monsalve, M.L. & Gómez, J. 2015. Visita de reconocimiento al Volcán Guacharacos (Ibagué, Tolima) y otros centros volcánicos del área. Servicio Geológico Colombiano, informe interno, 23 p. Bogotá. https://doi.org/10.32685/pub.esp.38.2019.10

Monsalve–Bustamante, M.L., Gómez, J. & Núñez–Tello, A. 2020. Rear–arc small–volume basaltic volcanism in Colombia: Monogenetic volcanic fields. In: Gómez, J. & Pinilla–Pachon, A.O. (editors), The Geology of Colombia, Volume 4 Quaternary. Servicio Geológico Colombiano, Publicaciones Geológicas Especiales 38, p. 353–396. Bogotá. https://doi.org/10.32685/pub.esp.38.2019.10

Montes, N., Velandia, F., Osorio, J., Audemard, F. & Diederix, H. 2005. Interpretación morfotectónica de la Falla de Ibagué para su caracterización paleosismológica, Universidad Industrial de Santander. Boletín de Geología, 27(44): 95–114. Bucaramanga.

Montes, C., Bayona, G., Cardona, A., Buchs, D.M., Silva, C.A., Morón, S., Hoyos, N., Ramírez, D.A., Jaramillo, C.A., & Valencia, V. 2012. Arc-continent collision and orocline formation: closing of the central American seaway.

Journal of Geophysical Research, Solid Earth, 117 (B4). https://doi.org/10.1029/2011JB008959

Montes, C., Cardona, A., Jaramillo, C., Pardo, A., Silva, J.C., Valencia, V., & Niño, H. 2015. Middle Miocene closure of the Central American Seaway. Science, 348 (6231), 226–229. https://doi.org/10.1126/science.aaa2815

Mora-Páez, H., Kellogg, J. N., Freymueller, J. T., Mencin, D., Fernandes, R. M., Diederix, H., LaFemina, P., Cardona-Piedrahita, L., Lizarazo, S., Peláez-Gaviria, H., Díaz-Mila, F., Bohórquez-Orozco, O., Giraldo-Londoño, L & Corchuelo-Cuervo, Y. 2019. Crustal deformation in the northern Andes–A new GPS velocity field. Journal of South American Earth Sciences, 89, 76-91. https://doi.org/10.1016/j.jsames.2018.11.002

Mora, A., Parra, M., Strecker, M.R., Sobel, E.R., Hooghiemstra, H., Torres, V., & Vallejo- Jaramillo, J. 2008. Climatic forcing of asymmetric orogenic evolution in the Eastern Cordillera of Colombia. Geol. Soc. Am. Bull., 120, 930–949. https://doi.org/10.1130/B26186.1

Mora, A., Villagómez, D., Parra, M., Caballero, V.M., Spikings, R., Horton, B.K., Mora–Bohórquez, J.A., Ketcham, R.A. & Arias–Martínez, J.P. 2020. Late Cretaceous to Cenozoic uplift of the northern Andes: Paleogeographic implications. In: Gómez, J. & Mateus–Zabala, D. (editors), The Geology of Colombia, Volume 3 Paleogene – Neogene. Servicio Geológico Colombiano, Publicaciones Geológicas Especiales, 37, p. 89–121. Bogotá. https://doi.org/10.32685/pub.esp.37.2019.04

Mora, S. 2022. Relatos de una tragedia. Universidad Central. Link de consulta: https://concentrika.ucentral.edu.co/relatos-de-una-tragedia/ (consulted in January 2026).

Moreno–Sánchez, M., Gómez–Cruz, A. & Buitrago–Hincapié, J. 2020. Paleozoic of Colombian Andes: New paleontological data and regional stratigraphic review. In: Gómez, J. and Mateus–Zabala, D. (eds) The Geology of Colombia, Volume 1 Proterozoic – Paleozoic. Servicio Geológico Colombiano, Bogotá, Publicaciones Geológicas Especiales, 35, 167–203. https://doi.org/10.32685/pub.esp.35.2019.09

Murcia, H.F., Hurtado, B.O., Cortés, G.P., Macías, J.L. & Cepeda, H. 2008. The ~ 2500 yr B.P. Chicoral non–cohesive debris flow from Cerro Machín Volcano, Colombia. Journal of Volcanology and Geothermal Research, 171(3–4): 201–214.

Murcia, H.F., Sheridan, M.F., Macías, J.L. & Cortés, G.P. 2010. TITAN2D simulations of pyroclastic flows at Cerro Machín Volcano, Colombia: Hazard implications. Journal of South American Earth Sciences, 29(2): 161–170. https://doi.org/10.1016/j.jsames.2009.09.005

Naranjo, J.L., Sigurdsson, H., Carey, S.N. & Fritz, W. 1986. Eruption of the Nevado del Ruiz volcano, Colombia, on 13 november 1.985: Tephra Fall and Lahars. Reprint Series. 29. August, 233: 961-963. https://doi.org/10.1126/science.233.4767.961

Naranjo, A., Horner, J., Jahoda, R., Diamond, L.W., Castro, A., Uribe, A., Pérez, C., Paz, H., Mejía, C. & Weil, J. 2018. La Colosa Au porphyry deposit, Colombia: Mineralization styles, structural controls, and age constraints. Economic Geology, 113(3), 553–578. https://doi.org/10.5382/econgeo.2018.4562

Navarro, S., Pulgarín, B., Monsalve, M.L., Cortés, G.P. & Calvache, M.L. 2011. Excursión Volcán Nevado del Ruiz–Armero, 26 años después, con alusión a los volcanes Cerro Bravo y Cerro Machín. XIV Congreso Latinoamericano de Geología y XIII Congreso Colombiano de Geología. 89 p. Medellín.

Nivia, Á., 1987. The geochemistry and origin of the Amaime and Volcanic sequences, SW Colombia. M. Phil. Thesis, University of Leicester, UK, 164 pp.

Nivia, Á., Marriner, G.F., Kerr, A.C. & Tarney, J. 2006. The 931 Quebradagrande Complex: A Lower Cretaceous ensialic marginal basin in the Central Cordillera of the Colombian Andes. Journal of South American Earth Sciences, 21, 423–436, https://doi.org/10.1016/j.jsames.2006.07.002

Núñez, A., Gómez, J. & Rodríguez, G. 2001. Vulcanismo básico al sureste de la ciudad de Ibagué, departamento del Tolima (Colombia). VIII Congreso Colombiano de Geología. Memorias CD ROM, 12 p. Manizales.

Ordóñez–Carmona, O., Restrepo-Alvarez, J.J., Pimentel, M.M. 2006. Geochronological and isotopical review of pre-Devonian crustal basement of the Colombian Andes. Journal of South American Earth Sciences, 21, 372–382. https://doi.org/10.1016/j.jsames.2006.07.005

Ordóñez-Carmona O., Pimentel M., & Laux, J.H. 2008. Edades U-Pb del Batolito Antioqueño. Boletín de Ciencias de la Tierra, 22, 129–130.

Osorio, J.A., Montes, N.E., Velandia, F.A., Acosta, J.E., Romero, J.A., Diederix, H. Audemard, F. & Núñez, A. 2008. Paleosismología de la Falla de Ibagué. Servicio Geológico Colombiano, Publicaciones Geológicas Especiales 29, 240 p. Bogotá.

Pankhurst, R.J., Rapela, C.W., & Fanning, C.M. 2000. Age and origin of coeval TTG, I- and S-type granites in the Famatinian belt of NW Argentina. Transactions of the Royal Society of Edinburgh: Earth Sciences, 91, 151–168. https://doi.org/10.1017/S0263593300007343

Parra, M., Mora, A., Jaramillo, C., Strecker, M.R., Sobel, E.R., Quiroz, L., Rueda, M., & Torres, V. 2009a. Orogenic wedge advance in the northern Andes: Evidence from the Oligocene-Miocene sedimentary record of the Medina Basin, Eastern Cordillera, Colombia. Geological Society of America Bulletin, 121, 780-800. https://doi.org/10.1130/B26257.1

Parra, M., Mora, A., Sobel, E.R., Strecker, M.R., & González, R. 2009b. Episodic orogenic front migration in the northern Andes: Constraints from low-temperature thermochronology in the Eastern Cordillera, Colombia. Tectonics, 28, TC:4004, https://doi.org/10.1029/2008TC002423

Peace, A. L., Phethean, J. J., Franke, D., Foulger, G. R., Schiffer, C., Welford, J. K., McHone G., Rocchi S., Schnabel M. & Doré, A. G. 2020. A review of Pangaea dispersal and Large Igneous Provinces–In search of a causative mechanism. Earth-Science Reviews, 206, 102902. https://doi.org/10.1016/j.earscirev.2019.102902

Pierson, T.C., Janda, R.J., Thouret, J-C. and Berrero, C.A. 1990. Perturbation and Melting of Snow and Ice by the 13 November 1985 Eruption of Nevado del Ruiz, Colombia, and Consequent Mobilization, Flow and Deposition of Lahars. Journal of Volcanology and Geothermal Research, 41, 17-66. https://doi.org/10.1016/0377-0273(90)90082-Q

Pindell, J.L. & Kennan, L. 2009. Tectonic evolution of the Gulf of Mexico, caribbean and northern South America in the mantle reference frame: An update. In: James, K.H., Lorente, M.A. and Pindell, J.L. (eds) The origin and evolution of the Caribbean Plate. Geological Society of London, Special Publication, 328, 1–55, https://doi.org/10.1144/SP328.1

Pindell, J., Villagómez, D., Molina–Garza, R., Graham, R. & Weber, B. 2020. A revised synthesis of the rift and drift history of the Gulf of Mexico and surrounding regions in the light of improved age dating of the Middle Jurassic salt. Geological Society, London, Special Publications, 504, 29–76. https://doi.org/10.1144/SP504-2020-43

Quiroga, D. E., Currie, C. A., & Pearse, J. 2024. Lithosphere removal in the Sierra Nevada de Santa Marta, Colombia. Journal of Geophysical Research: Solid Earth, 129, e2023JB027646. https://doi. org/10.1029/2023JB027646

Ramírez J. E. 1975. Historia de los terremotos en Colombia. Bogotá. Instituto Geográfico Agustín Codazzi, Subdirección de Investigaciones y Divulgación Geográfica

Ramos, V.A. & Aleman, A. 2000. Tectonic evolution of the Andes. In: Cordani, U.G., Milani, E. J., Thomaz Filha, A., Campos, D.A. (Eds.), Tectonic Evolution of South America. 31st International Geological Congress, Rio de Janerio, pp. 635–685.

Ramos, V.A. 2008. The basement of the Central Andes: the Arequipa and related terranes. Annual Reviews of Earth and Planetary Sciences, 36, 289–324. https://doi.org/10.1146/annurev.earth.36.031207.124304

Renzoni, G. 1962. Apuntes acerca de la litología y tectónica de la zona al Este y Sureste de Bogota, Bol. Geol.,Vol. X, 59·79 p. Bogotá, Colombia.

Restrepo, J. & Toussaint, J. 1976. Edades radiométricas 1015 de algunas rocas de Antioquia – Colombia. Pub. Esp., Geol., Departamento de Recursos Minerales, Facultad de Minas, Universidad Nacional de Colombia, Medellín, No. 6, pp. 1-24.

Restrepo-Pace P.A. 1995. Late Precambrian to Early Mesozoic tectonic evolution of the Colombian Andes, based on new geochronological, geochemical and isotopic data. PhD thesis, University of Arizona, 195 p.

Restrepo-Pace, P.A., Ruiz, J., Gehrels, G., & Cosca, M. 1997. Geochronology and Nd isotopic data of Grenville-age rocks in the Colombian Andes: new constraints for Late Proterozoic - Early Paleozoic paleocontinetal reconstructions of the Americas. Earth and Planetary Science Letters, 150, 427e441. https://doi.org/10.1016/S0012-821X(97)00091-5

Rodríguez, G., Sepúlveda, J., Ramírez, C., Ortiz, F., Ramos, K., Bermúdez, J., & Sierra, M. 2011. Cartografía Geológica y Exploración Geoquímica de la Plancha 443 Mitú. 163.

Rodríguez–García, G., Correa–Martínez, A.M., Zapata–García, G., Arango–Mejía, M.I., Obando–Erazo, G., Zapata–Villada, J.P. and Bermúdez, J.G. 2020) Diverse Jurassic magmatic arcs of the Colombian Andes: Constraints from petrography, geochronology, and geochemistry. In: Gómez, J. and Pinilla–Pachon, A.O. (eds) The Geology of Colombia, Volume 2 Mesozoic. Servicio Geológico Colombiano, Bogotá, Publicaciones Geológicas Especiales, 36, p. 117–170, https://doi.org/10.32685/pub.esp.36.2019.04

Rodríguez, G., Correa Martínez, A.M., Zapata, J.P., Ramírez, D.A. & Sábrica, C.A. 2022. Evolution of arc magmatic cycles from the Carboniferous to the Early Cretaceous in the western paleomargin of Gondwana, north of the Andes. Boletín Geológico, 49(2): 15–43. https://doi.org/10.32685/0120-1425/bol.geol.49.2.2022.663

Rossello, E.A. 2001. Sistemas tectónicos transcurrentes: una síntesis de sus condiciones mecánicas y aplicaciones geoeconómicas. Revista Asociación Geológica de Argentina, Serie D, Publicación Especial 5: 19–43. Buenos Aires.

Rueda, H. 2000. Depósitos de caída asociados a la actividad eruptiva del Volcán Cerro Machín: Caracterización y evaluación de su amenaza potencial. Tesis de pregrado, Universidad de Caldas, 107p. Manizales.

Santos, João O.S., Hartmann, L. A., Gaudette, H. E., Groves, D. I., Mcnaughton, N.J. & Fletcher, I. R. 2000. A New Understanding of the Provinces of the Amazon Craton Based on Integration of Field Mapping and U-Pb and Sm-Nd Geochronology. Gondwana Research, 3(4), 453–488. http://dx.doi.org/10.1016/S1342-937X(05)70755-3

Sarmiento, G. 1994. Estratigrafía y medios de depósito de la Formación Guaduas. Boletin Geológico. Volumen 32 N.1-3. INGEOMINAS Bogota.

Sarmiento-Rojas, L. F., Van Wess, J. D., & Cloetingh, S. 2006. Mesozoic transtensional basin history of the Eastern Cordillera, Colombian Andes: Inferences from tectonic models. Journal of South American Earth Sciences, 21(4), 383-411. https://doi.org/10.1016/j.jsames.2006.07.003

Sarmiento–Rojas, L.F. 2019. Cretaceous Stratigraphy and Paleo-Facies Maps of Northwestern South America. In: Cediel, F. and Shaw, R.P. (eds) Geology and Tectonics of Northwestern South America. Frontiers in Earth Sciences, Springer, Cham. https://doi.org/10.1007/978-3-319-76132-9_10

Silva–Arias, A., Páez–Acuña, L.A., Rincón–Martínez, D., Tamara–Guevara, J.A., Gómez–Gutiérrez, P.D., López–Ramos, E., Restrepo–Acevedo, S.M., Mantilla–Figueroa, L.C. &Valencia, V. 2016. Basement characteristics in the Lower Magdalena Valley and the Sinú and San Jacinto Fold Belts: Evidence of a Late Cretaceous Magmatic Arc at the South of the Colombian Caribbean. CT&F – Ciencia, Tecnología y Futuro, 6, 5–36. https://doi.org/10.29047/01225383.01

Spikings, R. A., Winkler, W., Hughes, R. A., & Handler, R. 2005. Thermochronology of allochthonous terranes in Ecuador: Unravelling the accretionary and post-accretionary history of the Northern Andes. Tectonophysics, 399(1-4), 195-220. https://doi.org/10.1016/j.tecto.2004.12.023

Spikings, R., Cochrane, R., Villagómez, D., van der Lelij, R., Vallejo, C., Winkler, W. & Beate, B. 2015. The geological history of northwestern South America: From Pangaea to the early collision of the Caribbean Large Igneous Province (290–75 Ma). Gondwana Research, 27(1): 95–139. https://doi.org/10.1016/j.gr.2014.06.004

Spikings, R. & Paul, A. 2019. The Permian – Triassic history of magmatic rocks of the northern Andes (Colombia and Ecuador): Supercontinent assembly and disassembly. In: Gómez, J. and Pinilla–Pachon, A.O. (eds) The Geology of Colombia, Volume 2 Mesozoic. Servicio Geológico Colombiano, Bogotá, Publicaciones Geológicas Especiales, 36, 1–43. https://doi.org/10.32685/pub.esp.36.2019.01

Sylvester, A.G. 1988. Strike slip faults. Geological Society of America Bulletin, 100:1666–1703. https://doi.org/10.1130/0016-7606(1988)100%3C1666:ssf%3E2.3.co;2

Tassinari, C.C., & Macambira, M.J.B. 1999. Geochronological provinces of the Amazonian Craton. Episodes, 22(3), 174–182. https://doi.org/10.18814/epiiugs/1999/v22i3/004

Thouret, J.M. Cantagrel, R. Salinas, A. Murcia. 1990. Quaternary eruptive history of Nevado del Ruiz (Colombia). Journal of Volcanology and Geothermal Research. Volume 41, Issues 1–4. 225-251 p. ISSN 0377-0273. https://doi.org/10.1016/0377-0273(90)90090-3

Toussaint, J.F., Restrepo, J.J. 1994. The Colombian Andes During Cretaceous Times. In: Salfity, J.A. (eds) Cretaceous Tectonics of the Andes. Earth Evolution Sciences. Vieweg+Teubner Verlag, Wiesbaden. https://doi.org/10.1007/978-3-322-85472-8_2

Toussaint, J.F. & Restrepo, J.J. 1978. Edad cretácea de una anfibolita granatífera de Pijao – Quindío. Pub. Esp., Geol., Departamento de Ciencias de la Tierra, Facultad de Ciencias, Universidad Nacional de Colombia, Medellín, No 17, Resumen, 1p

Tschanz, C.M., Marvin, R.F., Cruz, J., Mehnert, H.H., & Cebula, 1103 G.T. 1974. Geologic evolution of the Sierra Nevada de Santa Marta, Northeastern Colombia. Geological Society of America Bulletin, 85, 273e284. https://doi.org/10.1130/0016-7606(1974)85<273:GEOTSN>2.0.CO;2

Valencia, A. 2017. Proceso de la colonización antioqueña. Centro Cultural del Banco de la República en Manizales. Link de consulta: https://www.banrepcultural.org/rutas-colonizacion-antioquena/images/Colonizacion.pdf

Vallejo, C., Spikings, R. A., Luzieux, L., Winkler, W., Chew, D., & Page, L. 2006. The early interaction between the Caribbean Plateau and the NW South American Plate. Terra Nova, 18(4), 264-269. https://doi.org/10.1111/j.1365-3121.2006.00688.x

van der Lelij, R. 2013. Reconstructing North-Western Gondwana With Implications for the Evolution of the Iapetus and Rheic Oceans: A Geochronological, Thermochronological and Geochemical study (PhD thesis) Terre & Environment, 121. University of Geneva, Switzerland, p. 221. https://doi.org/10.13097/archive-ouverte/unige:31653

van der Lelij, R., Spikings, R., Ulianov, A., Chiaradia, M., & Mora, A. 2016. Palaeozoic to Early Jurassic history of the northwestern corner of Gondwana, and implications for the evolution of the Iapetus, Rheic and Pacific Oceans. Gondwana Research, 31, 271-294. http://dx.doi.org/10.1016/j.gr.2015.01.011

Van Houten, F.B. & Travis, R.B. 1968. Cenozoic deposits, Upper Magdalena valley, Colombia. American Asociation of Petroleum Geologist Bulletin, 52(4): 675–702. https://doi.org/10.1306/5D25C455-16C1-11D7-8645000102C1865D

Van Staal, C.R. & Hatcher, R.D. Jr. 2010. Global setting of Ordovician orogenesis. In: Finney, S.C. and Berry W.B.N. (eds) The Ordovician Earth System. Geological Society of America Special Paper, 466, 1–11. https://doi.org/10.1130/2010.2466(01)

Vargas, C. A., & Mann, P. 2013. Tearing and breaking off of subducted slabs as the result of collision of the Panama Arc-Indenter with northwestern South America. Bulletin of the seismological Society of America, 103(3), 2025-2046. https://doi.org/10.1785/0120120328

Vásquez, M., Altenberger, U., Romer, R. L., Sudo, M., & Moreno-Murillo, J. M. 2010. Magmatic evolution of the Andean Eastern Cordillera of Colombia during the Cretaceous: Influence of previous tectonic processes. Journal of South American Earth Sciences, 29(2), 171-186. https://doi.org/10.1016/j.jsames.2009.02.003

Velandia, F., Bermúdez, M.A., Kohn, B., Bernet, M., Zuluaga, C.A., & Brichau, S. 2021. Cenozoic exhumation patterns in the northern Andes: Constraints from the southern Bucaramanga Fault, Eastern Cordillera, Colombia. Journal of South American Earth Sciences, 111, 103473. https://doi.org/10.1016/j.jsames.2021.103473

Villagómez, D. & Spikings, R. 2013. Thermochronology and tectonics of the Central and Western Cordilleras of Colombia: Early Cretaceous – Tertiary evolution of the northern Andes. Lithos, 160–161: 228–249. https://doi.org/10.1016/j.lithos.2012.12.008

Villagómez, D., Spikings, R., Magna, T., Kammer, A., Winkler, W. & Beltrán, A. 2011. Geochronology, geochemistry and tectonic evolution of the Western and Central Cordilleras of Colombia. Lithos, 125(3–4): 875–896. https://doi.org/10.1016/j.lithos.2011.05.003

Villamizar-Escalante, N., Zuluaga, C. A., Bernet, M., Amaya, S., 1147 López-Isaza, J.A., García-Delgado, H., & Velandia, F. 2024. Deep-seated crustal faults and their role in the thermos-tectonic evolution of an active mountain belt: New evidence from the Northern Andes. Journal of Structural Geology, 185, 105177. https://doi.org/10.1016/j.jsg.2024.105177

Vinasco, C.J., Cordani, U.G., González, H., Weber, M. & Peláez, C. 2006. Geochronological, isotopic, and geochemical data from Permo–Triassic granitic gneisses and granitoids of the Colombian central Andes. Journal of South American Earth Sciences, 21, 355–371. https://doi.org/10.1016/j.jsames.2006.07.007

Viscarret, P., Wright, J., & Urbani, F. 2009. New U-Pb zircon ages of El Baúl Massif, Cojedes State, Venezuela. Revisita Técnica de la Facultad de Ingenieria Universidad del Zulia 32, 210–221.

Weber, B., Iriondo, A., Premo, W.R., Hecht, L., & Schaaf, P. 2007. New insights into the history and origin of the southern Maya block, SE Mexico: U-Pb-SHRIMP zircon geochronology from metamorphic rocks of the Chiapas massif. International Journal of Earth Sciences, 96, 253–269. https://doi.org/10.1007/s00531-006-0093-7

Weber, M., Gómez, J., Cardona, A., Duarte, E., Pardo, E. & Valencia, V. 2015. Geochemistry of the Santa Fé Batholith and Buriticá Tonalite in NW Colombia—Evidence of subduction initiation beneath the Colombian Caribbean Plateau. Journal of South American Earth Sciences, 62, 257–274. https://doi.org/10.1016/j.jsames.2015.04.002

Wilcox, R.E., Harding, T.P. & Seely, D.R. 1973. Basic wrench tectonics. American Association of Petroleum Geologists Bulletin 57(1): 74–96. https://doi.org/10.1306/819A424A-16C5-11D7-8645000102C1865D

Withjack, M.O., Schlische, R.W., & Olsen, P.E. 1998. Diachronous rifting, drifting, and inversion on the passive margin of central eastern North America; an analog for other passive margins. AAPG Bulletin. 82 (5A), 817–835. https://doi.org/10.1306/1D9BC60B-172D-11D7-8645000102C1865D

Zapata–Cardona, E., Hernández–González, J.S., Quiceno–Colorado, J.A., Ruiz–Jiménez, E.C., Moreno–Sánchez, M., Naranjo–Sierra, E., Toro–Toro. L.M. & Rincón–Alape, J. 2023. Petrogenesis and tectonic implications of the carboniferous El Carmen Pluton, central Colombian Andes: insights from whole-rock and mineral geochemistry, in situ zircon Lu–Hf isotopes and U–Pb geochronology. International Geology Review, 66, 2469–2494. https://doi.org/10.1080/00206814.2023.2286481

Zapata–Villada, J. P., Restrepo, J. J., Cardona-Molina, A., & Martens, U. 2017. Geoquímica y geocronología de las rocas volcánicas básicas y el Gabro de Altamira, Cordillera Occidental (Colombia): Registro de ambientes de Plateau y arco oceánico superpuestos durante el Cretácico. Boletín de Geología, 39(2), 13-30. https://doi.org/10.18273/revbol.v39n2-2017001

Zuluaga, C., & Stowell, H. 2012. Late Cretaceous–Paleocene metamorphic evolution of the Sierra Nevada de Santa Marta: Implications for Caribbean geodynamic evolution. Journal of South American Earth 1191 Sciences, 34, 1-9. https://doi.org/10.1016/j.jsames.2011.10.001

Zuluaga, C., Pinilla, A., & Mann, P. 2015. Jurassic silicic volcanism and associated continental-arc basin in Northwestern Colombia (southern boundary of the Caribbean Plate). In: Bartolini, C., Mann, P. (Eds.), Petroleum Geology and Potential of the Colombian Caribbean Margin. AAPG Memoir, 108, 137–160. https://doi.org/10.1306/13531934M1083640

Zuluaga, C.A., Amaya, S., Urueña, C., & Bernet, M. 2017. Migmatization and low-pressure overprinting metamorphism as record of two pre-Cretaceous tectonic episodes in the Santander Massif of the Andean basement in northern Colombia (NW South America). Lithos, 274, 123-146. http://dx.doi.org/10.1016/j.lithos.2016.12.036

Zuluaga, C.A. & López, J.A. 2019. Ordovician Orogeny and Jurassic Low-Lying Orogen in the Santander Massif, Northern Andes (Colombia). In: Cediel, F. and Shaw, R.P. (eds) Geology and Tectonics of Northwestern South America. Frontiers in Earth Sciences. 195-250. https://doi.org/10.1007/978-3-319-76132-9_4

Zuluaga, C.A., Gómez, J., Bernet, M., & Mateus–Zabala, D. 2026. Magmatism, metamorphism, and exhumation in the Colombian Andes: an introduction. Geological Society, London, Special Publications, 558.